Hungarian University of Agriculture and Life Sciences (MATE)

HTS-Based Virome Analysis of Solanaceous Crops and Weeds in Hungary and Kosovo

Burim Ismajli

GÖDÖLLŐ

2026

DOCTORAL (PhD) DISSERTATION

Burim Ismajli

GÖDÖLLŐ

2026

Name of Doctoral School: **Doctoral School of Natural Sciences**

Head of the Doctoral School: **Prof Dr. Erika Csákiné Michéli**,
full professor, MATE
core member of the Hungarian Academy of Sciences

Name of the Doctoral Program: **Doctoral Program of Biological Sciences**

Head of the Doctoral program: **Prof. Dr. Zoltán Nagy, DSc,**
full professor, MATE

Disciplinary: **Biological Sciences**

Supervisors: **Dr. Éva Várallyay, DSc.**
Scientific Advisor, MATE
corresponding member of the Hungarian Academy of Sciences
Institute of Plant Protection, Department of Plant Pathology,
Genomics Research Group, Gödöllő

Dr. habil. András Péter Takács
associate professor, MATE
Institute of Plant Protection, Department of Plant Protection,
Keszthely

approval of the supervisors:

....

Dr. Éva Várallyay **Dr. András Péter Takács**

TABLE OF CONTENTS

List of Abbreviations

General terms

Bspot: Brown spots

Chl: Chlorosis

Dback: Dieback

Dflow: Drying flowers

Dw: Dwarfism

Fdef: Flower deformation

Fdelays: Flowering delays

Fdying: Flower dying

H: Holes

H on leaf: Hole in leaf

Lcurl: Leaf curl

Ldef: Leaf deformation

Nec: Necrosis

P.A: Purple anthocyanin

Sh.i: Short internodes

Ul: Uneven leaves

Yflowers: Yellow flowers

Yfresh pouts: Yellowing on the fresh pouts

AGOs: Argonaute proteins

cDNA: Complementary DNA

CP: Coat protein

CRP: Cysteine-rich protein

DCLs: Dicer-like proteins

DNA: Deoxyribonucleic acid

DNase: Deoxyribonuclease

dsRNA: Double-stranded RNA

miRNA: MicroRNA

ORFs: Open reading frames

RNA: Ribonucleic acid

RNAi: RNA interference

RDRs: RNA-dependent RNA polymerases

RISC: RNA-induced silencing complex

siRNAs: Small interfering RNAs

sRNAs: Small ribonucleic acids

ssDNA: Single-stranded DNA

TNA: Total nucleic acids

VPg: Viral genome-linked protein

NABP: Nucleic acid binding protein

TGB2: Triple gene block protein 2

TGBp1: Triple gene block protein 1

SA: Salicylic acid

SNPs: Single nucleotide polymorphisms

ELISA: Enzyme-linked immunosorbent assay
DAS-ELISA: Double antibody sandwich enzyme-linked immunosorbent assay
HTS: High-throughput sequencing
sRNA HTS: Small RNA high-throughput sequencing
PCR: Polymerase chain reaction
RT-PCR: Reverse transcription-polymerase chain reaction
SDS (10%) – Sodium dodecyl sulfate (10%)
EB: Ethidium bromide

LB+AMP : Lysogeny Broth + ampicillin
LIG: Ligation mixture
TBE: Tris base, boric acid, and ethylenediaminetetraacetic acid

Bp: Base pair
ml: Milliliter
µl: Microliter
mins: Minutes
s/sec: Seconds
nt: Nucleotide
rpm: Revolutions per minute
RPM: Reads per million

K2022: Keszthely 2022

K2023: Keszthely 2023

Ko2023: Kosovo 2023

Virus names

BBWV1: Broad bean wilt virus 1

BBWV2: Broad bean wilt virus 2

BPEV: Bell pepper endornavirus

CMV: Cucumber mosaic virus

CMVS: Cucumber mosaic virus satellite RNA

LBVaV: Lettuce big-vein associated virus

ObPV: Obuda pepper virus

OxruMV1: Oxybasis rubra mitovirus 1

PCV2: Pepper cryptic virus 2

PotLV: Potato latent virus

PVH: Potato virus H

PVM: Potato virus M

PVY: Potato virus Y

RWMV: Ranunculus white mottle virus

TVCV: Tobacco vein clearing virus

TAV: Tomato aspermy virus

TuYV: Turnip yellows virus

1. INTRODUCTION

The Solanaceae family represents a cohesive group of dicotyledonous plants, encompassing a range of extensively cultivated crops. Within this family, various species have significant roles, whether as vital food sources, suppliers of bioactive compounds, or even as decorative ornamental plants (Gebhardt, 2016). Members of the Solanaceae family include well-known cultivated crops such as potato (*Solanum tuberosum*), tomato (*Solanum lycopersicum*), pepper (*Capsicum annuum*), among others, that thrive in regions across the globe with temperate or tropical climates (Hančinský et al., 2020). In addition to the extensively cultivated crops, the Solanaceae family also comprises a notable array of wild and weedy species. For instance, species such as *Solanum nigrum, Datura stramonium,* and *Solanum dulcamara* are frequently encountered in agricultural landscapes, often thriving as pervasive weeds near crop fields. Moreover, *Brassica napus*, although taxonomically a member of the Brassicaceae family, is commonly found in the same environments, further illustrating the complex interactions between cultivated and non-cultivated plants. This coexistence underscores the importance of considering both cultivated crops and wild species when studying plant communities, as these weeds can play significant roles in ecological dynamics, pathogen transmission, and the overall genetic diversity of agroecosystems. Aside from the commonly cultivated crops and weeds, the Solanaceae family is also home to various medicinal plants known for their alkaloid production. Notable examples include deadly nightshade (*Atropa belladonna*), black henbane (*Hyoscyamus niger*), and jimson weed (*Datura stramonium*) (Hančinský et al., 2020). Those plants have become staples in households worldwide, gracing kitchens, gardens, and fields, and contributing to global agriculture and culinary traditions (Olmstead et al., 2008). Over the last century, plants from the Solanaceae family have played a crucial role in genetic research, contributing significantly to advancements in our understanding of plant genetics (Gebhardt, 2016). Cultivated species from the Solanaceae family are frequently found thriving alongside their wild counterparts in the same ecosystems. In many cases, wild Solanaceae species are considered common weeds within these shared habitats. In diverse agricultural settings, Solanaceae plants are exposed to various infectious pathogens, including viruses (Hančinský et al., 2020). Plant viruses are responsible for widespread epidemics in significant crops, posing a significant challenge to global food security. Consequently, virologists

have traditionally prioritized their research efforts on economically vital cultivated crops, sometimes overlooking nearby weeds and wild plant species (Wren et al., 2006). In the realm of virus research, exploring the role of weeds as potential reservoirs has become pivotal. Scientists delve into the intricate dynamics between weeds and viruses, unravelling how these plants may serve as silent carriers. Understanding weed-associated viruses is crucial for devising effective strategies to mitigate agricultural threats and protect global crops. Weeds can act as reservoirs for both viruses and the insects that transmit them. In such circumstances, the spread of viruses can be highly pronounced (Duffus, 1971). Building on the interactions between cultivated solanaceous crops and solanaceous weeds, it is essential to expand our focus to virus detection and diagnostic methods that support integrated control strategies in agricultural ecosystems. Although virus detection has traditionally centered on economically important crops, effective management also requires investigating the weeds surrounding fields, which can serve as reservoirs for viruses and facilitate outbreaks in high-value crops. Integrated control strategies that combine early detection, robust diagnostics, and targeted management practices are crucial for mitigating virus spread and reducing yield losses (Jones, 2006). Conventional techniques, such as enzyme-linked immunosorbent assay (ELISA) and reverse transcription-polymerase chain reaction (RT-PCR), offer high sensitivity and specificity, but high-throughput sequencing, known as HTS, provides a comprehensive, unbiased analysis of the entire virome, unveiling both known and previously undescribed viruses that traditional methods might miss (Massart et al., 2022). By sequencing millions of nucleic acid molecules simultaneously, HTS exposes a wide spectrum of viral isolates within complex agricultural ecosystems. Its integration into routine monitoring facilitates rapid, proactive responses to emerging threats, reinforcing the importance of early and precise virus identification, whether in crops or neighbouring weeds for global food security. In short, incorporating advanced diagnostics like HTS alongside integrated management practices offers a promising pathway to sustain agricultural productivity amid the challenges posed by evolving plant pathogens.

2. OBJECTIVES TO ACHIEVE

1. Investigate the viromes of solanaceous weeds in Keszthely, Hungary, using high-throughput sequencing (HTS), and evaluate their role as virus reservoirs
2. To investigate and characterize the viromes of cultivated solanaceous crops in Kosovo using HTS.
3. To confirm detected viral infections through RT-PCR and to perform phylogenetic analyses to evaluate their evolutionary relationships.

3. LITERATURE REVIEW

3.1 Plant Viruses

Viruses are infectious agents invisible under a light microscope, yet despite their tiny size, they can cause significant disruption (Gergerich and Dolja, 2006). Plant viruses were first recognized as disease-causing agents in the late 19th century, when research on tobacco plants revealed that a mysterious infectious agent later known as tobacco mosaic virus was behind the characteristic mosaic symptoms. This landmark discovery not only identified the first plant virus but also laid the foundation for the field of plant virology (Van der Want and Dijkstra, 2006). Since that early discovery, it has become evident that plant viruses infect a remarkably wide range of hosts including vegetables, legumes, cereals, fruit crops, ornamentals, and even wild plant species and are estimated to account for approximately one-third of all known plant pathogens (Ibaba and Gubba, 2020). Plant viruses are obligate intracellular parasites, meaning they cannot reproduce independently but instead, they rely entirely on the host's cellular machinery to replicate their small genomes, which are typically composed of RNA or DNA enclosed within a protein capsid (Ibaba and Gubba, 2020). Upon infecting a susceptible host, they interfere with normal cellular processes, leading to a variety of symptoms such as mosaic patterns, leaf deformation, chlorosis, stunted growth, and tissue necrosis, all of which contribute to reduced plant vigor and productivity. These infections often translate into serious yield losses and in some epidemics (for example by certain potyviruses) crop yield was reported to decline by more than 90%. On the molecular side, most plant viruses have very compact genomes (often positive-sense RNA, though some have double-stranded RNA or single-stranded DNA and some plant virus groups possess double-stranded DNA genomes (e.g. caulimoviruses, type member: CaMV) with limited coding capacity. In fact, deep sequencing surveys and reviews emphasize that the plant virome is dominated by RNA viruses (Dolja et al., 2020), with positive-sense single-stranded RNA families (such as Potyviridae) making up the majority of known plant virus genera. Among virus families, Potyviridae (the largest plant RNA virus family) and Geminiviridae (a large ssDNA family) stand out as especially damaging: their members are widespread in crops and often cause devastating diseases in vegetables, legumes, cereals and other plants. Plant viruses hijack host resources at every step of the infection cycle (Hyodo and Okuno, 2020), as a result, the outcome of infection depends on complex virus–host interactions. Symptoms and severity vary greatly depending on the host

genotype, environmental conditions and the presence of vectors or co-infecting pathogens. Entry of plant viruses usually requires a wound or vector transmission: insects (aphids, whiteflies, thrips, beetles), nematodes or even pollen beetles can introduce virions by piercing the plant cuticle and cell wall. After entry and uncoating, the viral genome is translated and replicated using host enzymes, and progeny virions are assembled and spread from cell to cell (via plasmodesmata) and long-distance through the phloem (Nicaise, 2014). New plants become infected when these viruses are carried out to new hosts by vectors or human-mediated means (grafting, pruning or harvest tools, and planting of infected seed or vegetative propagules). Because there are no curative treatments once infection occurs, the early and accurate detection of plant viruses is an essential component of disease control (Jeong et al., 2014) and the management is based on integrated prevention: the use of certified virus-free seed or planting material, strict sanitation (sterilizing tools, rogueing infected plants, weed control) and suppression of vectors (insecticides, trap crops or netting) are combined with deployment of resistant cultivars. After identifying a virus, implementing appropriate integrated control strategies is crucial to limit its spread and reduce crop damage and yield loss. Equally important is preventing virus transmission through all dissemination pathways (López et al., 2009).

3.2 Plant-Virus Interactions and Resistance Mechanisms

To develop virus-resistant host plants, a variety of strategic approaches are currently available. Historically, plant breeders introduced resistance traits into susceptible genotypes through conventional breeding, often without a clear understanding of the underlying genetic mechanisms (Prins, 2003). However, advances in molecular biology have led to the identification, cloning, and functional characterization of numerous, usually dominant resistance (*R*) genes. This progress has significantly enhanced our understanding of plant innate immune responses and has enabled the application of *R* genes across species boundaries (Goldbach et al., 2003). These *R* genes typically encode proteins that recognize specific viral factors, activating downstream defense responses that inhibit viral replication or spread. Beyond natural resistance governed by *R* genes, RNA interference (RNAi) serves as a crucial sequence-specific gene silencing pathway, degrading viral RNAs and thereby limiting infection and genetically engineered strategies such as pathogen-derived resistance and transgenic expression of antiviral genes have expanded the toolkit for conferring virus resistance in plants (Bragard et al., 2013).

3.3 Plant Immune Responses to Viral Pathogens

During plant viral infections, the plant RNA interference (RNAi) defense pathway is activated as part of its antiviral response. This mechanism employs three distinct classes of proteins (Dicer-like proteins (DCLs), Argonaute proteins (AGOs), and RNA-dependent RNA polymerases (RDRs) to suppress gene expression at both the transcriptional and post-transcriptional levels, thereby enabling the plant to effectively counteract pathogen virulence (Baulcombe, 2004). In response to active viral invasion in the plant, double-stranded RNA (dsRNA) molecules are formed within the host cell. These dsRNAs are then cleaved by Dicer-like enzymes into small interfering RNAs (siRNAs). One strand of the siRNA is incorporated into the RNA-induced silencing complex (RISC), which guides the complex to recognize and bind complementary RNA sequences, specifically targeting viral RNAs for degradation since the siRNAs are derived from the infecting virus (Garcia-Ruiz et al., 2016). Within the RNA-induced silencing complex (RISC), the target viral RNA is cleaved, effectively blocking the virus and inhibiting its activity. (Figure 1). When this mechanism functions effectively, only a minimal amount of intact virus remains in the plant, while a high level of virus-specific siRNAs accumulate. These virus-derived siRNAs can be isolated and utilized as molecular markers for plant virus diagnostics.

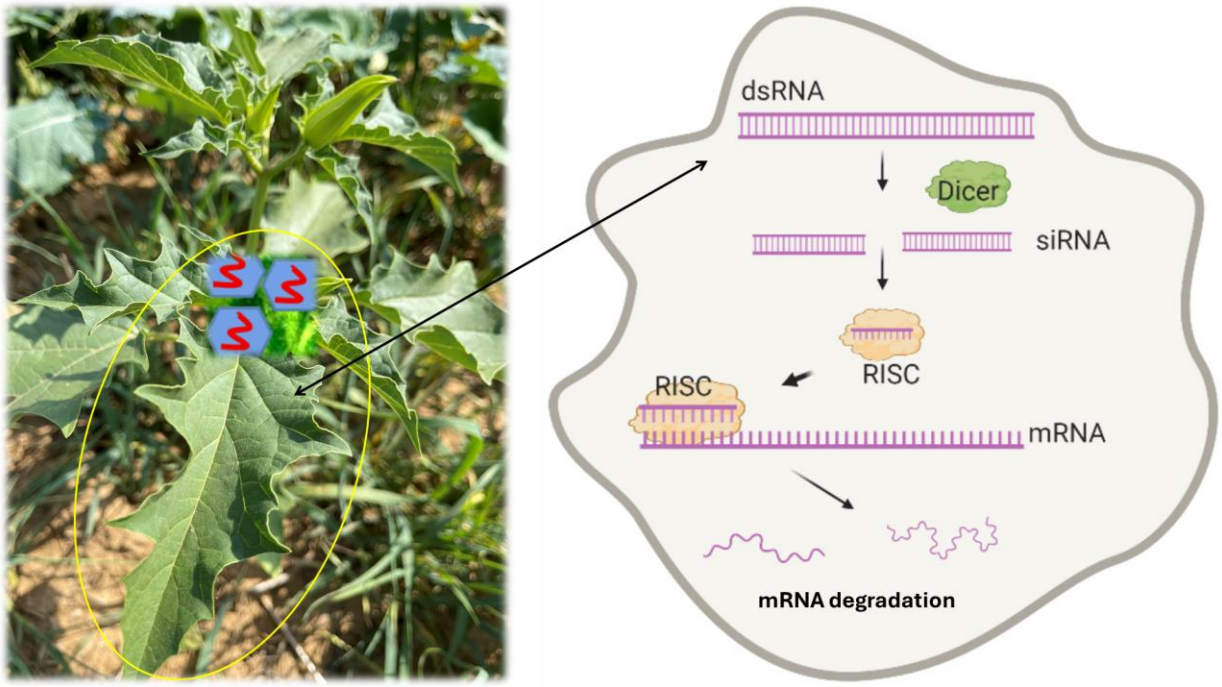

Figure 1. Author's sampling photo and RNAi mechanism cartoon from (Golubeva et al., 2021).

3.4 Viruses Infecting Solanaceous Crop

3.4.1 Cucumber mosaic virus

Cucumber mosaic virus (CMV) is the type species of the genus Cucumovirus in the family Bromoviridae and is distinguished by its unique tripartite, positive-sense RNA genome comprising RNA1, RNA2, and RNA3 which encodes essential proteins for replication, movement, and the formation of its icosahedral particles (Mochizuki and Ohki, 2012) This modular genome configuration not only permits rapid evolution and genetic recombination but also supports an extraordinarily broad host range, infecting over 1,200 plant species (Mochizuki and Ohki, 2012). The discovery of CMV dates back to 1916 when Doolittle and Jagger first reported viral diseases on cucurbits, marking the beginning of a long history as one of agriculture's most significant pathogens (Doolittle, 1916). As early as the 1970s, field surveys in India identified *S. nigrum* as a reservoir of CMV, among many weed species found infected in vegetable-growing areas (Kiranmai et al., 1998). More recently field surveys in Southern India from 2012 to 2014 documented severe virus-like symptoms in cucurbitaceous vegetables including Chinese cucumber (*Cucumis sativus*), *Trichosanthes cucumerina*, and bottle gourd (*Lagenaria siceraria*), such as stunted growth, mosaic mottling, puckering, and chlorosis with infection incidences ranging between 63% and 88% in different locales (Nagendran et al., 2018). These symptoms were replicated via mechanical inoculation, and subsequent testing with DAS-ELISA and RT-PCR confirmed the presence of CMV, revealing a coat protein gene sequence with over 92% nucleotide identity to CMV subgroup IB isolates (Nagendran et al., 2018). A 2016–2017 survey in Punjab, India confirmed CMV infection in *S. nigrum* (along with other viruses like PVY and PVM), indicating that nightshade can serve as a reservoir for crop viruses (Chaudhary et al., 2019). In Shiraz, Iran, a strain naturally infecting hoary cress (*Lepidium draba*) was identified that induced distinctive vein clearing and mosaic patterns on leaves. Detailed serological assessments and coat protein gene analysis including SDS-polyacrylamide gel electrophoresis and *Eco*RI restriction profiling facilitated its classification into defined subgroups, illustrating the genetic diversity within CMV populations (Rasoulpour and Izadpanah, 2008). CMV is notorious for its impact on crop yield and quality. For example, in the Pothwar region of Pakistan, surveys during 2015–16 documented cucumber crops exhibiting chlorotic lesions, necrotic spots, mosaic patterns, and stunting symptoms that have led to significant yield reductions (Asad et al., 2019). In response, extensive cultural practices and agrochemical applications are frequently employed, while breeding programs explore genetic

resistance, including marker-assisted selection, to mitigate these losses (Li et al., 2020). Molecular analyses in Kenya of African nightshade (*Solanum scabrum*, ANS) have revealed CMV isolates that group within subgroup I, suggesting that wild hosts serve as critical reservoirs facilitating the virus's spread to adjacent crops (Kimaru et al., 2020). Similarly, investigations in Brazil have found that weeds such as black nightshade (*Solanum americanum*) can harbor mixed infections often involving both CMV and Potato virus Y thereby acting as persistent virus reservoirs between cropping seasons (Moura et al., 2014). Complementary field surveys in Punjab, India, have confirmed the infection of *Solanum nigrum* by CMV alongside other viruses, further underscoring the importance of wild plants in the epidemiology of CMV (Chaudhary et al., 2019). Innovative control strategies have also been explored; for instance, the application of medicinal plant extracts on chili *(Capsicum annuum)* plantations has proven effective. Treatments using extracts from plants like *Annona muricata* and *Datura stramonium* have significantly reduced mosaic disease severity while enhancing plant growth and fruit yield, offering promising avenues for sustainable management (Hamidson et al., 2018). Large-scale surveys in southern Illinois, involving over 5,000 plants across approximately 55 species, have demonstrated that wild hosts such as eastern black nightshade (*Solanum ptycanthum*) and groundcherry (*Physalis heterophylla*) are major reservoirs for CMV. Multiple aphid species have been shown to efficiently transmit the virus from these wild hosts to commercial crops like bell pepper, leading to substantial economic losses since the early 1990s (Hobbs et al., 2000). In Ulleng-do, Korea, an isolate known as CMV-ZM was observed causing mottle and stunting symptoms on maize. Genetic comparisons of its RNA segments revealed high nucleotide sequence identities with subgroup I strains distinguishing it from subgroup II isolates and adding further insight into CMV classification (Kim et al., 2011). At the molecular level, the CMV 2b protein plays a pivotal role in the virus's pathogenicity. By inhibiting the plant's antiviral RNA silencing mechanisms and modulating jasmonic acid-mediated defense responses, the 2b protein not only enhances viral accumulation but also promotes aphid survival, thereby indirectly facilitating the spread of CMV (Ziebell et al., 2011). Finally, field studies in Santiago, Chile, focusing on weeds such as jimsonweed (*Datura stramonium*) and thornapple (*D. ferox*) have confirmed mixed infections that include CMV, along with Alfalfa mosaic virus and Potato virus Y. These observations emphasize the necessity for integrated weed management, as such alternative hosts play a critical role in maintaining and disseminating viruses in agricultural settings (Ormeño et al., 2006).

3.4.2 Broad bean wilt virus 1

Broad bean wilt virus 1 (BBWV-1) is a critical plant pathogen classified within the Fabavirus genus, exhibiting a bipartite genome composed of two single-stranded, positive-sense RNAs that govern its infection cycle and symptom development (Murphy et al., 2012). Genetic analyses have revealed considerable diversity among its isolates, with multiple genomic regions showing evidence of long-distance migration and significant gene flow that underscore the virus's dynamic evolutionary history (Ferriol et al., 2014). Notably, BBWV-1 has caused severe outbreaks in various regions, such as in Slovenia where infected pepper plants displayed discolorations, rings, and dark bumps on fruits, leading to dramatic yield losses (Mehle et al., 2008). In Singapore, detailed sequencing of an isolate uncovered a complex genome organization featuring conserved domains including protease cofactor, helicase, VPg, protease, and RNA-dependent RNA polymerase that illuminate its molecular functionality (Koh et al., 2001). Investigations of a Spanish isolate demonstrated that the virus's genome comprises two RNA segments with similarities to other members of the Comoviridae family, including conserved noncoding regions essential for replication (Ferrer et al., 2005). In New Zealand, BBWV-1 was diagnosed in *Tropaeolum majus* plants displaying severe mosaic and necrotic symptoms, with electron microscopy and molecular assays confirming its presence even in mixed viral infections (Ochoa-Corona et al., 2010). Comparative genomic studies have further distinguished BBWV-1 from BBWV-2, with differences in polyprotein sequences and variable homologies across isolates supporting their classification as two distinct species within the Fabavirus genus (Kobayashi et al., 2003). Metagenomic investigations in agroecosystems have also highlighted the unexpected diversity of BBWV-1, detecting it in wild nightshade populations and suggesting that non-cultivated hosts serve as important reservoirs for the virus (Rivarez et al., 2023). Advances in molecular biology have enabled the development of full-length cDNA clones of BBWV-1's genomic RNAs, and the resulting capped transcripts have successfully reproduced the infection cycle in multiple host plants under experimental conditions (Ferriol et al., 2016). Emerging high-throughput sequencing technologies have expanded the known host range of BBWV-1, revealing its presence in unconventional hosts such as *Ullucus tuberosus* and further broadening our understanding of its ecological distribution (Fox et al., 2019). Studies of Japanese isolates, particularly through complete sequencing of RNA-2, have reinforced the role of aphid-mediated

transmission and highlighted the virus's widespread geographical distribution (Kobayashi et al., 1999). Recent reports in Iran have identified BBWV-1 infecting ribwort plantain (*Plantago lanceolata*), where molecular assays on symptomatic plants have confirmed its presence, thereby extending its host list (Mehrvar et al., 2024). Overall, frequent reassortment between the two RNA segments among various populations points to a complex interplay of genetic factors that drive the evolution and spread of Broad bean wilt virus 1 (Ma et al., 2020).

3.4.3 Turnip yellows virus

Turnip yellows virus (TuYV) is a phloem-limited, aphid-transmitted polerovirus belonging to the family Solemoviridae, genus Polerovirus. It contains a single-stranded, positive-sense RNA genome of approximately 5.6 kb, organized into seven ORFs (0–2, 3a, 3–5), where ORF5 represents the most variable region among isolates (Filardo et al., 2021). TuYV is persistently transmitted, primarily by *Myzus persicae*, and infects a wide range of hosts across more than twenty plant families (Xiang et al., 2011, Slavíková et al., 2022). Early molecular studies distinguished TuYV from the closely related Brassica yellows virus (BrYV), although recombination between the two species has been documented, particularly within the P3–P5 genomic region (Buxton-Kirk et al., 2021). Later analyses further demonstrated substantial sequence variation across ORF0, ORF3a, and especially ORF5, supporting the existence of several phylogenetic groups within TuYV populations (Filardo et al., 2021). Occasional interspecies recombination, including BrYV/TuYV recombinants, has been confirmed in oilseed rape in Greece (Orfanidou et al., 2021). In terms of global spread, TuYV has been detected across all continents. A notable report came from China, where BrYV was initially differentiated as a distinct species infecting brassica crops (Xiang et al., 2011). In the Philippines, HTS-based diagnosis revealed TuYV group 2 in cabbage previously suspected to contain BrYV, confirmed by recombination analyses (Buxton-Kirk et al., 2021).Subsequent work in the UK identified TuYV as an emerging pathogen in peas, demonstrating widespread incidence across multiple regions and establishing its presence for at least a decade (Fowkes et al., 2021). TuYV was later also confirmed as a pathogen of N*arcissus*, marking its first record in ornamental species in the UK (Forde et al., 2023). In Australia, extensive HTS screening identified broad genetic diversity among isolates from canola and pulse crops, as well as the presence of TuYV group 2 in garlic for the first time (Filardo et al.,

2021, Nurulita et al., 2022). A complete genome sequence from Brazil further expanded the known geographic range, showing high similarity with Australian isolates and marking the first official Brazilian report (Greer et al., 2021). In Europe, TuYV has been shown to circulate widely in weeds and crop hosts. Field surveys in the Czech and Slovak Republics revealed infections in at least 26 weed and crop species, demonstrating the crucial role of weeds as reservoirs that sustain virus pressure in oilseed rape landscapes. Notably, *Solanum nigrum* was among weeds what was confirmed as a natural host of TuYV in these surveys (Slavíková et al., 2022), highlighting that solanaceous weeds may also contribute to the maintenance and spread of the virus within agricultural ecosystems. In Italy, TuYV was detected in *Phytolacca americana*, suggesting new ecological roles of this weed in virus maintenance (Kwak et al., 2024). Meanwhile, in Turkey, TuYV was identified in peanut (*Arachis hypogaea*), representing both the first national report and a new natural host (Karanfil, 2022). Genomic comparisons between TuYV in brassica hosts and in their aphid vectors demonstrated sequence differences between plant and aphid isolates, providing insights into virus population structure and transmission biology (Pimenta et al., 2024). TuYV was officially reported infecting rapeseed in Uruguay, supported by RT-PCR and ELISA confirmation, suggesting that the virus had likely been present for several years (Delfino et al., 2025).

3.4.4 Tobacco vein clearing virus

Tobacco vein clearing virus (TVCV) is a double-stranded DNA (dsDNA) plant pararetrovirus belonging to the genus Solendovirus within the family Caulimoviridae. Its circular dsDNA genome is approximately 7.7 kb in length and is characterized by site-specific discontinuities on both strands, a hallmark of pararetroviruses. The genome contains four open reading frames (ORFs) typical of Solendoviruses: ORF1 encoding the putative coat protein, ORF2 encoding a putative cell-to-cell movement protein, ORF3 encoding a large polyprotein that includes the conserved domains of aspartic protease, reverse transcriptase, and RNase H, and ORF4 encoding a putative trans-activator factor. These genomic and structural features clearly establish TVCV as a DNA pararetrovirus with replication dependent on reverse transcription rather than RNA intermediates, distinguishing it from RNA viruses and aligning it with other members of Caulimoviridae (Hull, 1984, Abass and Lahuf, 2023). TVCV was first described as a previously unknown caulimo-like

virus infecting the hybrid tobacco species *Nicotiana edwardsonii*. The virus produces isometric virions approximately 50 nm in diameter, composed of a 45 kDa capsid protein enclosing its 7,767 bp genome (Lockhart et al., 2000). Initial sequence comparisons demonstrated that TVCV is most closely related to Cassava vein mosaic virus (CsVMV), supporting its placement within pararetroviruses. Despite the similarity in genome organization, no serological relationship was detected between TVCV and other caulimoviruses, including Petunia vein clearing virus, even though both share certain biological traits (Lockhart et al., 2000). Biologically, TVCV exhibits an unusual transmission profile. In *N. edwardsonii* it is seed-transmitted to nearly 100% of progeny, yet it cannot be transmitted mechanically, by grafting, or by the aphid *Myzus persicae* to other *Nicotiana* species. Early hybridization studies revealed that the TVCV genome is integrated into the host nuclear DNA. Integration signals were detected in the genomes of *N. edwardsonii* and its male parent *N. glutinosa*, but not in its female parent *N. clevelandii*. Moreover, TVCV shared 78% identity with pararetrovirus-like sequences present in *N. tabacum* and showed hybridization to genomic DNA of *N. tabacum* and *N. rustica*. These findings provided some of the earliest evidence that TVCV can exist both as an episomal virus and as part of endogenous pararetroviral elements (EPRVs) embedded in host genomes. This suggested that episomal infections may originate from the activation of inherited pararetroviral integrants (Lockhart et al., 2000). Recent genomic investigations expanded the known host range of TVCV integrants (Abass and Lahuf, 2023) identified a TVCV-like EPRV integrated into the genome of *Solanum lycopersicum* in Iraq, sharing 81.60% identity with TVCV (AF190123.1). BLASTn analyses confirmed similar integrants in multiple cultivated and wild tomato accessions worldwide, representing the first Solendovirus-derived EPRV reported in tomato. Field virome studies have also detected abundant TVCV-related sequences in tomato and pepper. In Tennessee, TVCV reads were among the most prevalent in both tomato and pepper samples, with RT-PCR confirming their presence. The authors noted that some sequences may originate from expressed EPRVs, as endogenous TVCV-like elements have been reported in tomato genomes (Dias et al., 2023).

3.4.5 Potato virus M

Potato virus M (PVM) is a widely distributed plant pathogen belonging to the genus Carlavirus of the family Betaflexiviridae (Rupasov et al., 1989, Cavileer et al., 1998, Ge et al., 2014) and poses a significant threat to solanaceous crops such as potato and tomato. Initially detected in 1994 via enzyme-linked immunosorbent assays (ELISA) on potato certification samples from Idaho, the

virus was identified in both symptomatic plants exhibiting mottling, crinkling, leaf rolling, and stunting and asymptomatic hosts, leading to the recognition of a distinct strain designated PVM-ID owing to unique variations in its coat protein's amino-terminal region (Rupasov et al., 1989, Cavileer et al., 1998). Subsequent investigations expanded its reported host range to include tomato and *Chenopodium* species in northwestern India, where mixed infections with other viruses such as potato virus Y (PVY) and cucumber mosaic virus (CMV) were also observed, indicating a complex epidemiology and significant interspecies viral interactions (Chaudhary et al., 2019, Halabi et al., 2021, Chaudhary et al., 2023, Rivarez et al., 2023). Additional surveys in various regions including upstate New York and Hungary have reported PVM in wild hosts such as bittersweet nightshade (*Solanum dulcamara*), where the virus is maintained asymptomatically throughout the growing season, while studies in Southern Italy and the Czech Republic have documented its occurrence in tomato and other hosts, with certain isolates exhibiting unique transmission features such as tuber-borne spread and low-efficiency aphid transmission by *Myzus persicae* (Grieco et al., 1997, Salamon, 2006, Perry and McLane, 2011, Plchova et al., 2015). The genomic structure of PVM is characterized by a single-stranded, positive-sense RNA molecule that encodes multiple open reading frames (ORFs) responsible for replication, movement, and host interaction; detailed sequence analysis has revealed a genomic organization reminiscent of potexviruses, particularly in the arrangement of ORFs encoding the coat protein (CP) and triple gene block components (Rupasov et al., 1989, Su et al., 2017). Advanced molecular techniques such as reverse transcription-polymerase chain reaction (RT-PCR), cDNA library construction, and high-throughput sequencing have facilitated the development of an infectious full-length clone using an enhanced 35S promoter, thereby enabling detailed studies of viral replication and symptom development in experimental hosts (Flatken et al., 2008, Glasa et al., 2019). Phylogenetic analyses have classified PVM isolates into distinct evolutionary lineages including the PVM-o and PVM-d clades based on variations in critical genes such as TGB2, CP, and NABP; these studies have also revealed low genetic diversity in some populations, strong purifying selection pressures, and evidence for recent population expansion, as demonstrated by isolates from China, Iran, Ukraine and Slovakia (Ge et al., 2014, Tabasinejad et al., 2014, Mishchenko et al., 2018, Glasa et al., 2019). Moreover, PVM encodes specialized RNA silencing suppressors, notably a cysteine-rich protein (CRP) and triple gene block protein 1 (TGBp1), which inhibit both local and systemic RNA silencing, thereby enhancing viral RNA accumulation and facilitating intercellular

movement (Senshu et al., 2011). Further investigations involving Ukrainian tomato isolates have revealed high CP gene sequence identity with strains from Europe, India, and China, underscoring the virus's capacity for genetic exchange and recombination across diverse geographical regions (Mishchenko et al., 2018, Kumar et al., 2023). Detailed analyses of the molecular variability within the cysteine-rich protein region have identified up to 16 genotype groups among Iranian isolates, reflecting substantial differences in selective pressures across distinct ecological zones (Tabasinejad et al., 2014, Tabasinejad et al., 2015). Finally, comprehensive surveys in regions such as Russia have characterized the distribution and genetic variability of PVM in both potato leaves and tubers, providing valuable insights into its regional epidemiology and underscoring its widespread occurrence in global agroecosystems (Yanagisawa et al., 2021).

3.4.6 Potato virus H

Potato virus H (PVH) is a member of the genus Carlavirus within the family Betaflexiviridae that was initially discovered infecting potato crops in Inner Mongolia, China (Li et al., 2013). It possesses a single-stranded, positive-sense RNA genome of approximately 8.4 kilobases, encoding a replicase, movement proteins (the triple gene block), a coat protein, and a cysteine-rich protein (Li et al., 2013). Comparative genomic analyses reveal that PVH is markedly divergent from other carlaviruses with only 18–57% amino acid identity in its key proteins thereby substantiating its classification as a novel species. Electron microscopy has further confirmed the presence of flexuous filamentous virions approximately 570 nm in length, and serological studies indicate that PVH is immunologically distinct from related viruses (Li et al., 2013). Recent investigations have identified a highly divergent strain of PVH that exhibits only about 66% nucleotide identity with the original isolate and shows significant variation in its replicase gene, prompting proposals to refine species demarcation criteria for carlaviruses (Liu et al., 2020). In its primary host, potato, PVH infections are frequently mild or latent, producing only subtle symptoms such as slight leaf curling or faint mottling that often render field diagnosis challenging (Abouelnasr et al., 2014). Beyond potatoes, the host range of PVH has expanded to include other solanaceous plants. For instance, while pepino (*Solanum muricatum*) acts as an asymptomatic carrier, infections in tomato (*Solanum lycopersicum*) have been associated with leaf yellowing, curling, mottling, and deformed, discolored fruits; experimental inoculations have also confirmed its ability to infect

Nicotiana species, underscoring potential isolate-specific differences in host susceptibility (Xu et al., 2024). The virus is predominantly spread through vegetative propagation via infected potato tubers and mechanical transmission during routine agricultural practices, with field surveys in multiple Chinese provinces corroborating its widespread occurrence (Abouelnasr et al., 2014). Molecular surveys in South Asia, particularly in Bangladesh, have further detected PVH isolates closely related to the original strain, suggesting that the virus may be disseminated internationally through infected seed potatoes (Rashid et al., 2020). Notably, no occurrences of PVH have been reported in Europe or the Americas to date, and the European Union considers PVH an exotic quarantine pest (absent from EU, but potentially harmful) (EFSA, 2020). Field and laboratory studies additionally highlight that mixed viral infections are common in potato tubers. Various combinations encompassing PVH along with viruses such as Potato virus X, Potato virus S, Potato aucuba mosaic virus, Potato leafroll virus, and even Potato virus M have been observed, whereas viruses like Potato virus Y appear to be absent (Rashid et al., 2021).

3.4.7 Obuda pepper virus

Obuda pepper virus (ObPV) is a distinctive plant pathogen classified within the genus Tobamovirus of the family Virgaviridae, exhibiting the rigid rod-shaped morphology typical of the tobacco mosaic virus group. Its genome comprises a positive-sense single-stranded RNA of about 6.5 kb that encodes four main open reading frames a 126-kDa replication protein, a 183-kDa readthrough product, a 30-kDa cell-to-cell movement protein, and an approximately 18-kDa coat protein mirroring the classic organization found in other tobamoviruses (Ikeda et al., 1993, Padgett and Beachy, 1993). Initially described in the early 1980s in Óbuda (Budapest), Hungary, ObPV was first reported as a new pepper strain of tomato mosaic virus isolated from *Capsicum annuum*, with parallel observations from Bulgaria further supporting its distinctiveness from other TMV-like strains (Csillery et al., 1983, Stoimenova, 1984) . Subsequent molecular studies, including the cloning of a full-length cDNA, demonstrated that ObPV is infectious in plants and identified a single nucleotide substitution in the 126-kDa replicase gene as the key factor responsible for its ability to break tobacco *N*-gene resistance (Padgett and Beachy, 1993). The primary host of ObPV is *Capsicum annuum*, where infection manifests as systemic mosaic, mottling, leaf distortion, and severe stunting, often accompanied by reduced fruit size and yield (Igwegbe, 1983). Moreover,

infections in wild solanaceous weeds such as black nightshade (*Solanum nigrum*) have been reported, resulting in marked biomass reduction an observation that has even led to exploration of the virus as a potential biocontrol agent (Kazinczi et al., 2006). Notably, like other tobamoviruses, ObPV is highly stable and efficiently transmitted by mechanical means, with contaminated seeds also being implicated as a potential route of natural spread. In terms of its epidemiological footprint, although originally documented in Hungary, ObPV has been recognized as one of the more widespread pepper-infecting tobamoviruses in Europe, co-circulating with viruses such as Pepper mild mottle virus in Capsicum crops (Kumari et al., 2023).

3.4.8 Lettuce big-vein associated virus

Lettuce big vein associated virus (LBVaV) belongs to the Varicosavirus family and is one of the principal agents involved in lettuce big vein disease (LBVD). Its genome is segmented into two single-stranded RNA molecules; RNA1 is approximately 6797 nucleotides long and encodes a large L polymerase protein that shows significant homology with those of plant rhabdoviruses (Sasaya et al., 2002), while RNA2 is about 6081 nucleotides in length and contains five major open reading frames, including the coat protein gene (Sasaya et al., 2004). LBVaV is frequently detected in mixed infections with Mirafiori lettuce big-vein virus (MiLBVV), together causing symptoms such as reduced growth, mosaic discoloration, chlorotic vein banding, and leaf deformations on lettuce (Albert et al., 2019). Worldwide, LBVD has led to substantial yield losses ranging from 30% to 70% and extensive studies across various regions including Europe, the Americas, and parts of Africa have documented its incidence and genetic diversity (Hayes et al., 2006, Bernal-Vicente et al., 2018, Hernandez et al., 2020). Comparative phylogenetic analyses of LBVaV isolates from Australia, Japan, and Europe have revealed distinct clades that underscore its geographical strain differentiation (Navarro et al., 2005a, Maccarone et al., 2010). Advanced molecular techniques, including RT-PCR, molecular dot blot hybridization, and high-throughput sequencing, have been pivotal in detecting and characterizing LBVaV in symptomatic and asymptomatic plants (Navarro et al., 2004, Navarro et al., 2005b). Additional work has demonstrated that common weeds can serve as reservoirs, facilitating spread via soil-borne fungal vectors such as species of *Olpidium*, which are key to disease transmission (Navarro et al., 2005b, Pavan et al., 2008, Verbeek et al., 2013, Ochoa-Martínez et al., 2014). Population genetics studies,

as well as investigations in Turkey and Jordan, have provided further insights into the virus–vector relationships and the evolutionary pressures acting on LBVaV (Salem et al., 2020, Zelyüt and Ertunç, 2021). Moreover, outbreaks in regions such as South Africa and Brazil, along with host-range expansions to species like tomato, emphasize the virus's emerging epidemiological significance (Sanches et al., 2008, Tomašechová et al., 2021). Together, these findings supported by integrated genomic and phylogenetic analyses highlight the complex biology of LBVaV and underscore the need for continued research into its management and control (Sasaya et al., 2002, Sasaya et al., 2004).

3.4.9 *Oxybasis rubra* mitovirus 1

Mitoviruses represent an intriguing group of small RNA viruses that are vertically transmitted and occur in a broad range of hosts including fungi, plants, and animals (Jacquat et al., 2023). Among these, *Oxybasis rubra* mitovirus 1 (OxruMV1) was discovered in the transcriptome of red goosefoot (*Chenopodium rubrum*), marking its initial identification and highlighting its potential significance in plant-associated viral diversity (Nibert et al., 2018). OxruMV1 possesses an approximate 2.7 kb positive-sense RNA genome that encodes a single RNA-dependent RNA polymerase, a defining feature of mitoviruses that confirms its genetic identity. Its complete genome, deposited in GenBank under accession NC_076526, (GenBank, 2023), validates its streamlined organization and has led to its formal classification within the family Mitoviridae, specifically in the genus Duamitovirus a lineage reserved for mitoviruses infecting plants as opposed to fungi (Nibert et al., 2018). This virus replicates within host mitochondria and is maintained through vertical transmission, yet it appears to establish a largely cryptic infection in *Oxybasis rubra*, with no disease symptoms detected (Mihara et al., 2016). Furthermore, the absence of in-frame UGA codons in the RNA-dependent RNA polymerase gene underscores its adaptation to the plant mitochondrial genetic code, emphasizing the evolutionary specialization of these viruses. Phylogenetic analyses have placed OxruMV1 in a well-supported monophyletic clade alongside other plant mitoviruses, thereby reinforcing the distinct evolutionary trajectory of this virus within Mitoviridae (Alvarez-Quinto et al., 2023).

3.4.10 Broad bean wilt virus 2

Broad bean wilt virus 2 (BBWV2), belonging to the genus Fabavirus within the Secoviridae family, is a widely distributed viral pathogen that affects a variety of economically important crops, including peppers, in regions worldwide (NAKAMURA et al., 1998, Seo et al., 2017). The virus has a bipartite genome composed of two single-stranded positive-sense RNAs: RNA1 (5,960 nucleotides) and RNA2 (3,600 nucleotides). Each RNA segment encodes a single open reading frame (ORF) that is translated into a polyprotein precursor, which is then cleaved into functional proteins. RNA1 produces five proteins, including the RNA-dependent RNA polymerase (RdRp), while RNA2 generates three proteins, including the movement protein and coat proteins (Kwak et al., 2013b, Seo et al., 2017). BBWV2 is aphid-transmitted (especially by *Aphis gossypii* and *Myzus persicae*) in a nonpersistent manner and has a wide host range that spans both dicotyledonous and some monocotyledonous plants (Lee et al., 2000, Ferrer et al., 2011, Kwak et al., 2013b). Symptoms of BBWV2 infection vary by host and include mosaic patterns, chlorosis, necrotic spots, vein clearing, wilting, and plant stunting. In peppers, infection can lead to distinctive symptoms such as necrotic spots on leaves and stems, stunted growth, and apical necrosis. These symptoms have been observed in naturally infected plants and reproduced in inoculation studies (Lee et al., 2000, Kwak et al., 2013a). BBWV isolates are divided into two species: Broad bean wilt virus 1 (BBWV1) and Broad bean wilt virus 2 (BBWV2). While these species have similar genome structures and functions, their nucleotide sequence identity is relatively low, ranging from 39% to 67%. Negative selection and recombination are key factors driving this diversity (Ferrer et al., 2011). The virus can co-infect plants with other viruses such as Cucumber mosaic virus (CMV), Pepper mottle virus (PepMoV), Pepper mild mottle virus (PMMoV), and Potato virus Y (PVY), which can exacerbate disease severity in affected crops.

3.4.11 Potato virus Y

Potato virus Y (PVY) is a filamentous, non-enveloped virus from the Potyvirus genus within the Potyviridae family. It has a single-stranded, positive-sense RNA genome of approximately 9.7 kb, encoding a large open reading frame (ORF) and a smaller ORF called PIPO. Initially identified in the 1930s, PVY infects a broad range of hosts, predominantly within the Solanaceae family, and is found worldwide. PVY is spread by more than 40 aphid species, including *Myzus persicae*, through a nonpersistent transmission mechanism (Scholthof et al., 2011, Wylie et al., 2017). The

virus causes symptoms such as stunting, leaf distortion, vein clearing, necrosis, and mosaic patterns. PVY strains, including PVYO (ordinary or common strain), PVYN (necrotic strain), PVYC (potato stipple streak strain), PVYNTN (tuber necrosis strain), and PVYEU (European strain), produce different symptoms and can affect potato tubers. PVYO isolates typically cause mosaic symptoms on tobacco and potato, along with leaf drop in potatoes. PVYN isolates lead to partial or complete leaf necrosis in infected plants. The PVYC strain is primarily associated with stipple streak symptoms in potatoes. In the 1980s, new variants like PVYNTN were identified, which can cause potato tuber necrosis. PVYEU, primarily found in Europe, is associated with necrotic symptoms in some plants. PVY is globally distributed and has a significant economic impact (Scholthof et al., 2011, Wylie et al., 2017). From 2005 to 2007, PVY was the most common virus found in single infections. Mixed infections with tobacco mosaic virus (TMV) and cucumber mosaic virus (CMV) were also observed during this period. Infected plants exhibited symptoms like stunting and necrosis, while no viruses were detected in symptomless samples (Stanković et al., 2011). PVY strains infecting pepper plants have been classified into pathotypes based on the symptoms they induce, such as vein-banding or veinal necrosis, with distinct types based on resistance gene interactions (Fanigliulo et al., 2005, Moodley et al., 2014). Studies on PVY's genetic diversity have shown significant variability in its population. Sequencing of viral RNA and virus-derived small interfering RNAs (siRNAs) has provided insights into viral evolution, revealing shifts in haplotype frequencies and the role of host responses like salicylic acid (SA) signaling in influencing virus structure (Shukla et al., 1994, Kutnjak et al., 2015, Kutnjak et al., 2017).

3.4.12 Pepper cryptic virus 2

Pepper cryptic virus 2 (PCV-2) is classified as a bipartite double-stranded RNA virus within the genus Deltapartitivirus, part of the family Partitiviridae, which consists of isometric viruses with segmented dsRNA genomes. This family includes genera such as Alphacryptovirus and Betacryptovirus, known to infect plants. These viruses are effectively transmitted through pollen and seeds but are not spread via grafting or mechanical inoculation, and they lack known natural vectors. Mixed infections involving PCV-2 and other cryptoviruses or host-specific pathogenic viruses are common in pepper plants (Sabanadzovic and Valverde, 2011). The first documented case of PCV-2 infection in pepper plants was reported in China in 2015, where twenty *Capsicum*

annuum plants exhibited mosaic, crinkle, and stunting symptoms (Sun et al., 2017). Following this, the presence of PCV-2 in chili cultivars was confirmed in India through RT-PCR and partial sequencing of the coat protein gene, marking the first occurrence of this cryptovirus in Indian chili plants. Symptoms were observed in various genotypes, with some displaying prominent yellowing, while others, such as Chilli Black Megha (CBM), appeared symptomless (Saritha et al., 2016). In Europe, PCV-2 was first reported in Slovakia after testing various symptomatic sweet pepper and chili plants in 2018 and 2019. This study represented the first identification of PCV-2 in Slovakia and revealed mixed infections involving PCV-2 with other viruses, including PVY and CMV. The observed symptoms, such as mosaic patterns and leaf mottling, could not be definitively attributed to a single virus, suggesting possible synergistic interactions among these viruses (Tomašechová et al., 2019, Tomašechová et al., 2020). In Poland, high-throughput sequencing (HTS) of two symptomatic pepper samples revealed the presence of both PCV-2 and Bell pepper alphaendornavirus (BPEV), in mixed infections with other viruses, which marked the first identification of these persistent viruses in the country (Minicka et al., 2024). In Tennessee, USA, RT-PCR confirmed the presence of PCV-2 in pepper samples, which exhibited both symptomatic and symptomless plants (Dias et al., 2023). Despite the identification of PCV-2 in various regions and its association with mixed infections, it remains uncertain whether PCV-2 is the primary cause of disease symptoms, as specific symptoms directly linked to this virus have yet to be documented. Phylogenetic analysis conducted on PCV-2 revealed three distinct groups of isolates based on RNA1 and RNA2 sequences (Jo et al., 2022).

3.4.13 Bell pepper endornavirus

Bell pepper endornavirus (BPEV) (Alphaendornavirus capsici), classified within the family Endornaviridae, is a persistent double-stranded RNA virus known to infect economically important crops, particularly peppers (Okada et al., 2011). It has a genome approximately 14.7 kb in length and is transmitted through seeds but not via graft inoculation. The BPEV genome comprises a single open reading frame (ORF) that encodes a large polyprotein with several conserved functional domains. The incidence of BPEV and its associated symptoms, such as mild crinkling and chlorosis on young leaves, has been observed in various regions. Studies have reported significant virus infections in bell pepper plants, including acute viruses that lead to reduced fruit yield and quality (Valverde et al., 2019). In Tennessee, a comprehensive survey revealed BPEV as

the most abundant virus detected in field-grown tomatoes and peppers (Dias et al., 2023). In Poland, high-throughput sequencing identified BPEV in mixed infections with other viruses, confirming its prevalence in the region (Minicka et al., 2024). In Slovakia, researchers determined the complete polyprotein-coding genomic sequence of a BPEV isolate, showing nucleotide identities ranging from 86.1% to 98.6% compared to other isolates (Tomašechová et al., 2019). Similarly, transcriptome analysis in Colombia confirmed the presence of BPEV in commercial chili and bell pepper samples, marking the first report of this virus group in the country (Muñoz-Baena et al., 2017). In a separate study, a new endornavirus infecting hot peppers was identified, demonstrating high similarity to BPEV (Lim et al., 2015). BPEV's impact is evident, with severe symptoms reported in bell pepper cultivars, while commercially developed hot pepper cultivars displayed mild symptoms (Jo et al., 2022). The family Endornaviridae includes viruses that infect various hosts, and recent studies suggest the activation of viral immune silencing machinery by BPEV, indicating the potential for a novel silencing suppressor (Sela et al., 2012). Furthermore, research in the Middle East including Lebanon and Syria confirmed the presence of BPEV in sweet pepper plants, marking a significant expansion of its known geographic distribution (Abou Kubaa et al., 2024). Finally, high-throughput sequencing of symptomatic plants from Panama resulted in the assembly of the complete BPEV genome, contributing to our understanding of its genetic diversity and marking the first report of STV and BPEV in that region (Galipienso et al., 2021).

3.4.14 *Ranunculus* white mottle virus

Ranunculus white mottle virus (RWMV) (Ophiovirus ranunculi) is a member of Aspivirideae in the Ophiovirus genus. The virus was first identified in ornamental plants, with its initial discovery reported in 1990 from *Ranunculus* hybrid plants in Northern Italy, where it exhibited symptoms such as mosaic patterns and leaf distortion (Vaira et al., 1997, Vaira et al., 2002, Maria Laura, 2012). Following this, RWMV was detected in various host plants, including tomato and pepper, throughout Europe, highlighting its expanding geographic distribution. In May 2016, a co-infection involving RWMV was observed in tomato plants in Slovakia, indicating its presence alongside Lettuce big-vein associated virus (Tomašechová et al., 2021). Subsequent reports from Slovenia in 2017, 2019, and 2020 confirmed the virus in both tomato and pepper plants, marking the first detection of RWMV in these crops in Europe and emphasizing the importance of monitoring its impact (Rivarez et al., 2023) . The virus's incidence was found to be particularly

severe in pepper plants, with symptoms closely resembling pepper yellows disease, reported at 70-80% in Greece (Gavrili et al., 2024). RWMV is characterized by a multipartite genome structure, typically comprising three or four segments encapsidated separately (García et al., 2017). The full genome sequences of the four RNAs are also available from NCBI GenBank, sequenced by the DSMZ from a *Lactuca sativa* plant collected in Germany (OR879093-6). Despite its presence across various regions, the pathogenic impact of RWMV remains uncertain, primarily due to its consistent association with mixed infections and low incidence rates in symptomatic plants (Vaira et al., 2002). The virus has not been directly linked to known vectors, further complicating its management (Rivarez et al., 2023). Overall, the documentation of RWMV across multiple host species and regions underscores the necessity for further research to assess its pathogenic potential, develop sensitive molecular diagnostic tools, and implement effective monitoring strategies for its control in agricultural settings.

3.5 Detection of Plant Viruses

3.5.1 Serological and Molecular Approaches for Plant Virus Detection

The early and accurate detection of plant viruses is essential for effective disease management and prevention of economic losses. Because viral symptoms are often variable and can resemble those caused by abiotic stresses, symptom-based diagnosis alone is unreliable. Over the past three decades, the enzyme-linked immunosorbent assay (ELISA), a serology-based technique, has been widely used for virus detection (Jeong et al., 2014). ELISA is one of the most sensitive serological techniques, suitable for routine testing without requiring expensive equipment. In many plant viruses, the direct double-antibody sandwich (DAS-ELISA) method offers narrow specificity, allowing differentiation between strains or even between intact and degraded viral forms. In contrast, indirect ELISA methods detect a broader range of serologically related viruses and are often more sensitive than direct assays (Koenig and Paul, 1982). The microplate method using enzyme-labeled antibodies enables highly sensitive detection and quantification of diverse plant viruses in both purified samples and crude plant extracts. Virus concentration is determined photometrically based on color intensity, making this technique a reliable and efficient tool for both field diagnostics and research applications (Clark and Adams, 1977). However, its application has gradually declined due to limitations such as the availability and cost of virus-specific

antibodies, the need for large sample volumes, and the time required to complete the assays. To overcome these limitations, molecular techniques have been developed, providing higher sensitivity and specificity.

3.5.2 PCR-Based Techniques for Plant Virus Detection

To overcome the limitations of serological methods, molecular approaches such as the polymerase chain reaction (PCR) have been developed, offering much higher sensitivity and specificity. The polymerase chain reaction (PCR) is a simple yet powerful molecular technique that enables the exponential amplification of specific DNA sequences through *in vitro* synthesis. The process consists of three essential steps: (a) denaturation of the target DNA to separate the strands, (b) annealing of two oligonucleotide primers to the complementary regions of the single strands, and (c) extension of the primers by a thermostable DNA polymerase (Henson and French, 1993). Since its introduction, PCR has evolved into several variants, among which reverse transcriptase PCR (RT-PCR) is widely used for the detection of RNA viruses (Singh, 1998). This method enables the amplification of specific viral genomic regions, allowing rapid, precise, and cost-effective identification of diverse plant viruses, even at very low concentrations. Typical approaches to sample preparation involve the extraction of total plant nucleic acids, purification of the virus, or isolation of viral nucleic acids. These methods are often labor-intensive, involving tissue grinding, centrifugation, and the use of organic solvents or ethanol precipitation. Moreover, they typically produce larger quantities and higher purity of viral nucleic acids than are required for PCR analysis. In recent years, several simplified protocols have been developed for preparing large numbers of plant samples for PCR applications. The most straightforward approach involves adding plant tissue directly to the PCR reaction mixture; however, this method is only effective when the reaction can tolerate inhibitory compounds naturally present in plant tissues (Thomson and Dietzgen, 1995).

3.5.3 High-Throughput Sequencing (HTS) and Small RNA-Based Approaches for Plant Virus Detection

Over the past decade, high-throughput sequencing (HTS) has revolutionized plant virology by enabling the discovery of an unprecedented number of viruses, thereby expanding our understanding of viral diversity and revealing the viromes of numerous agricultural crops (Villamor et al., 2019). The technique, also known as next-generation sequencing, has become an essential tool for both the detection of known viruses and the discovery of novel ones, while also supporting studies on genetic diversity, small RNAs, gene expression, and epidemiology (Maree et al., 2018). The continuous improvement and decreasing cost of HTS platforms have facilitated their integration into plant diagnostics, surveillance, and quarantine programs; however, challenges remain in data management, bioinformatics, and the standardization of analytical protocols (Maina et al., 2024). Complementary to HTS, small RNA (sRNA) sequencing has provided valuable insights into plant–virus interactions. Plants recognize viruses through the RNA interference (RNAi) pathway, in which double-stranded viral RNA is processed into 21–24 nt small RNAs that can be reassembled *in silico* to identify the infecting virus (Santala and Valkonen, 2018). Small RNAs serve as key regulators of gene expression and play critical roles in antiviral defense, while viruses, in turn, evolve suppressors to counteract RNA silencing. Recent studies have advanced understanding of these molecular interactions and highlighted the potential of sRNA-based approaches for virus detection and plant immunity research (Deng et al., 2022).

3.6 Virus Reports in Wild Solanaceous Hosts

Wild solanaceous weeds such as *Solanum nigrum, Datura stramonium,* and *Solanum dulcamara* represent important components of agroecosystems, often acting as unnoticed reservoirs for numerous plant viruses. These species are widely distributed across different geographical regions and can harbor viruses that also infect cultivated crops, thereby playing a crucial role in the maintenance and epidemiology of viral diseases. The presence of such alternative hosts facilitates virus survival during periods when susceptible crops are absent, allowing reintroduction of infections into production fields, once favorable conditions return. Over the years, various studies conducted worldwide have reported natural infections of these weeds by several economically important plant viruses, many of which are associated with severe yield reductions in Solanaceaeous crops. The findings indicate that *S. nigrum*, *D. stramonium, and S. dulcamara* are

frequently associated with diverse plant viruses, confirming their role as natural hosts and contributors to the complex virus–host interactions within Solanaceae ecosystems.

3.6.1 GenBank-Based Reports of Plant Viruses and Viroids Where *Solanum nigrum* Served as Host

Solanum nigrum (commonly known as black nightshade) is a weed plant belonging to the Solanaceae family. This family comprises numerous genera well known for their therapeutic, nutritional, and ornamental importance. In addition to *S. nigrum*, the Solanaceae family includes several economically significant crops such as potato (*Solanum tuberosum*), tomato (*Solanum lycopersicum*), and pepper (*Capsicum spp*.), as well as ornamental species like *Petunia*, and other medicinal plants including *Atropa belladonna L.* (deadly nightshade), *Datura stramonium* L. (Jimson weed), and *Hyoscyamus niger* L. (black henbane). *Solanum nigrum*, also known by the local names Makoi or black nightshade, commonly grows as a weed in moist environments and can adapt to a wide range of soil conditions, including dry, stony, shallow, or deep soils. It is widely distributed in tropical and subtropical agroclimatic regions and can be cultivated by sowing seeds during April–May in well-fertilized nursery beds. In addition to its medicinal value, the species is also used in land reclamation due to its hardiness and adaptability. *S. nigrum* is known by different names across various regions of the world (Jain et al., 2011). It is called black nightshade or black berry nightshade in Australia; black nightshade, annual nightshade, common nightshade, or garden nightshade in Europe; black nightshade in New Zealand; and simply nightshade in South Africa (Rani et al., 2017).

Beyond its medicinal and ecological importance, *S. nigrum* has also gained considerable attention in plant virology. This species has been reported as a natural host for numerous plant viruses, often serving as a reservoir from which infections can spread to cultivated crops. Its wide distribution and ability to survive in diverse environments make it an ideal bridge host, sustaining virus populations between cropping seasons. Over the years, a variety of viruses infecting *S. nigrum* have been identified and molecularly characterized in different parts of the world. A complete compilation of molecularly documented cases where *Solanum nigrum* has served as a host for plant viruses, along with their corresponding GenBank accession numbers, has been prepared. *Solanum*

nigrum has been reported as a host for numerous plant viruses across a wide range of geographical regions, demonstrating its significant role in virus ecology and epidemiology.

This species has been identified as a natural host for members of the genus Topcuvirus in the USA (Briddon et al., 1996) and China, where Tomato pseudo-curly top virus was detected. It was also found to host several begomoviruses across different regions, including Ageratum yellow leaf curl virus and Chilli leaf curl virus in India (Venkataravanappa et al., 2023), Ageratum enation virus and Crassocephalum yellow vein virus in China, Bhendi yellow vein mosaic virus (Iqbal et al., 2023), Parthenium leaf curl virus and Papaya leaf curl virus in Pakistan, and Papaya leaf crumple virus in India (Kumar et al., 2024), Solanum leaf curl virus, Whitefly-transmitted Indian begomovirus, and Cotton leaf curl virus in India (Biswas et al., 2025). Moreover, Tomato yellow leaf curl virus, a widespread begomovirus, was reported in *S. nigrum* from multiple countries, including Cyprus (Papayiannis et al., 2011), Tunisia (Mnari-Hattab et al., 2014), Mauritius (Lobin et al., 2023), Portugal (Fiallo-Olivé et al., 2019), Morocco (Belabess et al., 2015), India (Ansar et al., 2021) as well as from China, Pakistan, and Tunisia (direct submissions in GenBank). Additionally, *S. nigrum* has been reported as a host for cytorhabdoviruses in China, where Tomato yellow mottle-associated virus was identified (Li et al., 2023), and for nucleorhabdoviruses in Greece, where Eggplant mottled dwarf virus was identified (Pappi et al., 2016). Infections caused by tospoviruses have been recorded in India, where Groundnut bud necrosis virus was found (Amruta et al., 2020), and in China, where Tomato spotted wilt virus was detected. Furthermore, an ophiovirus, Ranunculus white mottle virus, was reported in Slovenia (Rivarez et al., 2023).

A complete summary of reported virus and viroid cases where *S. nigrum* served as a host, including information on the viral genus, virus name, abbreviation, GenBank accession number, geographical origin and citation is provided in Table 1 and Table 2.

Table 1: Plant viruses and viroids reported in *Solanum nigrum* as a weed host

Genus	Virus name	Abbr.	Genbank accession number	Geo. origin	Citation
Topcuvirus	Tomato pseudo-curly top virus	TPCTV	NC_003825, X84735	USA	(Briddon et al., 1996)
			OR460679-81, OR428173-75	China	Zhang,K. (direct submission)
Begomovirus	Ageratum yellow leaf curl virus	AYLCV	KJ028213	India	Kumar,J. (direct submission)
	Ageratum enation virus	AEV	OK044277	China	Zhong,J. (direct submission)
	Bhendi yellow vein mosaic	BYVMV	OL436195, OL436204-05	Pakistan	(Iqbal et al., 2024)
	Chilli leaf curl virus	ChiLCV	OL687162, OL687164	India	(Venkataravanappa et al., 2023)
	Crassocephalum yellow vein virus	CRAYVV	MK626675	China	Zhao,L. (direct submission)
	Cotton leaf curl virus	CLCuV	KJ028212	India	(Biswas et al., 2025)
	Papaya leaf curl virus	PaLCuV	OR041641	Pakistan	Ullah,A. (direct submission)
	Parthenium leaf curl virus	/	OR041651		
	Papaya leaf crumple virus	PaLCuV	KJ028210	India	(Kumar et al., 2024)
	Solanum leaf curl virus	/	JN009667	India	Marwal,A. (direct submission)
	Tomato yellow leaf curl virus	TYLCV	OM022935-37	Pakistan	Sattar,M.N. (direct submission)
			AJ620187-88		Briddon,R.W. (direct submission)
			AM849548		Tahir,M. (direct submission)
			OM102559		Ilyas,M. (direct submission)
			KY112754	India	Ansar,M. (direct submission)
			MW724714		Sharma,J. (direct submission)
			MH465599, MH465600		(Ansar et al., 2021)
			KJ028211		Kumar,J. (direct submission)
			PX252061		Nagendran,K. (direct submission)
			OK128315	China	Zhong,J. (direct submission)
			FN822928	Cyprus	(Papayiannis et al., 2011)
			GU322874	Tunisia	(Mnari-Hattab et al., 2014)
			OK391173	Mauritius	(Lobin et al., 2023)
			KU958507, KU958510	Tunisia	Zammouri,S. (direct submission)
			JN859138	Portugal	(Fiallo-Olive et al., 2019)
			LN846597	Morocco	(Belabess et al., 2015)
	Whitefly-transmitted Indian begomovirus	/	DQ339123, DQ339130	India	Sivalingam,P.N. (direct submission)
Cytorhabdovirus	Tomato yellow mottle-associated virus	TYMaV	MW527091	China	(Li et al., 2023)
Nucleorhabdovirus	Physostegia chlorotic mottle virus	PhCMoV	OQ318171	Netherlands	(Temple et al., 2024)
	Eggplant mottled dwarf virus	EMDV	HG794537, HG794538	Greece	(Pappi et al., 2016)
Tospovirus	Groundnut bud necrosis virus	GBNV	KY490685-87	India	Laxmidevi,V. (direct submission)
			KY491041, KY491043-45, KX244329, KX244332, KX244334, KX244337-40		(Amruta et al., 2020)
	Tomato Spotted Wilt Virus	TSWV	PV637928	China	Zhong,J. (direct submission)
Ophiovirus	Ranunculus white mottle virus	RWMV	OL472203-06	Slovenia	(Rivarez et al., 2022)

Furthermore, the list of viruses hosted by *Solanum nigrum* continues with fabaviruses. Infections by fabaviruses were reported in France, where Broad bean wilt virus 1 was detected (Ma et al., 2020), and in China, where Broad bean wilt virus 2 was reported. This species was also identified as a host for nepoviruses, specifically Artichoke yellow ringspot virus in Greece (Karapetsi et al., 2021), and for torradoviruses, represented by Tomato torrado virus in Spain (Alfaro-Fernández et al., 2010). In addition, *S. nigrum* was reported to host a mandarivirus, namely Citrus yellow vein clearing virus, in Turkey. Reports also include its role as a host for carlaviruses, such as Potato virus S in Iran (Hosseini and Salari, 2017) and Potato virus M in India, and for alfamoviruses, including Alfalfa mosaic virus detected in China, Iran and Spain (Bergua et al., 2014).

Moreover, *S. nigrum* has been associated with cucumoviruses, particularly Cucumber mosaic virus, reported from Tunisia (Khaled-Gasmi et al., 2020), India, and China.

Infections caused by criniviruses have been documented in Greece, where Cucurbit yellow stunting disorder virus was found, and in Saudi Arabia, with Tomato chlorosis virus was identified in *S. nigrum* (Shakeel et al., 2017). Similarly, poleroviruses were detected in Saudi Arabia, represented by Cucurbit aphid-borne yellows virus (Amer et al., 2025), and in India, with Pepper vein yellows virus reported (Knierim et al., 2013).

The potyvirus group is represented by a diverse set of viruses infecting *S. nigrum*, including Chilli veinal mottle virus in China and India (Nadu et al., 2009); Moroccan watermelon mosaic virus in Turkey; Potato virus Y reported in China (Fan et al., 2021), Tunisia, India, France (Moury et al., 2002, Moury et al., 2014), and Syria (Chikh Ali et al., 2010); Pepper veinal mottle virus in Taiwan (Cheng et al., 2011); Solanum nigrum potyvirus in India; Tobacco vein banding mosaic virus in China (Bi et al., 2020); Watermelon mosaic virus in Spain (Peláez et al., 2021); and Wild tomato mosaic virus in China (Zhang et al., 2019). Also *S. nigrum* was identified as a host for several tobamoviruses, including Cucumber green mottle mosaic virus in Australia (Mackie et al., 2023), Tomato mosaic virus in Kenya and India, Tomato brown rugose fruit virus in Jordan (Salem et al., 2022), Youcai mosaic virus in China, and Yellow tailflower mild mottle virus in Australia (Xu et al., 2022). For Alphanucleorhabdoviruses, Physostegia chlorotic mottle virus was recorded in Netherlands (Temple et al., 2024).

Beyond viruses, *S. nigrum* has also been recognized as a host for viroids, specifically members of the genus Pospiviroid, including Chrysanthemum stunt viroid in Russia (Matsushita et al., 2021) and Potato spindle tuber viroid in Australia (Mackie et al., 2016), (Table 2).

Table 2: Plant viruses and viroids reported in *Solanum nigrum* as a weed host

Fabavirus	Broad bean wilt virus 1	BBWV1	MN216346-55/59/62/64/69-83/88	France	(Ma et al., 2020)
	Broad bean wilt virus 2	BBWV2	OP785725-26	China	Qiu,Y. (direct submission)
Nepovirus	Artichoke yellow ringspot virus	AYRSV	MT228909	Greece	(Karapetsi et al., 2020)
Torradovirus	Tomato torrado virus	ToTV	GQ397371/74/86/93/402/409/419/427/436/445	Spain	(Alfaro-Fernandez et al., 2010)
Mandarivirus	Citrus yellow vein clearing virus	CYVCV	KU669036	Turkey	Onelge,N. (direct submission)
Carlavirus	Potato virus S	PVS	MF773983	Iran	(Hosseini et al., 2017)
	Potato virus M	PVM	MH038049	India	Chaudhary,P. (direct submission)
Alfamovirus	Alfalfa mosaic virus	AMV	PP179213-215	China	Chen,Z. (direct submission)
			KM655873-74	Iran	Arabshah,Z. (direct submission)
			JQ691165-67, JQ691225-27, JQ691285-87, JQ691345-47	Spain	(Bergua et al., 2014)
Cucumovirus	Cucumber mosaic virus	CMV	MN639221	Tunisia	(Khaled-Gasmi et al., 2020)
			MH038051	India	Chaudhary,P. (direct submission)
			MG014232	China	Geng,G. (direct submission)
Crinivirus	Cucurbit yellow stunting disorder virus	CYSDV	LT992900	Greece	Orfanidou,C. (direct submission)
	Tomato chlorosis virus	ToCV	KT888064	Saudi Arabia	(Shakeel et al., 2017)
Polerovirus	Cucurbit aphid-borne yellows virus	CABYV	MH192389	Saudi Arabia	(Amer,M.A et al., 2025)
	Pepper vein yellows virus	PeVYV	JX427531	India	(Knierim et al., 2013)
Potyvirus	Chilli veinal mottle virus	ChiVMV	MG674070-72	China	Yang,C. (direct submission)
			GU294786-88	India	(Manoranjitham et al., 2009)
			ON838425-26	China	Wan,Q., (direct submission)
	Moroccan watermelon mosaic virus	MWMV	MW362133	Turkey	Yesil,S. (direct submission)
	Potato virus Y	PVY	MN833214	China	(Kai et al., 2021)
			MH644177	Tunisia	Tayahi,M. (direct submission)
			MH208451	India	Chaudhary,P. (direct submission)
			KF670578/586/588	France	(Moury et al., 2013)
			AB461465-66/87	Syria	(Ali et al., 2010)
			AB295475	Syria	(Ali et al., 2007)
			AJ439544	France	(Moury et al., 2002)
	Pepper veinal mottle virus	PVMV	FJ617225	Taiwan	(Cheng et al., 2011)
	Solanum nigrum potyvirus	/	AJ609501	India	Mehra,A. (direct submission)
	Tobacco vein banding mosaic virus	TVBMV	MN331841	China	(Bi et al., 2020)
			PP908787	China	Feng,Y. (direct submission)
	Watermelon mosaic virus	WMV	MN814366-68	Spain	(Pelaez et al., 2021)
	Wild tomato mosaic virus	WTMV	MH807178	China	Zhang L. (direct submission)
			MK070541	China	(Shang et al., 2019)
			PP854832	China	Chen,Z. (direct submission)
Tobamovirus	Cucumber green mottle mosaic virus	CGMMV	OQ198376	Australia	(Mackie et al., 2023)
	Tomato mosaic virus	ToMV	PP869351, PP885707, PP885709	Kenya	Kirasi,P.M. (direct submission)
			KX424990	India	Jamuna,S. (direct submission)
	Tomato brown rugose fruit virus	ToBRFV	OP009341-42	Jordan	(Salem et al., 2022)
	Youcai mosaic virus	YoMV	OR261028-030	China	Gu,X.T. (direct submission)
	Yellow tailflower mild mottle virus	YTMMV	ON733061-86, ON733090-92	Australia	(Xu et al., 2022)
Pospiviroid	Chrysanthemum stunt viroid	CSVd	LC523688-89	Russia	(Matsushita et al., 2021)
	Potato spindle tuber viroid	PSTVd	ON478339-47	Russia	Mironenko,N.V., (direct submission)
			KP454037, KP454041, KJ857498	Australia	(Mackie et al., 2016)

3.6.2 GenBank-Based Reports of Plant Viruses and Viroids Where *Datura stramonium* Served as Host

Datura stramonium L., commonly known as jimsonweed, is a wild-growing species belonging to the Solanaceae family. It is a cosmopolitan plant, widely distributed and easily accessible across various ecosystems. The species is well known for producing a range of toxic tropane alkaloids, including atropine, hyoscyamine, and scopolamine (Gaire and Subedi, 2013), which make it this weed relevant also for pharmacological and toxicological applications. The genus *Datura*

(Solanaceae) encompasses several well-known solanaceous plants, sharing phylogenetic proximity with major crops such as potato, tomato, pepper, and even coffee. The classification of species within the *Datura* genus is largely based on genetic markers, reflecting its remarkable degree of intraspecific variation, likely driven by frequent mutations and wide ecological adaptation. This genus exhibits a broad distribution, occurring with high abundance in temperate, tropical, and subtropical regions. All parts of *D. stramonium* are highly toxic to humans and other mammals due to its alkaloid content (Mukhtar et al., 2019). Beyond its toxicological significance, *D. stramonium* also holds phytopathological importance, as it can act as a natural reservoir and host for a wide range of plant viruses. Several studies have demonstrated its susceptibility to infection by viruses belonging to different genera and families. Specifically, *Datura stramonium* has been reported as a host for begomoviruses in several countries, including Venezuela, where Datura leaf distortion virus was identified (Fiallo-Olivé et al., 2013). Tomato yellow leaf curl virus was detected in Iraq; Sudan (Mohammed et al., 2018); India (Saha et al., 2014); China (Dong et al., 2007); Iran (Hosseinzadeh et al., 2014); and Cyprus (Papayiannis et al., 2011). It was also found to serve as a host for tospoviruses in three different countries: in Brazil, where both Groundnut ringspot virus and Tomato chlorotic spot virus were reported (Bertran et al., 2011, de Oliveira et al., 2022); in the United States, where Tomato spotted wilt virus and Tomato chlorotic spot virus were detected (Webster et al., 2013, Marshall, 2016); and in Spain, where Tomato spotted wilt virus was identified (Debreczeni et al., 2011). In addition to these cases, *D. stramonium* was also reported to host viruses from five other genera, including criniviruses in Greece, where Cucurbit yellow stunting disorder virus was identified, and in South Africa, where Tomato chlorosis virus was detected; potyviruses in India where *Datura stramonium* potyvirus was identified, China; Tobacco vein banding mosaic virus, and Italy where Henbane mosaic virus was detected (Pecman et al., 2018); necroviruses in the United Kingdom where Tobacco necrosis virus was reported; tobamoviruses in Iran where Tomato brown rugose fruit virus was recorded; and turncurtoviruses also in Iran where Turnip curly top virus was reported.

In contrast to *Solanum nigrum*, according to NCBI, no records have yet described *D. stramonium* as a host for viroids. Nonetheless, the frequent detection of diverse plant viruses in this species highlights its potential role as a natural virus reservoir, possibly contributing to the epidemiology and spread of viral diseases among cultivated solanaceous crops. A complete summary of reported

virus and viroid cases where *D.stramonium* served as a host, including viral genus, virus name, abbreviation, GenBank accession number, geographical origin, and citation is provided in Table 3.

Table 3: Plant viruses and viroids reported in *Datura stramonium* as a weed host

Genus	Virus name	Abbr.	Genbank accession number	Geo. origin	Citation
Begomovirus	Datura leaf distortion virus	/	NC_018715/17, JN848773-74	Venezuela	(Fiallo-Olive et al., 2013)
	Tomato yellow leaf curl virus	TYLCV	OQ595415-417	Iraq	Owaid,S.M. (direct submission)
			MG868938	Sudan	(Mohammed et al., 2018)
			JN676054	India	(Saha et al., 2013)
			OM677619, OM721652-54, OM743926-30, ON307484	China	Hao,H. (direct submission)
			KC106635-47	Iran	(Hosseinzadeh et al., 2014)
			FR682612	Cyprus	(Papayiannis et al., 2011)
			EF011559-61	China	(Dong et al., 2007)
Tospovirus	Groundnut ringspot virus	GRSV	MW629022	Brazil	(Oliveira et a., 2022)
	Tomato spotted wilt virus	TSWV	KU179548-49	USA	(Marshall et al., 2016)
			HQ537114	Spain	(Debreczeni et al., 2011)
	Tomato chlorotic spot virus	TCSV	KC969451-52/60-61/70-71	USA	(Webster et al., 2018)
			HQ700667	Brazil	(Bertran et al., 2011)
Crinivirus	Cucurbit yellow stunting disorder virus	CYSDV	LT992897	Greece	Orfanidou,C. (direct submission)
	Tomato chlorosis virus	ToCV	KT989862	South Africa	Moodley,V. (direct submission)
Potyvirus	Datura stramonium potyvirus	/	AJ783710	India	Singh,M.K. (direct submission)
	Tobacco vein banding mosaic virus	TVBMV	ON924220	China	Knierim,D. (direct submission)
	Henbane mosaic virus	HMV	MH779473	Italy	(Pecman et al., 2018)
Necrovirus	Tobacco necrosis virus	TNV	OL311682	UK	Knierim,D. (direct submission)
Tobamovirus	Tomato brown rugose fruit virus	ToBRFV	OM501085	Iran	Salehzadeh,M. (direct submission)
Turncurtovirus	Turnip curly top virus	TCTV	MF536416	Iran	Kamali,M. (direct submission)

3.6.3 GenBank-Based Reports of Plant Viruses and Viroids Where *Solanum dulcamara* Served as Host

Solanum dulcamara (bittersweet or climbing nightshade) is one of the few Solanaceae species native to Europe. As a common and widely distributed weed, it is highly adaptable to diverse ecological niches, ranging from moist woodland edges to riparian zones and agricultural areas. *S. dulcamara* has long been recognized as an alternative host for numerous plant pathogens and pests responsible for major diseases in solanaceous crops, particularly potato pathogens such as *Phytophthora infestans*. Interestingly, while this species can harbor various pathogens, it is also considered a potential source of resistance genes, making it valuable for breeding and plant protection programs. Despite its ecological significance and genetic potential, *S. dulcamara* has remained underexplored at the genomic level. However, with the advent of next-generation sequencing technologies, recent efforts have sought to accelerate research on this non-model species and better understand its genetic diversity and plant–pathogen interactions (D'Agostino et

al., 2013). Beyond its role in fungal and bacterial pathosystems, *S. dulcamara* has also been found to interact with plant viruses, serving as a natural virus reservoir in certain cases. Although viral reports involving this weed are limited compared to other solanaceous hosts, its susceptibility to viral infection indicates potential epidemiological importance. To date, all documented cases where *S. dulcamara* has been reported as a host concern infections by members of the Carlavirus genus, specifically Potato virus M (PVM) which was detected in the United States in 2011 (Perry and McLane, 2011). This finding emphasizes the potential of *S. dulcamara* to act as a viral reservoir. Unlike *Solanum nigrum*, which has been reported to host certain viroids such as Pospiviroid species, *S. dulcamara* has not been found to serve as a host for any viroids to date. This distinction further highlights the species-specific interactions between solanaceous weeds and different groups of plant pathogens. A complete summary of recorded virus–host associations of *S. dulcamara* including virus genus, virus name, abbreviation, GenBank accession number, geographical origin, and references is presented in (Table 4) below.

Table 4: Plant viruses and viroids reported in *Solanum dulcamara* as a weed host

Genus	Virus name	Abbr.	Genbank accession number	Geo. origin	Citation
Carlavirus	Potato virus M	PVM	HQ446853	USA	(Perry et al., 2011)

4. MATERIAL AND METHODS

4.1 Sample collection in Keszthely

In 2022, the first field study in Keszthely (K2022) focused on asymptomatic weed plants growing naturally around cultivated crops. Sampling was carried out in two fields (Field I and Field II). In field I, we sampled *Solanum nigrum* and *Datura stramonium*, which naturally emerged among pepper, eggplant, and tomato crops. Five samples were collected from each plant, and the sampling was performed on leaves or flowery shoots (Table 8). On field II we sampled five *S. nigrum* plants, growing in an area previously used for wheat and potato cultivation, and the same sampling approach was applied.

In 2023, the Keszthely field study (K2023) was extended to include symptomatic weeds and two additional species, again sampled from two fields (Field III and Field IV), following the same strategy as in K2022 (Figure 6). Field III included *S. nigrum* with ten samples (Figure 4), *D. stramonium* with ten samples, and *Brassica napus* with three samples, with leaves, flowery shoots, fruits, or seeds collected depending on the plant (Table 9). Field IV focused on *Solanum dulcamara*, from which eight plants were sampled, including leaves, flowery shoots, and fruits (Table 9).

In *Solanum nigrum* of K2023 from Field III, observed symptoms included leaf curl, mutations, leaf deformation, uneven leaves, dwarfism in young leaves, purple anthocyanin accumulation, and the presence of holes on leaves. Some plants exhibited combinations of these symptoms, such as leaf curl with dwarfism or uneven leaves with holes (Figure 2).

Figure 2. Representative images of *S. nigrum,* S3: 1–10, K2023, showing observed virus-related symptoms.

In the *Datura stramonium* samples from field III, symptoms were also highly variable and included uneven leaves, delayed flowering (T4), flower deformation, brown spots on leaves and seeds, leaf curl, chlorosis, drying flowers, yellow flowers, and deformed or yellowish fruits. Several plants displayed multiple concurrent symptoms (Figure 3).

Figure 3. Representative images of *D. stramonium,* D2: 1–10, K2023, showing observed virus-related symptoms.

In *Brassica napus* from Field III, most plants were asymptomatic, with only occasional leaf holes or insect damage (e.g., by *Phylliades* spp.) (Figure 4).

Figure 4. Representative images of *B. napus,* B: 1–3, K2023, showing observed virus-related symptoms.

In *Solanum dulcamara* from Field IV, symptoms ranged from chlorosis and leaf deformation to holes, edge anthocyanin, brown spots, necrosis, and flower or fruit damage, some of which were associated with insect activity (Figure 5).

Figure 5. Representative images of *S. dulcamara,* B: 1–3, K2023, showing observed virus-related symptoms.

4.2 Sample collection in Kosovo

Symptomatic and asymptomatic potato, tomato, and pepper plants were collected during the summer of 2023 from different locations in Kosovo (Ko2023) (Figure 6). A total of 30, potentially virus-infected symptomatic samples were collected from four regions: Pestovë, Barilevë, Bradash, and Gjurakoc. For each crop species, four symptomatic plants were selected and sampled for virome analysis. Potato samples (cv. Agria) were collected from Pestovë and Barilevë. Tomato samples included the traditional cultivar "Shijaka" from Bradash and Gjurakoc, as well as cultivar "Belle" from Barilevë. Pepper plants were sampled in Barilevë and Bradash. In Barilevë, the cultivar "Somborka," grown from commercially purchased seeds, was cultivated following tomato as the preceding crop. Weed control relied on herbicide application, resulting in approximately 3% weed cover. In Bradash, the pepper cultivar "Shorok Shari" (Babure) was grown in open fields using seedlings produced through the traditional Albanian substrate-based method. Tomato was also the preceding crop at this location, and herbicide-based management reduced weed cover to about 5%.

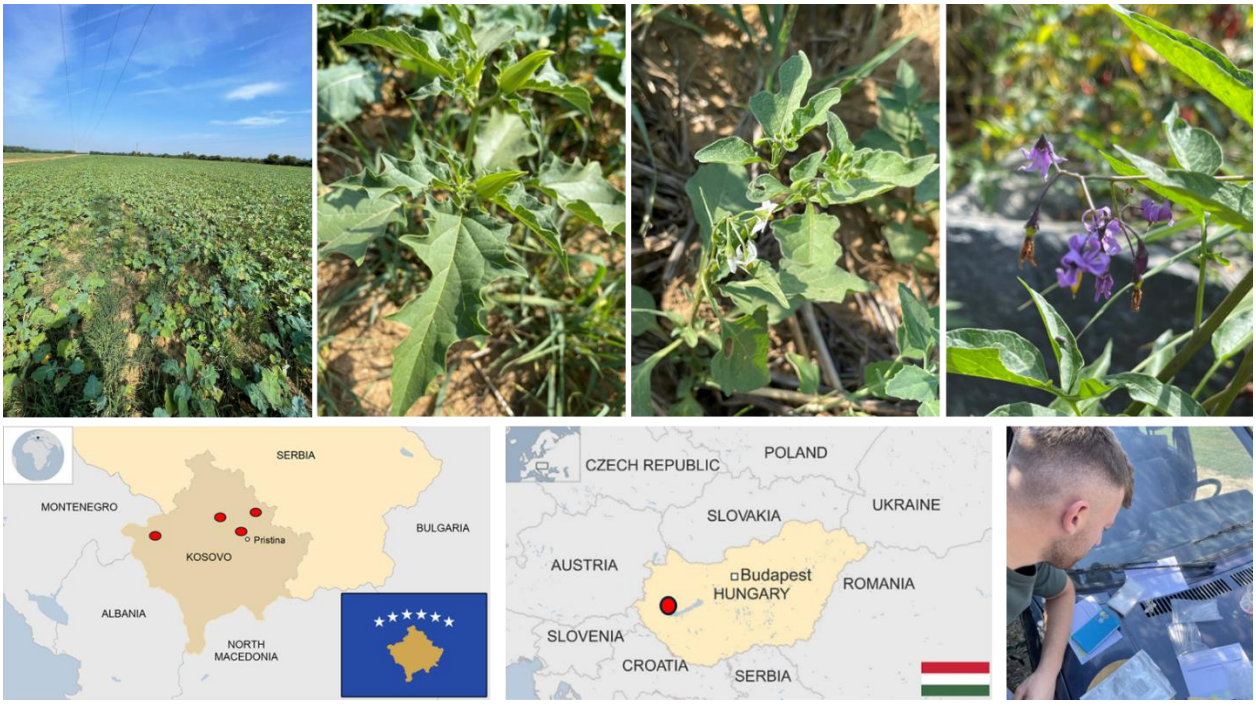

Figure 6. Author's images documenting some of the sampled fields, along with maps illustrating the study areas in Kosovo and Keszthely, Hungary

4.3 RNA Isolation

4.3.1 Phenol-chloroform extraction method

Total RNA was extracted using the phenol-chloroform extraction method, with all procedures carried out on ice to preserve RNA integrity. The extraction buffer was freshly prepared by combining 7 ml sterile water, 1 ml of 10× elution buffer (Tris-HCl, pH 8.5), and 2 ml Sodium Dodecyl Sulfate (10% SDS). Initially, 2–3 leaf pieces originating from 2–3 leaves of the same plant were homogenized using a mortar and pestle. A volume of 650 µL of the prepared extraction buffer was then added to the homogenate, which was subsequently transferred into labeled Eppendorf tubes containing 600 µL of phenol and immediately placed on ice. The samples were vigorously vortexed and centrifuged at 15,000 rpm for 5 minutes at room temperature. In the next step, 600 µL of phenol-chloroform:isoamyl alcohol (24:1) was added to fresh, labeled tubes kept on ice. The supernatant from the previous centrifugation step was carefully pipetted into these tubes, followed by vortexing and centrifugation at 15,000 rpm for 5 minutes. This step was repeated using 600 µL of chloroform to further purify the sample.

After the final centrifugation, the supernatant was transferred to new tubes containing 20 µl of 4 M sodium acetate and 1 ml of 96% ethanol, pre-prepared and kept on ice. To promote nucleic acid precipitation, these tubes were gently inverted several times and incubated on ice for 15 minutes before centrifugation at 15,000 rpm for 10 minutes. After centrifugation, the supernatant was discarded carefully to retain the visible white nucleic acid pellet. The pellet was washed with 1 mL of 70% ethanol, followed by centrifugation at 15,000 rpm for 3 minutes at room temperature. Residual ethanol droplets were removed, and the pellet was air-dried. The resulting total nucleic acids (TNA) were dissolved in 30 µL of sterile water by gentle vortexing for a few seconds. The TNA solutions were then stored at –70 °C until further use.

Total nucleic acids were checked by running an aliquot on a 1.2% agarose gel after denaturation with a buffer mix (2 µl sample, 3 µl water, 5 µl formamide denaturing buffer, FDE) at 65°C for 5 minutes to ensure proper strand separation.

4.3.2 TRIzol extraction method

For peppers only, RNA was isolated exclusively using TRIzol reagent. Following sample collection, leaf tissue (2–3 pieces from 2–3 leaves of the same plant) were homogenized in a grinder with 1 mL TRIzol reagent and vortexed to ensure thorough lysis. To the homogenate, 200 µL chloroform (without isoamyl alcohol or other additives) was added, and samples were vortexed vigorously for 15 s, then incubated on ice for 10–15 min. Samples were centrifuged at 12,000 rpm for 15 min at 4 °C to achieve phase separation, and the upper aqueous phase was carefully transferred to a fresh tube. RNA was precipitated by adding 500 µL isopropanol and gently inverting the tube several times, followed by centrifugation at 12,000 rpm for 10 min at 4 °C. The resulting RNA pellet was washed with 1 mL 70% ethanol and centrifuged at 7,500 rpm for 10 min at 4 °C. The supernatant was discarded, and the pellet was air-dried for 5–8 min, avoiding complete drying to preserve solubility, then resuspended in 30–50 µL nuclease-free water with gentle vortexing. RNA was stored at –70 °C, and integrity was confirmed by running a small aliquot on a 1.2% agarose gel after denaturation at 65 °C for 5 min.

4.4 Total Nucleic Acid Preparation and RNA Sequencing (RNA-Seq)

To ensure sufficient data quality, RNA extractions from the same plants within each field were combined. For each plant, two independent RNA extractions were performed and subsequently pooled, resulting in a single RNA sample per individual. Pooling was then further extended across individuals, first generating a representative pool of all individuals of each species and then producing one large pool of all contaning 15µl in K2022, 20µl in K2023 and 15µl in Ko2023 (Table 5), which were subsequently sent for sequencing.

This pooling strategy helped to ensure that the final samples contained sufficient RNA from all individuals, providing a balanced and reliable representation of each dataset for high-quality sequencing.

Table 5. Pooling strategy of field samples

	Field	Name of the sampled	TNA	Species pool			Large Pool
K2022	**I**	***S. nigrum***	S1/1	1µl	5µl	S1/pool	K2022 big pool
			S1/2	1µl			
			S1/3	1µl			
			S1/4	1µl			
			S1/5	1µl			
		D. stramonium	D1	1µl	5µl	D/pool	
			D2	1µl			
			D3	1µl			
			D4	1µl			
			D5	1µl			
	II	***S. nigrum***	S2/1	1µl	5µl	S2/pool	
			S2/2	1µl			
			S2/3	1µl			
			S2/4	1µl			
			S2/5	1µl			

	Field	Name of the	TNA	Species pool			Large
Ko2023		*Solanum tuberosum*	Po1	5µl	5µl	Po/pool	Ko 2023 big pool
			Po2	5µl			
			Po3	5µl			
			Po4	5µl			
		Solanum lycopersicum	T1	5µl	5µl	T/pool	
			T2	5µl			
			T3	5µl			
			T4	5µl			
		Capsicum annuum	Pe1	5µl	5µl	Pe/pool	
			Pe2	5µl			
			Pe3	5µl			
			Pe4	5µl			

	Field	Name of the sampled plant	TNA	Species pool			Large Pool
K2023	**III**	***S. nigrum***	S3/1	1µl	5µl	S3/1 pool	K2023 big pool
			S3/2	1µl			
			S3/3	1µl			
			S3/4	1µl			
			S3/5	1µl			
			S3/6	1µl			
			S3/7	1µl			
			S3/8	1µl			
			S3/9	1µl			
			S3/10	1µl			
		D. stramonium	D2/1	1µl	5µl	D2/pool	
			D2/2	1µl			
			D2/3	1µl			
			D2/4	1µl			
			D2/5	1µl			
			D2/6	1µl			
			D2/7	1µl			
			D2/8	1µl			
			D2/9	1µl			
			D2/10	1µl			
		Brassica napus	B1	1µl	5µl	B/pool	
			B2	1µl			
			B3	1µl			
	IV	***Solanum dulcamara***	Sd1	1µl	5µl	Sd/pool	
			Sd2	1µl			
			Sd3	1µl			
			Sd4	1µl			
			Sd5	1µl			
			Sd6	1µl			
			Sd7	1µl			
			Sd8	1µl			

4.4.1 DNase treatment prior to RNA-seq

Prior to RNA sequencing, the pooled total nucleic acid (TNA) samples were subjected to DNase treatment to remove any residual genomic DNA. DNase digestion was performed using RNase-free DNase I (Thermo Fisher Scientific) following the manufacturer's instructions. After treatment, the resulting high-quality, DNA-free RNA samples were submitted for ribodepleted RNA-seq. Sequencing was carried out by NOVOGEN using the Illumina platform, generating 150 bp paired-end reads optimized for ncRNA-focused analyses.

4.5 Preparation of Small RNA Libraries

4.5.1 Isolation of the sRNA Fraction from Total RNA

Gel-based isolation of the small RNA fraction prior to library preparation is crucial for obtaining high-quality reads. For this, we utilized the TruSeq® Small RNA Library Prep Kit from Illumina. The objective of this protocol is to ligate adapters to both ends of the RNA molecule, followed by reverse transcription and amplification to create a cDNA library. A subsequent gel purification step prepares the library for clustering and sequencing. The TruSeq® Small RNA Library Prep Kit offers fast and efficient sample preparation, allowing direct small RNA library generation from total RNA. Its streamlined workflow enables cost-effective studies of small RNA transcripts across all species. The kit supports multiplexed sequencing and analysis using 48 unique indexes, and facilitates microRNA (miRNA) and small RNA discovery and profiling. The six-base indexes distinguish samples within a single flow cell lane, while the incorporation of RNA 3' adapters targets small RNAs and miRNAs generated by Dicer or other RNA-processing enzymes. Indexes are added during PCR amplification, which minimizes ligation bias and ensures accurate miRNA expression measurement.

4.5.2 Small RNA library preparation

Library preparation for Ilumina sequencing is based on the use of the Trueseq small RNA kit of Illumina. According to the kit description libraries can be prepared from 1µg total RNA; however, more reads with higher quality can be gained if the library is prepared from gel-purified small RNA fractions prepared from 10-30µg total RNA. While the quality of the reads depends on the quality of RNA, the number of reads (depth for sequencing) correlates with the sequencing equipment used and the number of combined libraries. On the average, HiSeq produces 140 million reads/cartridge, which allows to combine several libraries in a single sequencing unit. During library preparation 5’ and 3’ adapters are ligated to the initial small RNAs. Indexes are positioned on the reverse PCR primers as a stretch of 6 different bases. During sequencing the sequence of this index is determined and reads are sorted on this basis.

4.5.3 Purification of sRNA fraction from extracted RNA

For isolating small RNAs, we prepared an 8% TBE denaturing polyacrylamide gel containing urea and pre-ran the gel at 100 V for 30 minutes. Before loading, we washed the wells with 1x TBE buffer. Next, we mixed 20 µg of extracted total RNA with an equal volume of FDE (FDE is not just a dye; it also contains formaldehyde, which aids in denaturing the samples) in a microcentrifuge tube, denatured the sample at 65°C for 20 minutes, then cooled it on ice and briefly centrifuged. The samples were loaded, and the gel was run at 50 V until the samples entered the gel from the wells. Afterward, we ran the gel at a constant voltage of 100 V for 1 hr 30 mins, until the bromophenol blue dye reached the bottom of the gel and it is crucial to ensure that the dye does not run out, as the small RNAs are located just above this level. After disassembling the gel apparatus, the entire gel was stained by soaking in 60 mL of 1x TBE buffer containing 3 µL of 0.5 µg/mL ethidium bromide for 5 minutes, using separate containers for each gel to avoid cross-contamination. The gel was then visualized on a UV transilluminator (the Bio-Rad ChemiDoc Imaging system). The desired small RNA fraction (typically 15-30 nt, just above the bromophenol blue zone) was excised with a sterile blade. The gel pieces were placed in a sterile 0.5 mL microcentrifuge tube, which had been punctured 3-4 times with a 21-gauge needle, and transferred to a 2 mL microcentrifuge tube. The microtubes containing the gel slices were centrifuged at maximum speed (13000 rpm) for 2 minutes at room temperature to ensure the gel passed through the holes in the bottom of the tube. The 0.5 mL tube was then discarded, and 500 µL of sterile 0.3 M NaCl was added to the gel debris. The tube was gently shaken and incubated overnight at 4°C for RNA elution.

The next day, the eluate and gel debris were transferred to a Spin X cellulose acetate filter tube and centrifuged at 6000 rpm for 2 minutes. This step was repeated, and the Spin X column containing the gel debris was discarded. The eluate was mixed with 600 µL of 100% isopropanol and 1 µL of GlycoBlue, then gently inverted (not vortexed) and incubated at -70°C for 2 hours 30 minutes. Afterward, the precipitated RNA was centrifuged at maximum speed at 4°C for 20 minutes. The supernatant was carefully removed, and the RNA pellet was washed twice with 1 mL of 70% ice-cold ethanol. The pellet was air-dried before resuspending in 12 µL of MilliQ water. Following this, the 3' and 5' adapter ligation steps were performed.

4.5.4 3’ adapter ligation

Adapter ligation is a critical and essential step in library preparation. During this process, DNA adapters with known sequences are ligated to the RNA molecules, enabling their amplification and sequencing in later steps using specific primers. To prevent contamination and RNA degradation by RNases, it is crucial to perform this procedure under a laminar flow hood. For each sample, the ligation mixture was prepared by combining 1 µl of ligation buffer (HML), 0.5 µl of RNase inhibitor, and 0.5 µl of T4 RNA ligase 2 (truncated) in sterile PCR tubes on ice. The mixture was pipetted up and down several times and centrifuged to ensure uniformity.

To ligate the 3' adapter, the thermocycler was preheated to 70°C, and 2.5 µl of purified small RNA from each sample was added to a sterile PCR tube, along with 0.5 µl of RNA 3' adapter (RA3) and then mixed thoroughly, then centrifuged briefly. The tube was then placed on ice. The reaction mixture was denatured at 70°C for 2 minutes in the thermocycler and immediately transferred to ice afterward.

Next, the thermocycler was set to 28°C, and 2 µl of the ligation mixture was added to the denatured RNA. The mixture was gently mixed by pipetting and incubated at 28°C for 1 hour. The 3' adapter ligation reaction was terminated by adding 0.5 µl of ice-cold stop solution (STP), followed by gentle mixing by pipetting up and down several times. The incubation continued at 28°C for an additional 15 minutes before the tubes finally were placed on ice.

4.5.5 5’ adapter ligation

To ligate the 5' adapter, the thermocycler was preheated to 70°C, and 0.5 µl of RNA 5' adapter (RA5) was added to sterile PCR tubes. The mixture was incubated at 70°C for 2 minutes and then placed on ice. The thermocycler was preheated to 28°C. Next, 0.5 µl of 10 mM ATP and 0.5 µl of T4 RNA ligase were pipetted into separate sterile PCR tubes and placed on ice. The total volume of the denatured 5' adapter was added to this mixture, bringing the total volume to 1.5 µl. The 5' adapter mixture was then added to the 3' adapter reaction tube and thoroughly mixed by pipetting. The final volume for the 3' and 5' adapter ligation reaction was 7 µl. This reaction tube was placed into the preheated thermocycler and incubated at 28°C for 1 hour, after which the 3'-5' adapter ligation reaction was placed on ice.

4.5.6 Reverse transcription

For reverse transcription, the thermocycler was first preheated to 70°C. We then combined 1 µl of RNA RT primer (RTP) with 7 µl of the 3'–5' adapter-ligated reaction. The mixture was gently mixed by pipetting the entire volume up and down and then incubated at 70°C for 2 minutes. Afterward, the tubes were placed on ice. The thermocycler was then preheated to 50°C. Next, the RT reaction mixture was prepared in PCR tubes by adding 1 µl of ultrapure water, 2 µl of 5x reaction buffer, 0.5 µl of 12.5 mM dNTP mix, 1 µl of RNase inhibitor, and 1 µl of RevertAid H-reverse transcriptase. The mixture was thoroughly mixed by pipetting up and down, then briefly centrifuged. The 5.5 µl of RT reaction mixture was added to the 3'–5' adapter-ligated/primer mixture prepared in the first step, bringing the total volume of the RT reaction to 12.5 µl. The reaction was then incubated for 1 hour at 50°C, after which the tubes were placed on ice.

4.5.7 PCR Amplification for sRNA Libraries

The PCR reaction mixture was prepared in a separate sterile PCR tube on ice by pipetting 4.25 µl of MilliQ pure water, 1.25 µl of PCR mix (PML), 1 µl of RNA PCR primer (RP1), and 1 µl of RNA PCR primer index (RPIX). The mixture was gently mixed by pipetting up and down several times, briefly centrifuged, and placed back on ice. Next, 6.25 µl of cDNA was added to the PCR reaction mixture, bringing the total volume to 25 µl. The entire volume was mixed gently by pipetting up and down, centrifuged briefly, and kept on ice.

The PCR reaction was then denatured in a thermocycler for 30 seconds at 98°C, followed by 16 cycles of amplification, with each cycle consisting of 10 seconds at 98°C for denaturation, 30 seconds at 60°C for annealing, and 15 seconds at 72°C for elongation. The reaction was finalized with a 10-second extension at 72°C. At this point, the amplified small RNA library was ready for purification.

4.5.8 Purification of the small RNA library

Small RNA libraries were purified using a custom protocol based on the TruSeq Small RNA Library Preparation Kit (Illumina, San Diego, CA, USA). Two size markers were used: a 20 bp

DNA ladder and a 50 bp low-molecular-weight ladder, each loaded into the outermost wells of the gel (on each side of the gel). The amplified PCR product (25 µl) was mixed with 5 µl of 6x Orange DNA dye and loaded into two adjacent wells between the markers. Next the gel was ran at 50 V until the samples fully entered the gel from the wells. Electrophoresis was performed at a constant voltage of 100 V for 2 hours, allowing the dye to migrate towards the bottom of the gel. After electrophoresis, the size markers and amplified small RNA library were visualized using a UV transilluminator. The gel region corresponding to the target size range (140–145 nt) was carefully excised and transferred into punctured 0.5 ml microcentrifuge tubes placed inside 2 ml collection tubes. DNA was eluted by adding 0.3 M NaCl and gently shaking the tubes overnight at 4°C. The following day, the eluate was separated from the gel debris using a mini spin column. To precipitate the DNA, 1 µl of GlycoBlue and 1 ml of 100% ethanol were added to the eluate, followed by incubation at -70°C for 2 hours. The sample was then centrifuged at full speed at 4°C for 20 minutes. After discarding the supernatant, the RNA pellet was washed with 1 ml of 70% ice-cold ethanol. The pellet was dried in a SpeedVac concentrator for 5 minutes and then resuspended in 12 µl of sterile 1x TE resuspension buffer. The purified small RNA libraries were stored at -70°C until sequencing.

4.5.9 Sequencing the prepared libraries using Illumina platform

Sequencing was carried out using single indexing on a HiScanSQ platform (50 bp, single-end reads) by UD-Genomed (Debrecen, Hungary).

4.6 Bioinformatics methods for sequence analysis

4.6.1 Bioinformatics analysis of the HTS reads, sRNA, RNAseq

The genomic sequences obtained in FastQ file format underwent bioinformatics analysis using the CLC Genomics Workbench (Qiagen, Hilden, Germany). The CLC Genomics Workbench is an advanced bioinformatics platform designed for efficient analysis and visualization of sequencing data. Initially, quality control (QC) procedures were conducted within the software to eliminate low-quality reads and ensure high accuracy of downstream analyses. Additionally, the size distribution of the sequenced reads was assessed, with particular emphasis on the detection of

small RNA populations of 21, 22, and 24 nucleotides (nt) in length. Subsequently, a non-redundant read list was generated to consolidate identical sequences and streamline further analyses. For virus detection, high-quality reads were assembled de novo into longer contiguous sequences (contigs) using the assembly algorithm integrated into CLC Genomics Workbench.

For RNA-seq data analysis, following data importation, read trimming was performed to remove adapters and low-quality bases, and FastQC reports were generated to confirm data integrity. The trimmed paired-end reads were then assembled into contigs through *de novo* assembly. Resulting contigs underwent BLAST searches against a curated reference database comprising sequences of all currently known plant-infecting viruses, downloaded from NCBI GenBank (accessed on 31 July 2023). Additionally, sequence reads were directly mapped onto reference genomes of viruses identified by contigs that showed zero E-value hits during BLAST analysis. Consensus sequences generated from the mappings allowed us to quantify viral genome coverage.

4.7 Validation of virus presence with RT-PCR

4.7.1 Design of PCR Primers

Viruses identified through bioinformatics analysis were subsequently validated using virus-specific primers designed for targeted experimental confirmation (Table 6). Primers were designed using Geneious Prime (2024.0.7) based on reference genomes and assembled contigs, primarily targeting the coat protein (CP) gene region due to its conserved nature, virus-specific sequences and common use in phylogenetic analyses. Primers were designed to produce amplicons of varying sizes and were checked for specificity by BLASTing using the National Centre for Biotechnology Information (NCBI) (www.ncbi.nml.nih.gov).

This design strategy ensured reliable amplification of the target regions and enabled accurate validation of the HTS-derived viral detections in the investigated samples. Overall, the primer sets provided a solid basis for validating viral presence across samples.

Table 6. PCR primers used for virus detection in experiments K2022, K2023, and Ko2023.

	Virus		Primer Name	Primer Sequence (5'-3')	Position on the reference genome	Genome used as a reference	Annealing temperature (°C)
K2022 and K2023	CMV	RNA 1	CMV RNA 1_429F	TCGGAGGAAGTTGGGTCACAC	429-449	NC_002034	62°C
			CMV RNA 1_2401R	GACAGAATCGGCTGTTCGAAC	2401-2381		
			CMV_RNA1_429F	TCGGAGGAAGTTGGGTCACAC	429-449		62.5°C
			CMV_RNA1_1623R	GATGATATCACGTCCCAYTC	1623-1604		
		RNA 2	CMV RNA 2_178F	GTGAACAACGCGAAGATGCTG	179-198	NC_002035	63°C
			CMV RNA 2_2005R	GGTTCCATCACCTTAGCTTCC	2005-1985		
			CMV_RNA2_1116F	GGTCACAAGAGAGTAGGTAC	1116-1135		60.5°C
			CMV_RNA2_2875R	GCCGTWAGCTGGATGGACAAC	2875-2855		
		RNA 3	CMV RNA 3_416F	TTCCACTGATGCTGAAGGGTC	416-436	NC_001440	66°C
			CMV RNA 3_2032R	AGCTGGATGGACAACCCGTTC	2032-2012		
	BBWV1	RNA 1	BBWV1 RNA1_1167F	CACTCTTGTCAGCTCGTGGT	1167-1186	NC_005289, C_131	58°C
			BBWV1 RNA 1_4081R	CTTTCTCCCCTGGCTTCCTG	4081-4062		
		RNA 2	BBWV1 RNA 2_347F	TGCGAGAGTACTCAGGCATTC	368-388	NC_005289	58°C
			BBWV1 RNA 2_3343R	TTTAACAAAGCAGTGGAACCCA	3365-3344		
	TuYV		TVCV_1226F	ACACCAGGATATATAGAAAG	1226-1245	NC_003378	55°C
			TVCV_1941R	TAACAAGTACATTCTGTTAGT	1921-1941		
	TVCV		TuYV_3595F	CACAACGCCGACCTAGACGAC	3595-3615	NC_003743	55°C
			TuYV_4748R	CATCCCTATCTCCATCATCCG	4748-4728		
	PVM		PVM_7344F	GCTGATTTTGAGGGGAAGGA	7312-7331	NC_001361	58.7°C
			PVM_8128R	CCATTCATACCACCTGTCACC	8096-8076		
	PVH		PVH_6739F	GATAATCTGCATTCACTCCC	6739-6758	NC_018175	55.7°C
			PVH_7749R	AGCATGTGGTTCCATACGAT	7749-7730		
	ObPV		ObPV_2956F	GATGAGACTGAGAAGAGGAG	2937-2956	NC_003852	64.5°C
			ObPV_3679R	GCGGCAGTTCTTATGACAGG	7707-7688		
	LBVaV	RNA1	LBVaV_RNA1_5870F	AGCAACTGGAATGCTCTCGC	5870 - 5889	NC_011558	51.1°C
			LBVaV_RNA1_6442R	TCTATCCATCCACCGCTTGC	6423-6442		
		RNA2	LBVaV_RNA2_437F	GAGGTCTGTTGATCCCGTGG	446-465	NC_011568	58.7°C
			LBVaV_RNA2_1239R	TGTACCTCTTCCTCTCCGGG	1248-1229		
	OxruMV1		OxruMV1_1096F	TTCTCGCCTGGTATCTTATTC	1096-1116	NC_076526	55.7°C
			OxruMV1_1664R	GCCCAAGAACCGTAGTAGCCC	1664-1644		
Ko2023	CMV	RNA1	CMV RNA1_429F	TCGGAGGAAGTTGGGTCACAC	429-449	NC_002034	60.5
			CMV RNA1_1623R	GATGATATCACGTCCCAYTC	1623-1604		
		RNA2	CMV RNA2_1116F	GGTCACAAGAGAGTAGGTAC	1116-1135	NC_002035	60.5
			CMV RNA2_2875R	GCCGTWAGCTGGATGGACAAC	2875-2855		
		RNA3	CMV RNA3_224F	GGCTRCTGAGTGTGACCTAGG	224-244	NC_001440	60.5
			CMV RNA3_1575R	TGCGCGAAACAAGYTTCTTATC	1575-1554		
	BBWV2	RNA1	BBWV2 RNA1_434F	CCATTTCAGCCGCGTATGTG	434-453	c46	62.5
			BBWV2 RNA1_1410R	CGCACGGATCTTCTGCATTG	1410-1391		
		RNA2	BBWV2 RNA 2_921F	TTGGGACGCTTATTGGGCAT	921-940	c27	62.3
			BBWV2 RNA 2_2023R	CCTCTCATCCACGCACAGTT	2023-2004		
	PVY	PVY	PVY_127F	GGAAACCATTTCAACTCAAC	127-146	NC_001616	58.0
			PVY_469R	CTGGAAGTGATATTCTTCCC	469-450		
	PCV2	RNA1	PVC2 RNA1_639F	ACACCCGCACACAATTAACG	639-658	NC_034159	60.5
			PVC2 RNA1_1176R	CCGATTAGTGAATCATCTCC	1176-1157		
		RNA2	PVC2 RNA2_858F	AGGCAACTACTCTATGGAGG	858-877	NC_034167	60.5
			PVC2 RNA2_1272R	CCTATCTGCTTCTCCTGTAG	1272-1253		
	BPEV	BPEV	BPEV_1380F	TGTGGACGCAATGTACGACA	1380-1399	c136	60.5
			BPEV_2429R	ACCAACCTGCAACACTCACA	2429-2410		
	RWMV	RWMV	RWMV_1085F	CCTCTCATTTCGTCCAGCACT	1085-1105	c1885	60.5
			RWMV_1413R	CTTTGCGGTGGAAGAGGTGA	1413-1394		

4.7.2 Gradient PCR and Optimization of Annealing Temperature

Primers were diluted according to the manufacturer's protocol, and a gradient PCR was performed to determine the optimal annealing temperature for each primer pair. This step was necessary to

ensure specific amplification and to avoid non-specific products or primer-dimer formation. The gradient ranged from 51.1 to 66 °C (Table 6), allowing evaluation of primer behavior across a wide temperature interval. For each primer pair, PCR reactions were set up under different conditions, varying only the annealing temperature, to identify the temperature that produced a strong and specific band of the expected size. This optimization step ensured that only the most suitable temperature was chosen for the subsequent PCR reactions performed on individual samples.

4.7.3 PCR Reaction Setup and Cycling Parameters

PCR reactions were prepared individually for each plant sample, containing the following components per reaction: 3 µl of 5× Q5 reaction buffer or 5X Phire Reaction Buffer, 0.3 µl of 10 mM dNTP mix, 10 µl of MilliQ pure water, 0.3 µl of Q5 DNA polymerase or Phire DNA Polymerase, 0.75 µl forward primer (10 µM), and 0.75 µl reverse primer (10 µM). In the next step, new sterile PCR tubes were clearly labelled and placed on ice within a laminar flow cabinet to maintain sterile conditions. Subsequently, 0.5 µl of the cDNA template from each pooled plant sample or individuals were transferred into the appropriately labelled tubes. To each tube, 14.5 µl of the prepared PCR master mix was added, and the reaction mixtures were briefly centrifuged to achieve a homogeneous final volume of 15 µl. The samples were then loaded into the thermocycler for PCR amplification. The annealing temperatures used for each virus assay are listed in (Table 6). A summary of all PCR parameters is provided in Table 7, with conditions adjusted according to amplicon size and the polymerase used, following the recommendations of the respective reaction buffer.

Table 7. PCR parameters used for amplifications

PCR steps	Temperature (°C)	Duration of the step	
		Q5	Phire
Initial heating step	98	30 s	30 s
Denaturation	98	30 s	10 s
Annealing	51.1 - 66	30 s	10 s
Elongation	72	1-3 min	20 s
Final extension	72	2 min	1 min
Number of cycles	40 cycles		

4.7.4 cDNA Synthesis

The synthesis of complementary DNA (cDNA) was carried out using the RevertAid™ First Strand cDNA Synthesis Kit (Thermo Fisher Scientific, Waltham, MA, USA) or Thermo Scientific Maxima™ Reverse Transcriptase (Thermo Fisher Scientific, Waltham, MA, USA) with random primers, according to the manufacturer's protocol. RNA extracts obtained from a pool consisting of ten plant species, along with total nucleic acids extracted from each individual plant, were used as templates for the cDNA synthesis reaction. The cDNA synthesis reaction was carried out using 1.75 µl of template RNA combined with 0.25 µl of random hexamer primer, resulting in an initial reaction volume of 2 µl. Subsequently, this mixture was supplemented with a master mix containing the following reagents per single reaction: 1 µl of 5× reaction buffer, 0.5 µl of 10 mM dNTP mix, 0.25 µl of RiboLock RNase inhibitor, and 0.25 µl of RevertAid reverse transcriptase. The cDNA synthesis was then carried out at 25 °C for 10 min, followed by 42 °C for 60 min, 45 °C for 10 min, and a final step at 70 °C for 10 min. After completion of the reaction, the resulting cDNA was diluted according to the protocol.

4.7.5 Actin Test

The quality of the cDNA was confirmed in an RT-PCR reaction using actin-specific primers serving as a conserved housekeeping gene for cDNA quality assessment. Subsequently, RT-PCR was performed using Q5 Hot Start High-Fidelity DNA Polymerase (New England Biolabs, Ipswich, MA, USA) to amplify targeted viral genomic regions, utilizing primer-specific annealing temperatures and optimized cycling parameters.

4.7.6 PCR Amplification of RNA-seq Libraries

PCR amplification was performed using either Q5 DNA polymerase (New England Biolabs) or Phire DNA polymerase (Thermo Fisher Scientific) in reaction mixtures containing 3 µL of 5× Q5 or Phire reaction buffer, 0.3 µL of 10 mM dNTP mix, 10 µL of MilliQ water, 0.3 µL of the respective DNA polymerase, and 0.75 µL (10 µM) each of forward and reverse primers per reaction. The prepared PCR master mix consisted of 14.5 µl of the reaction mixture combined with 0.5 µl of cDNA template for a final reaction volume of 15 µl per reaction.

4.7.7 Preparation and running of gels

As the PCR cycling approached completion, a TBE agarose gel was prepared. Initially, 30-40 µl of agarose solution was accurately dispensed into a glass tube, to which 1 µl of ethidium bromide was added for staining. Wells were then carefully formed within the gel. For electrophoresis, 4 µl of DNA loading dye was combined with the PCR products in separate tubes. Subsequently, 6 µl of each mixture was loaded into the prepared wells. The first well was designated for the DNA ladder, receiving 2.5-3 µl of the M100bp plus ladder to facilitate molecular size estimation. Given the specific positions of the forward and reverse primers on the viral genome, the anticipated size of the amplified PCR product was determined. The gel electrophoresis was conducted at 116 V for 30-40 minutes. Following the run, the gel was imaged using the Bio-Rad ChemiDoc Imaging System to document the results.

4.7.8 Purification of PCR products

Purification of PCR products was performed using the NucleoSpin Gel and PCR Clean-up Mini Kit (Macherey-Nagel– 11/2024, Rev. 09), following the manufacturer's protocol. The procedure began with the extraction of DNA from agarose gels. DNA fragments were excised, and for every 100 mg of agarose gel (<2% concentration), 200 µL of Buffer NTI was added. Samples were then incubated at 50°C for 10 minutes, with brief vortexing every 2–3 minutes, until the gel slices were completely dissolved. Following dissolution, DNA binding was performed by placing a NucleoSpin® Gel and PCR Clean-up Column into a 2 mL collection tube and loading up to 700 µL of the dissolved sample. The column was centrifuged at 11,000 × g for 30 seconds. The flow-through was discarded, and the remaining sample (if any) was loaded and centrifuged again using the same conditions. To wash the silica membrane, 700 µL of Buffer NT3 was added to the column, followed by centrifugation at 11,000 × g for 30 seconds. This washing step was repeated once more to minimize chaotropic salt carry-over and ensure a high A260/A230 ratio. Drying of the silica membrane was achieved by centrifuging the column for 1 minute at 11,000 × g to completely remove residual wash buffer. Care was taken to prevent contact between the spin column and the flow-through during handling. To ensure the complete evaporation of any remaining ethanol, columns were additionally incubated at 70°C for 5 minutes. Finally, DNA elution was performed by transferring the column into a clean 1.5 mL microcentrifuge tube, adding 30 µL of Buffer NE,

incubating at room temperature for 1 minute, and centrifuging at 11,000 × g for 1 minute. The purified DNA was collected and used for the subsequent ligation steps.

4.7.9 Ligation process

The ligation process was performed following the protocol provided by the Thermo Scientific CloneJET PCR Cloning Kit. This kit is designed as an advanced positive selection system, optimized for the highly efficient cloning of PCR products generated by Pfu DNA polymerase, Taq DNA polymerase, Thermo Scientific™ DreamTaq™ DNA polymerase, or other thermostable DNA polymerases. In addition, the kit is suitable for the cloning of any DNA fragment, whether blunt- or sticky-ended. Central to the kit is the pJET1.2/blunt cloning vector, which carries a lethal gene that is disrupted upon the successful ligation of an insert. Consequently, only recombinant plasmids are able to propagate in *Escherichia coli* host cells, eliminating the need for blue/white screening and enhancing selection efficiency. The vector also features an expanded multiple cloning site, and a T7 promoter for *in vitro* transcription, along with included sequencing primers for easy verification of cloned inserts. pJET1.2/blunt is a linearized vector with 5'-phosphorylated ends, eliminating the need for phosphorylation of PCR primers, and is capable of accommodating inserts ranging from 6 bp to 10 kb in size. Blunt-ended PCR products produced by proofreading DNA polymerases can be directly ligated into the vector within 5 minutes. PCR products containing 3'-dA overhangs, typically generated by non-proofreading polymerases such as Taq, are first treated with a proprietary thermostable blunting enzyme provided in the kit before proceeding to ligation. The resulting ligation products are directly suitable for transformation into standard *E. coli* laboratory strains. For the ligation reaction, the following mixture was prepared: 10 µL of 2× Reaction Buffer, 1 µL of pJET1.2/blunt Cloning Vector, 1 µL of T4 DNA Ligase, and 8 µL of the purified PCR product from the previous step, totaling 20 µL. The mixture was briefly vortexed, centrifuged for 3–5 seconds, and incubated at room temperature for 10 minutes. The resulting ligation mixture was then directly used for bacterial transformation.

4.7.10 Bacterial tranformation process

Fourteen-milliliter (14 mL) sterile ligation tubes were labeled accordingly and placed on ice. Subsequently, 5 µL of the ligation mixture and 100 µL of competent cell suspension were added to each tube, followed by the transformation steps (Figure 7).

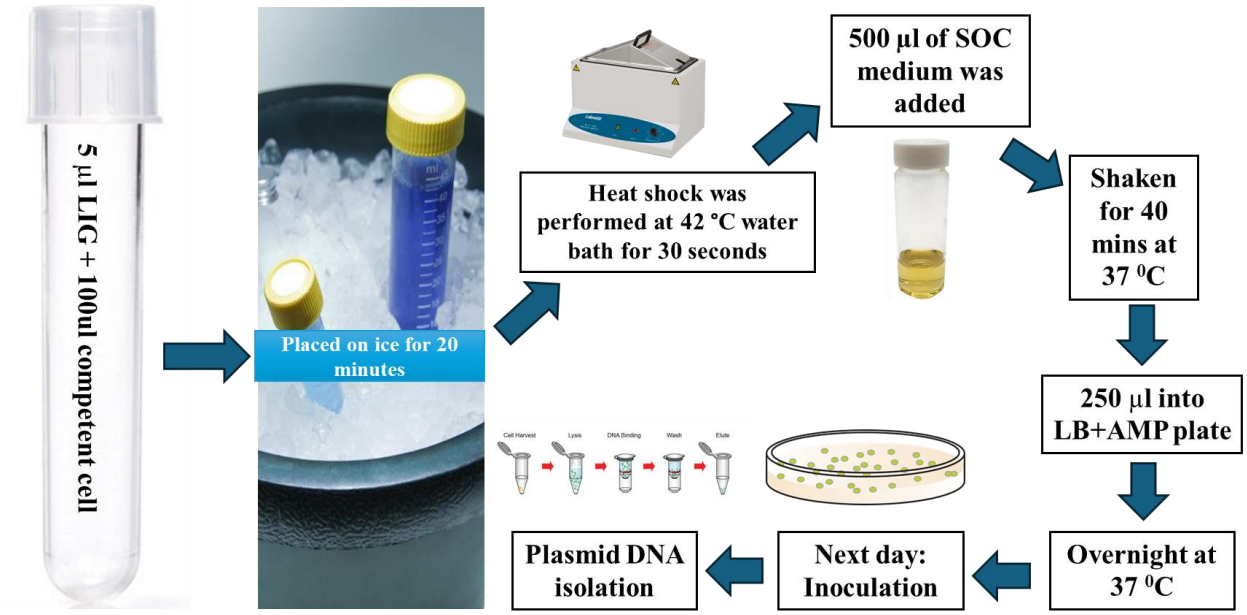

Figure 7. Bacterial transformation process.

4.7.11 Plasmid DNA isolation

Plasmid DNA was purified using the NucleoSpin® Plasmid / Plasmid (NoLid) kit (MACHEREY-NAGEL, 07/2010, Rev. 07), designed for the isolation of high-copy plasmid DNA from *E. coli*. The procedure began with the cultivation and harvesting of bacterial cells: 1–5 mL of a saturated *E. coli* LB culture was centrifuged for 30 seconds at 11,000 × g in a standard benchtop microcentrifuge. The supernatant was discarded carefully to remove as much residual liquid as possible. The cell lysis process followed. First, 250 µL of Buffer A1 was added to the pellet, and the cells were thoroughly resuspended by vortexing or pipetting until no clumps remained. Next, 250 µL of Buffer A2 was added, and the mixture was gently inverted 6–8 times to avoid shearing genomic DNA. The lysate was incubated at room temperature for up to 5 minutes, or until lysate appeared clear. Following lysis, 300 µL of Buffer A3 was added, and the mixture was again inverted 6-8 times gently to ensure thorough mixing. For lysate clarification, the sample was

centrifuged for 5 minutes at 11,000 × g at room temperature. If the supernatant was not clear, centrifugation was repeated. To bind the plasmid DNA, the cleared lysate was transferred onto a NucleoSpin® Plasmid / Plasmid (NoLid) column placed in a 2 mL collection tube. Up to 750 µL of the supernatant was loaded at a time and centrifuged for 1 minute at 11,000 × g. This step was repeated until the entire lysate was processed. The bound DNA was then washed. An additional wash step using 500 µL of Buffer AW preheated to 50 °C was performed to enhance the purity and improve subsequent sequencing and enzymatic reactions. Following this, 600 µL of Buffer A4 (ethanol-supplemented) was added, and the column was centrifuged for 1 minute at 11,000 × g. After discarding the flow-through, the column was returned to the collection tube and centrifuged again to ensure complete removal of residual wash buffer. For DNA elution, the column was transferred to a clean 1.5 mL microcentrifuge tube, and 50 µL of Buffer AE was added directly to the membrane. After a one minute incubation at room temperature, the plasmid DNA was eluted by centrifugation for 1 minute at 11,000 × g.

A digestion mix was then prepared, consisting of 2 µL Tango buffer, 0.2 µL *Xho*I, 0.2 µL *Xba*I, and 5.6 µL MilliQ water. In a new tube, 8 µL of this digestion mix was combined with 2 µL of the purified plasmid DNA to produce the digested plasmid sample. Both digested and undigested plasmid samples were analyzed by agarose gel electrophoresis. After confirming successful digestion, the plasmid products were submitted for Sanger sequencing.

4.7.12 Analyzing Sanger sequences

During the initial sequence analysis, chromatograms were checked in Chromas, a free viewer suitable for single-read DNA sequencing. Chromas was used to assess peak clarity and identify mixed or ambiguous bases (Figure 8), and sequences were exported in FASTA or text format for further analysis in CLC Genomics Workbench. Single nucleotide polymorphisms (SNPs) were identified based on consistent base substitutions and confirmed when present in both forward and reverse reads. When mixed peaks or sequence heterogeneity were detected, additional bioinformatics evaluation was performed in CLC.

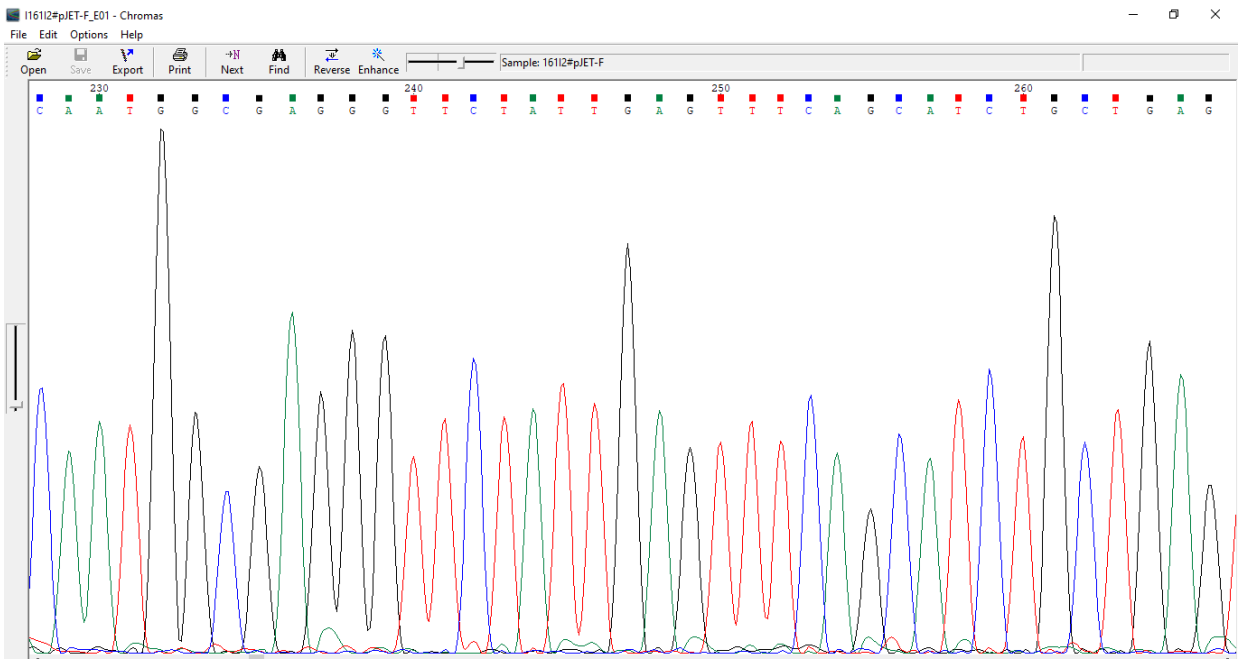

Figure 8. Chromatographic representation of a sequence opened in Chromas 2.1

4.7.13 Phylogenetic analysis

To compare and phylogenetically analyze the virus variants present in the samples multiple sequence alignments were performed using Geneious Prime with the MUSCLE algorithm. Evolutionary relationships were inferred using the Jukes-Cantor model and the Neighbor-Joining method. Phylogenetic trees were constructed based on the optimal model for each alignment, with 1,000 bootstrap replicates to assess reliability. The trees were scaled, with branch lengths representing the number of substitutions per site. The closest relatives of the viruses, as indicated in the tree legend, were used as outgroups.

5. RESULTS AND DISCUSSION

Weed samples from experiments K2022 and K2023 and cultivated crop samples from experiment Ko2023 were collected. The observations displayed a wide spectrum of symptoms, ranging from asymptomatic plants to severe morphological alterations indicative of virus activity.

5.1 Weed Sampling in experiment K2022

During the K2022 sampling, weed species including *Solanum nigrum* and *Datura stramonium* from Field I, as well as *S. nigrum* plants from Field II, were carefully investigated, and no visible symptoms indicative of viral infection were observed in any of the collected samples (Table 8).

Table 8. Weed sampling workflow in experiment K2022

	Field	Name of the sampled plant species	Code of the individual plant	Symptoms	Sampled in:
K2022	I	*Solanum nigrum*	S1/1	Symptomless	leaf, flowery shoot
			S1/2		leaf, flowery shoot
			S1/3		leaf, flowery shoot
			S1/4		leaf, flowery shoot
			S1/5		leaf, flowery shoot
		Datura stramonium	D/1		leaf
			D/2		leaf
			D/3		leaf
			D/4		leaf
			D/5		leaf
	II	*Solanum nigrum*	S2/1		leaf, flowery shoot
			S2/2		leaf, flowery shoot
			S2/3		leaf, flowery shoot
			S2/4		leaf, flowery shoot
			S2/5		leaf, flowery shoot

5.2 Weed Sampling in experiment K2023

While no visible symptoms were observed during the K2022 sampling, the K2023 sampling revealed a remarkable diversity of viral symptoms across several plant species (Table 9).

Table 9. Weed sampling workflow in experiment K2023 with observed viral symptoms. Lcurl: Leaf curl, Ldef: Leaf deformation, Ul: Uneven leaves, sh.i: Short internodes, Dw: Dwarfism, P.A: Purple-anthocyanin, Fdelays: Flowering delays, Dback: Dieback, Fdef: Flower deformation, Bspot: Brown spots, Chl: Chlorosis, Dflow: Drying flowers, Yflowers: Yellow flowers, Yfresh pouts: Yellowing on the fresh pouts, H: Holes, Fdying: Flower dying, H on leaf: Hole in leaf, anthocya..: Anthocyanin on the edges of leaves, Nec: Necrosis.

	Field	Name of the sampled plant species	Code of the individual plant	Symptoms	Sampled in:
K2023	III	*Solanum nigrum*	S3/1	Lcurl, Mutation	leaf, flowery shoot, fruits
			S3/2	Ldef	leaf, flowery shoot
			S3/3	Lcurl, Ul	leaf, flowery shoot, fruits
			S3/4	Lcurl, sh.i, Dw	leaf, flowery shoot, fruits
			S3/5	Dw, Lcurl, Ldef	leaf, flowery shoot, fruits
			S3/6	Dw, P.A	leaf, flowery shoot, fruits
			S3/7	Ul, Dw, Lcurl	leaf, flowery shoot, fruits
			S3/8	Ul, Dw, Lcurl	leaf, flowery shoot, fruits
			S3/9	Dw, Ul, Lcurl,holes	leaf, flowery shoot, fruits
			S3/10	Dw, Ul,Lcurl, holes	leaf, flowery shoot, fruits
		Datura stramonium	D2/1	Ul	leaf
			D2/2	T4, Fdelays, Dback	leaf
			D2/3	Fdef, Bspot, Ldef	leaf, flowery shoot
			D2/4	Lcurl, Ul, Chl, Dflow	leaf, flowery shoot
			D2/5	Lcurl, Ul, Yflowers	leaf, flowery shoot, seeds
			D2/6	Lcurl, Lholes, Ul	leaf, seeds
			D2/7	Def fruit, Yflowers	leaf, flowery shoot, seeds
			D2/8	Chl, Yfresh pouts	leaf, flowery shoot, seeds
			D2/9	Strong ldef, Chl, H	leaf
			D2/10	Ldef, Chl, Fdying	leaf, seeds
		Brassica napus	B1	No visible symtom	leaf
			B2	No visible symtom	leaf
			B3	Holes, Phylliades sp	leaf
	IV	*Solanum dulcamara*	Sd1	Chl, Ul, H on leaf	leaf, fruits
			Sd2	Ul, holes, anthocya..	leaf
			Sd3	Strong ldef, H	leaf
			Sd4	Brwon spots, Ldef, H	leaf, fruits
			Sd5	Dead flow, H, Nec	leaf, flowery shoot, fruits
			Sd6	Ldef, Lcurl, Nec, H	leaf
			Sd7	H, purple spots, Ldef	leaf
			Sd8	Anthocyanin, Nec	leaf, fruits

5.3 Cultivated Crop Sampling in experiment Ko2023

During the Ko2023 survey of cultivated crops, *Solanum tuberosum*, *Solanum lycopersicum*, and *Capsicum annuum* were sampled. These crops exhibited varying degrees of virus-like symptoms, primarily on leaves. While some plants showed clear symptoms, others were asymptomatic or displayed virus-like symptoms, reflecting the heterogeneous nature of symptom development within the field (Table 10).

Table 10. Crop samples from experiment Ko2023 with observed viral symptoms:. VLS: Virus-like symptoms, IVC: Interveinal chlorosis, M: Mosaic, Mpatterns: Mottling patterns, Ldef: Leaf deformation, Chlo: Chlorosis, SG: Stunted growth.

	Name of the sampled plant species	Code of the individual plant	Symptoms	Sampled in:
Ko2023	*Solanum tuberosum*	Po1	Asymptomatic	leaf
		Po2		leaf
		Po3	IVC	leaf
		Po4		leaf
	Solanum lycopersicum	T1	VLS	leaf
		T2		leaf
		T3		leaf
		T4		leaf
	Capsicum annuum	Pe1	VLS	leaf
		Pe2	M, Mpatterns, Ldef, Chlo, SG	leaf
		Pe3		leaf
		Pe4		leaf

5.4 HTS results

5.4.1 Results of the K2022 Weed Sampling

For the K2022 sampling, a single sRNA library (255_KSOL) and a single total RNA library (SOL_KES_10) were prepared to represent all sampled plant species, including *Solanum nigrum* and *Datura stramonium* from Field I and *S. nigrum* from Field II. In the case of sRNA for K2022, sequencing produced 21,955,551 reads, of which 21,573,415 high-quality redundant reads remained after trimming. These represented 3,178,957 non-redundant sRNA sequences, from which 3,177 contigs were assembled. For RNA-Seq of the same samples, 16,253,182 reads were

generated in total. After trimming and quality control, 15,972,388 reads were retained, resulting in the assembly of 132,523 contigs (Table 11).

Table 11. Initial statistics of the RNAseq and sRNA HTS for K2022 samples

Year	HTS	**Library code**	**Sequenced reads**	**Trimmed reads all (containing redundants)**	**Non-redundant reads**	**Number of contigs**
K2022	sRNA	255_KSOL	21 955 551	21 573 415	3 178 957	3177
	RNAseq	SOL_KES_10	16 253 182	15 972 388	n/a	132 523

BLAST analysis of contigs derived from sRNA and RNA-Seq revealed the presence of four viruses: Cucumber mosaic virus (CMV; RNA1, RNA2, and RNA3), Broad Bean Wilt Virus 1 (BBWV1; RNA1 and RNA2), Turnip yellow virus (TuYV) and Tobacco vein-clearing virus (TVCV) (Table 12).

Table 12. Bioinformatics results from RNA-Seq and sRNA-HTS analyses identified the viruses present in K2022 samples

			RNAseq					
K2022	**Virus**		**GenBankId of the reference genome**	**number of contigs**	**number of mapped reads**	**coverage of the viral genome (%)**	n/a	n/a
	CMV	**RNA 1**	NC_002034	1	115006	99%	n/a	n/a
		RNA 2	NC_002035	1	100107	99%		
		RNA 3	NC_001440	2	105966	99%		
	BBWV1	**RNA 1**	NC_005289	1	58198	98%		
		RNA2	NC_005290	1	42076	97%		
	TVCV		NC_003378	19	95208	89%		
	TuYV		NC_003743	5	12627	90%		
				sRNAseq				
K2022	**Virus**		**GenBankId of the reference genome**	**number of contigs**	**number of non-redundant reads**	**number of redundant reads, mapped to the virus**	**RPM**	**coverage of the viral genome (%)**
	CMV	**RNA 1**	NC_002034	62	14643	234654	10914	99%
		RNA 2	NC_002035	54	12327	190706	8870	99%
		RNA 3	NC_001440	31	24898	804366	37412	99%
	BBWV1	**RNA 1**	NC_005289	16	1187	5377	250	98%
		RNA2	NC_005290	5	525	2612	121	97%
	TVCV		NC_003378	25	2274	14799	688	80%
	TuYV		NC_003743	0	239	621	29	43%

Each virus was represented by at least one contig showing significant homology (0 E-value) to reference genomes of known plant-infecting viruses. Mapping of viral reads to the respective

genomes indicated high genome coverage in both sequencing approaches. For CMV, sRNA libraries showed 99% coverage for RNA1, RNA2, and RNA3 which was mirrored in the RNA-Seq data. BBWV1 coverage from sRNA reads was 98% for RNA1 and 97% for RNA2, with identical coverage observed in RNA-Seq libraries. TVCV coverage was 80% in sRNA results and 89% in RNA-seq results, while TuYV showed lower genome coverage in sRNA sequencing with 43% compared to RNA-seq with 90% (Table 12).

5.4.1.1 Size distribution analysis of viral reads obtained from sRNA in experiment Keszthely, 2022

In the K2022 experiment, the size distribution analysis of viral reads obtained from sRNA high-throughput sequencing (sRNA HTS) in this library showed that the majority of mapped reads for CMV were 21 nucleotides in length, all three RNAs of CMV were dominated by 21-nt reads (Figure 9) while BBWV1 RNA1 and RNA2 were predominantly 22 nucleotides in length. Mapped sRNA reads for both TVCV and TuYV were predominantly 24 nt in length (Figure 10). These distinct size classes highlight differences in how the host plant processes each virus through RNA silencing. The predominance of specific sRNA lengths suggests virus-specific interactions with the host defense machinery.

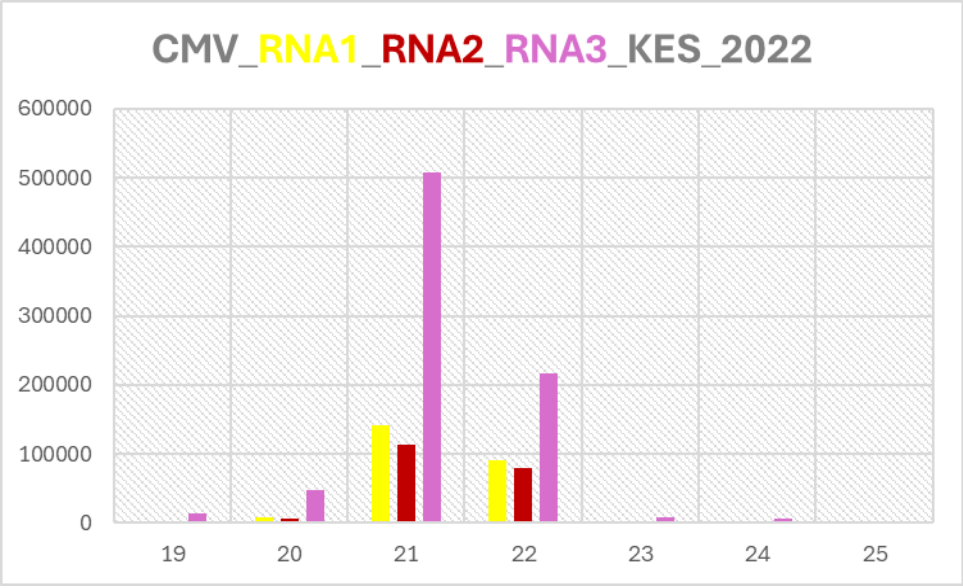

Figure 9. Size distributions of of viral reads mapped in the K2022 sRNA library in case of CMV RNA1, RNA2 and RNA3

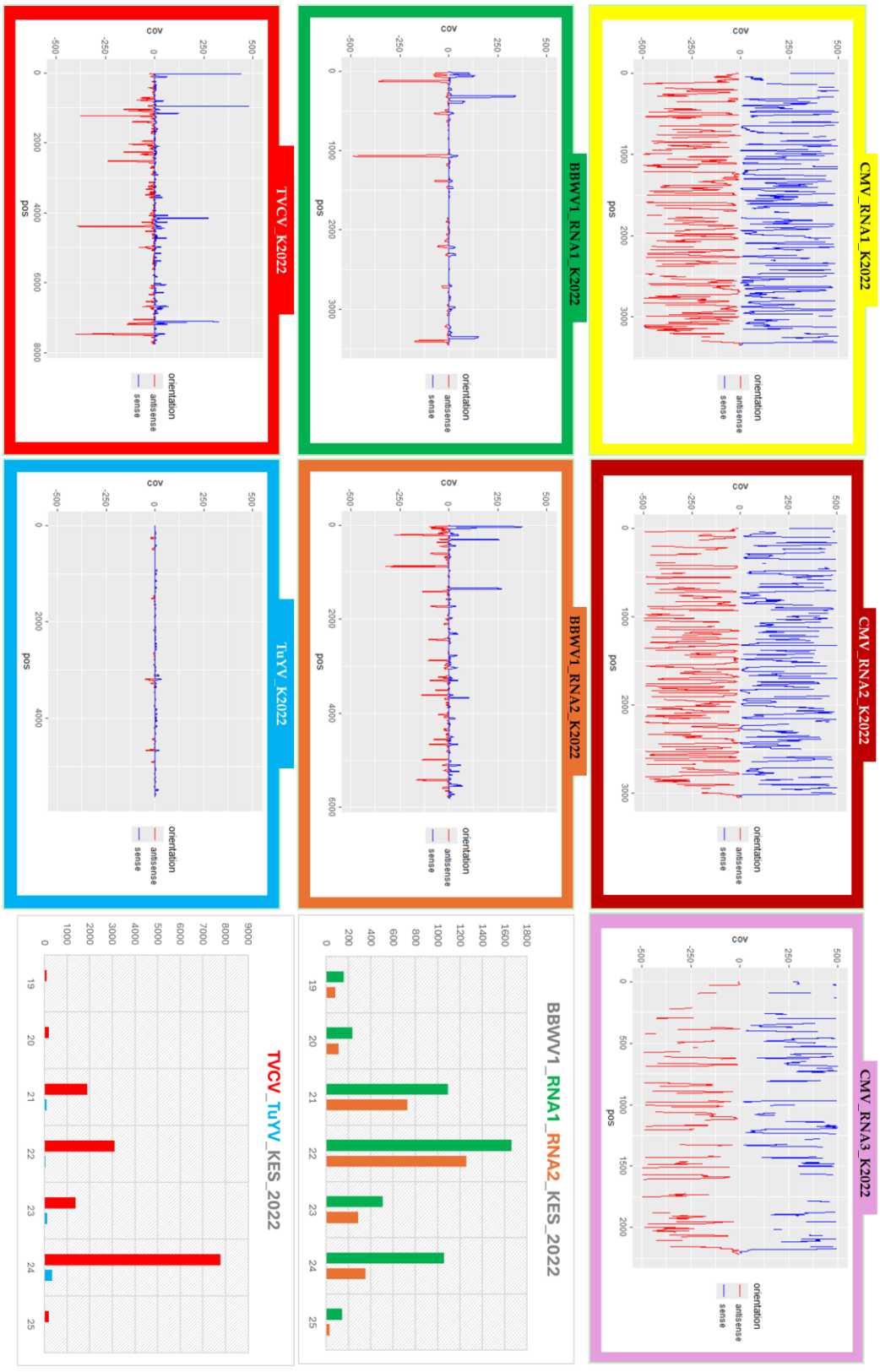

Figure 10. Investigation of viral reads mapped in the K2022 sRNA library showed both the coverage of the viral genome by sRNAs and the distribution of their sizes.

5.4.2 Results of the Keszthely, 2023 Weed Sampling

For the K2023 sampling, a single total RNA library was prepared for all samples (SOL_KES_17). A total of 23,061,440 reads were generated, and after trimming (including redundant sequences), 22,913,754 high-quality reads were retained, from which 71,700 contigs were assembled (Table 13).

Table 13. Initial statistics of the RNAseq for the K2023 samples.

Year	HTS	**Library code**	**Sequenced reads**	**Trimmed reads all (containing redundants)**	**Non-redundant reads**	**Number of contigs**
K2023	RNAseq	SOL_KES_17	23 061 440	22 913 754	n/a	71 700

BLAST analysis of the contigs identified seven viruses with significant similarity (E-value = 0): Potato virus M (PVM), Potato virus H (PVH), Obuda pepper virus (ObPV), Tobacco vein clearing virus (TVCV), Lettuce big-vein associated virus (LBVaV), Oxybasis rubra mitovirus 1 (OxruMV1), and Potato latent virus (PotLV). Genome coverage varied among viruses: 82% for PVM, 90% for PVH, 33% for ObPV, 45% for TVCV, 99% for LBVaV (both RNA1 and RNA2), 72% for OxruMV1, and 31% for PotLV (Table 14).

Table 14. Bioinformatics results showing the viruses identified in the K2023 samples through RNA-Seq analysis.

	Virus		**RNAseq**			
			GenBankId of the reference genome	**number of contigs**	**number of mapped reads**	**coverage of the viral genome (%)**
K2023	**PVM**		NC_001361	6	582615	82%
	PVH		NC_018175	11	90905	90%
	ObPV		NC_003852	2	47	33%
	TVCV		NC_003378	11	2452	45%
	LBVaV	**RNA1**	NC_011558	1	56368	99%
		RNA2	NC_011568	1	16005	99%
	OxruMV1		NC_076526	6	411315	72%
	PotLV		NC_011525	2	113601	31%

5.4.3 Results of the Kosovo, 2023 Cultivated Crop sampling

For the Ko2023 sampling, a total RNA library (SOL_KOS_18) was prepared to represent all sampled plant species. A total of 21,558,420 reads were obtained. Following trimming and quality control, 21,442,968 reads were retained. *De novo* assembly of these reads resulted in 40,362 contigs (Table 15).

Table 15. Initial statistics of the RNAseq for Ko2023 samples.

Library code	Sequenced reads	Trimmed reads all (containing redundants)	Non-redundant reads	Number of contigs
SOL_KOS_18	21 558 420	21 442 968	n/a	40362

For all datasets, the assembled contigs were further analyzed by BLAST against reference genomes of known plant-infecting viruses. For Ko2023, nine viruses were detected via BLAST of contigs, each represented by at least one contig with significant homology (E-value = 0): Cucumber mosaic virus (CMV), Broad bean wilt virus (BBWV2), Potato virus Y (PVY), Pepper cryptic virus 2 (PCV2), Bell pepper endornavirus (BPEV), Ranunculus white mottle virus (RWMV), Tobacco vein clearing virus (TVCV), Tomato aspermy virus (TAV), and CMV satellite RNA (CMVs). Mapping of viral reads to the genomes showed high coverage: 100% for all three CMV RNAs, 96% for BBWV2 RNA1, 99% for BBWV2 RNA2, 99% for PVY, 99% for PCV2 (RNA1 and RNA2), 98% for BPEV, >97% for all four RWMV RNAs, 85% for TVCV, 65% for TAV, and 99% for CMV satellite RNA. The contigs usually covered the whole genome of the viruses, except in the case of TVCV, TAV and CMV satellite. Here the contigs were shorter than the viral genome itself, or despite their length, only some of their part showed similarity to the viruses. Direct BLAST of the contigs to the GenBank records revealed that they show high similarity to Solanaceae genomes, indicating that these hits are generated from the host genome. These similar parts in the case of TAV and CMVsat were short. In the case of TVCV, the identity of the contigs to the reference genome was quite long which could indicate the presence of host integrated parts of a previous infection (Table 16). Hits to the other six viruses appeared valid and were analyzed further using virus-specific RT-PCR.

Table 16. Bioinformatics results indicating viruses present in the investigated samples of experiment Ko2023.

	Virus		GenBank ID of the reference	Virus hit		
				number of contigs	number of mapped reads	coverage of the viral genome (%)
Ko2023	CMV	RNA1	NC_002034	2	387085	100%
		RNA2	NC_002035	4	319933	100%
		RNA3	NC_001440	9	1248670	100%
	BBWV2	RNA1	NC_003003	7	124493	96%
		RNA2	NC_003004	5	211548	99%
	PVY		NC_001616	6	610666	99%
	PCV2	RNA1	NC_034159	2	27242	99%
		RNA1	NC_034167	1	6786	99%
	BPEV		NC_039216	1	54178	98%
	RWMV	RNA1	NC_043389	2	227	99%
		RNA1	OR879093	3	494	98%
		RNA2	OR879094	1	1037	98%
		RNA3	OR879095	1	2460	97%
		RNA4	OR879096	1	800	97%
	TVCV		NC_003378	35	877	85%
	TAV		NC_003837	1	299906	65%
	CMVs		NC_002602	2	165732	99%

5.5 RT-PCR Validation of HTS Results for the Keszthely, 2022 Weed Survey

5.5.1 Molecular Detection and Phylogenetic Analysis of CMV

In the RNAseq dataset for CMV, we had one, one and two contigs mapped to the three segments of the CMV genome, respectively (Figure 11a). 115,006 reads mapped to RNA1, 100,107 reads mapped to RNA2 and 105,966 reads mapped to RNA3 covering 99% of the CMV genome (Table 12). While in the case of sRNAseq, we had sixty-two, fifty-four, thirty-one contigs mapped to the three segments of the CMV genome (Table 12). 234,654 reads mapped to RNA1, 190,706 reads mapped to RNA2 and 804,366 mapped to RNA3 covering 99% of the viral genome (Table 12).

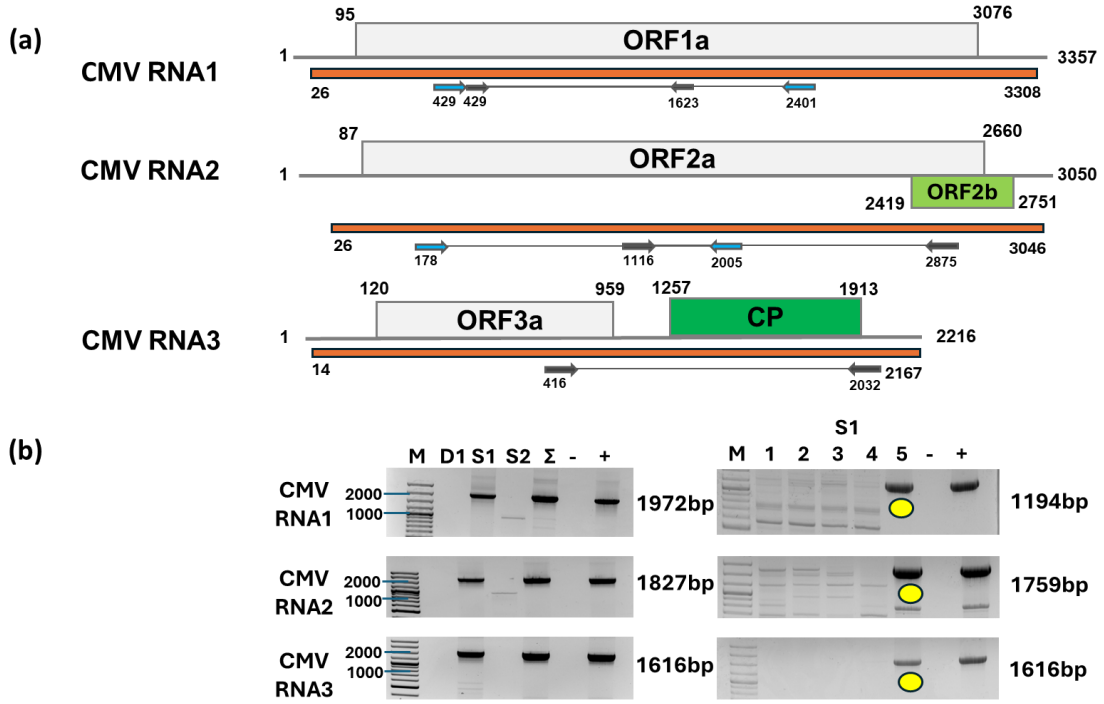

Figure 11. Summarized result of the HTS and its validation for the presence of CMV. (a) Schematic representation of the CMV genome, and the position of the primers used for RT-PCR validation. The orange line indicates the region covered by HTS sequencing results (b) the results of RT-PCR validation of the virus. M - represents the GeneRuler 100 bp Plus DNA Ladder, D1 - indicates the *Datura stramonium* pool, S1 - the *Solanum nigrum* pool of field I, S2 - the *Solanum nigrum* pool of field II, Σ - denotes the combined pool of D1, S1, and S2, - / + stand for negative and positive controls, S1: 1-5 denotes individuals of *Solanum nigrum* from field I. Yellow dots indicate the products which were cloned and sequenced.

To validate the presence of all three segments of CMV and investigate its presence in the different species and individuals, we designed primers based on the contig sequences and sequences of diverse CMV variants (Table 6). RT-PCR revealed the presence of CMV in *Solanum nigrum* field.

Only one individual, S1/5, was infected with the virus (Figure 11b). In the case of the infected individual, we cloned and sequenced the PCR product of RNA 1, RNA2 and RNA3 originating from the PCR using the cDNA prepared from the individuals as a template. After Sanger sequencing we checked for the possible presence of SNPs. As the sequence of the PCR product showed no SNP, we cloned and sequenced these products amplified from the RNA1, RNA2 and RNA3 and used them for phylogenetic analysis. Sequencing of the presenting CMV variants revealed that the S1/5 was infected with a variant belonging to the subgroup IA of CMV (Figure 12/a,b and c).

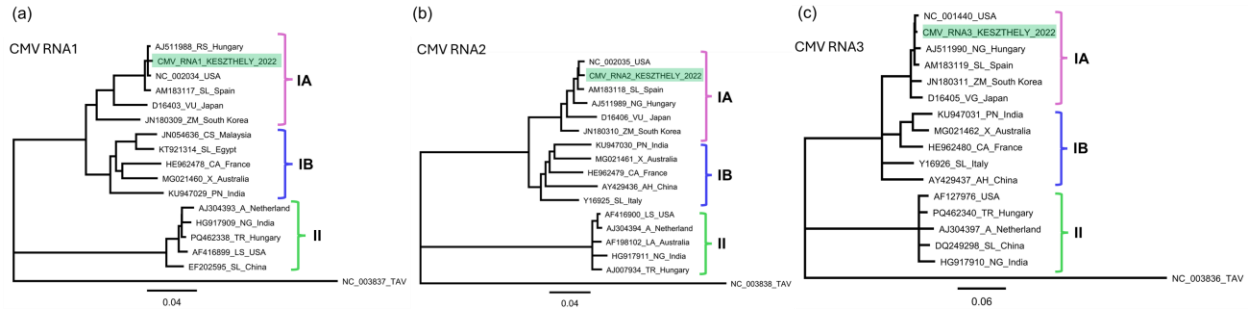

Figure 12. Phylogenetic analysis of CMV variants. (a) CMV RNA1, (b) CMV RNA2 and (c) CMV RNA3. The phylogenetic analysis was performed using the Geneious Tree Builder, applying the Tamura–Nei model and the neighbor-joining method with 1000 bootstrap replicates. Distinct colors represent the clustering of CMV subgroups. The CMV variants identified in our investigation are highlighted with green boxes. The sequences are indicated by their GenBank accession numbers. The middle panel of these indicates the host plant species, by using the following abbreviations: CA—*Capsicum annuum*, CS—*Cucumis sativus*, SL—*Solanum lycopersicum*, X—*Xanthosoma*, PN—*Piper nigrum*, RS—*Raphanus sativus*, VU—*Vigna unguiculata*, ZM—*Zea mays*, A—*Alstroemeria*, NG—*Nicotiana glutinosa*, TR—*Trifolium repens*, LS—*Lactuca saligna*, AH—*Arachis hypogaea*, and LA—*Lupinus angustifolius*.

5.5.2 Molecular Detection and Phylogenetic Analysis of BBWV1

According to the RNAseq results, one contig corresponding to RNA1 and one contig corresponding to RNA2 showed high identity to BBWV1 RNA1 and RNA2, respectively. In the sRNAseq data, sixteen contigs were associated with RNA1 and five with RNA2 (Figure 13a). A total of 58,198–5,377 reads were mapped to RNA1 and 42,076–2,612 reads to RNA2, resulting in 98% and 97% genome coverage of the BBWV1 segments, respectively (Table 12).

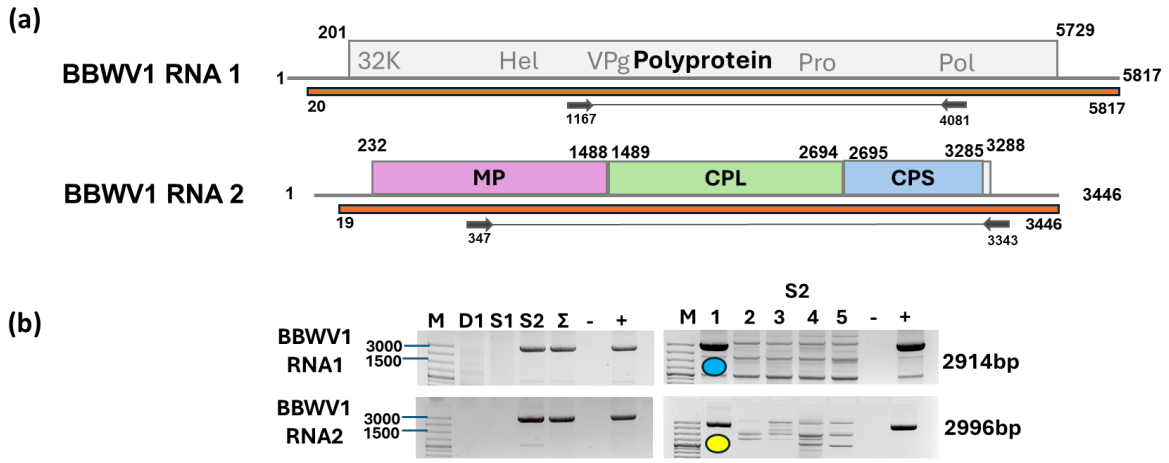

Figure 13. Summarized result of HTS and its validation for the presence of BBWV1. (a) Cartoon representation of the BBWV1 genome and the position of the primers used for RT-PCR validation. The orange line indicates the region covered by HTS sequencing results. (b) shows results of validation of the presence of BBWV2 using RT-PCR. M - represents the GeneRuler 100 bp Plus DNA Ladder, D1 - indicates the *Datura stramonium* pool, S1 - *Solanum nigrum* pool of field I, S2 - the *Solanum nigrum* pool of field II, Σ - denotes the combined pool of D1, S1, and S2, - / + stand for negative and positive controls, S2: 1-5 denotes individuals of *Solanum nigrum* from field II. Yellow dot indicate the product which were cloned and sequenced and blue dot represent PCR products that was purified and subjected to sequencing.

Validation of BBWV1 by RT-PCR revealed that only sample S2/1 was infected with this virus (Figure 13b). The PCR product obtained from this infected sample was directly sequenced without cloning for RNA1, whereas in the case of RNA2, the product was cloned and subsequently Sanger sequenced and then used for the phylogenetic tree (Figure 14).

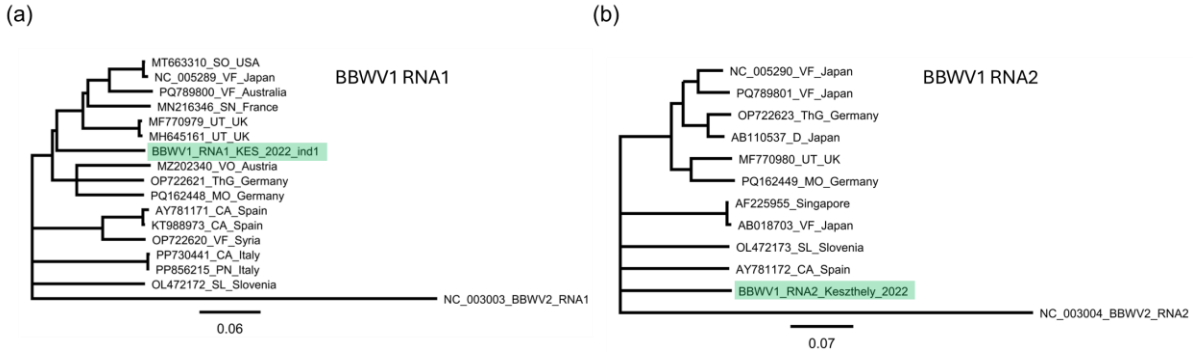

Figure 14. Phylogenetic analysis of BBWV1 variants (a) BBWV1 RNA1 and (b) BBWV1 RNA2. The phylogenetic analysis was performed using the Geneious Tree Builder, applying the Tamura–Nei model and the neighbor-joining method with 1000 bootstrap replicates. The BBWV1 variants identified in our investigation are highlighted with green boxes. The sequences are indicated by their GenBank accession numbers. The middle panel of these indicates the host plant species by using the following abbreviations: VF—*Vicia faba*, SO—*Spinacia oleracea*, SN—*Solanum nigrum*, UT—*Ullucus tuberosus*, ThG—*Thunbergia grandiflora*, VO—*Verbena officinalis*, MO—*Melissa officinalis*, CA—*Capsicum annuum*, SL—*Solanum lycopersicum*, PN—*Piper nigrum*, D—*Delphinium spp*.

The BBWV1 RNA1 sequence from *S. nigrum* in experiment K2022 groups within the European clade but forms its own distinct branch. Its closest relative is the UK isolate-MF770979, showing 85.233% nucleotide identity in the pairwise matrix, which confirms that the Keszthely variant is related to this UK strain but still represents a clearly separate lineage (Figure 14a). While the BBWV1 RNA2 sequence from K2022 forms a separate branch within the broader BBWV1 RNA2 diversity, positioned toward the base of the European–Asian clade. According to the pairwise identity matrix, its closest relative is the Japanese isolate, NC_005290, showing 81.615% nucleotide identity. Although it clusters near several Asian and European isolates, the branch separation indicates that the Keszthely RNA2 represents a genetically distinct variant, sharing its highest similarity with a *Vicia faba*–derived strain from Japan but still diverging substantially from all known sequences (Figure 14b).

5.5.3 Molecular Detection of TVCV

RNA-seq analysis showed nineteen contigs matching TVCV, covering eighty-nine percent of the viral genome (Figure 15a). A total of 95,208 reads mapped to the virus, while in sRNA twenty-five contigs corresponding to TVCV were obtained, representing eighty percent coverage of the viral genome, including 2,274 non-redundant reads and 14,799 redundant reads, with an RPM of 688 (Table 12). RT-PCR assays confirmed the presence of TVCV in all *Solanum nigrum* individuals from population S1, indicating that the virus is widespread within this group. A similar pattern was observed in population S2, where every tested plant also showed a positive result (Figure 15b).

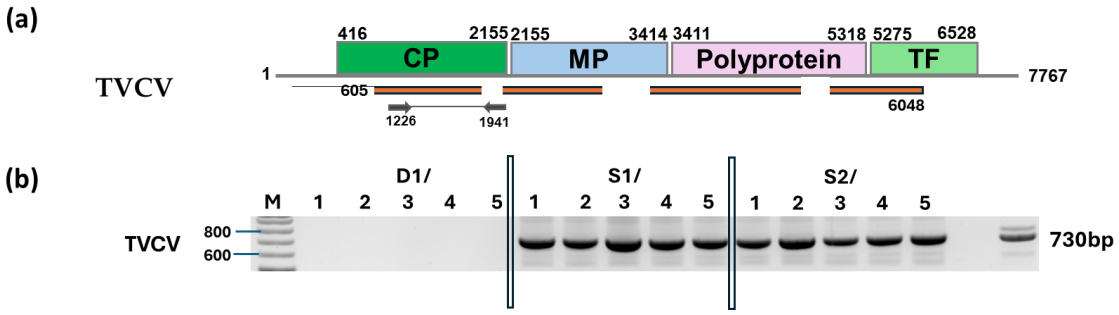

Figure 15. Summarized result of HTS and its validation for the presence of TVCV (a) Illustration representing the TVCV genome and the position of primers used for RT-PCR validation. The orange line indicates the region covered by HTS sequencing results. (b) shows results of validation of the presence of TVCV using RT-PCR. M - represents the GeneRuler 100 bp Plus DNA Ladder, D1/ 1-5 - indicates the *Datura stramonium* individuals of Field I, S1/1-5 – *Solanum nigrum* pool of field I, S2/1-5 – *Solanum nigrum* individuals of field II.

5.5.4 Molecular Detection of TuYV

RNA-seq analysis generated five contigs corresponding to TuYV, covering approximately ninety percent of the viral genome, with a total of 12,627 reads mapped to the virus (Figure 16a). In contrast, sRNA sequencing did not produce TuYV-specific contigs, although mapped reads collectively represented about forty-three percent of the viral genome, including 239 non-redundant reads and 629 redundant reads, corresponding to an RPM of 29 (Table 12).

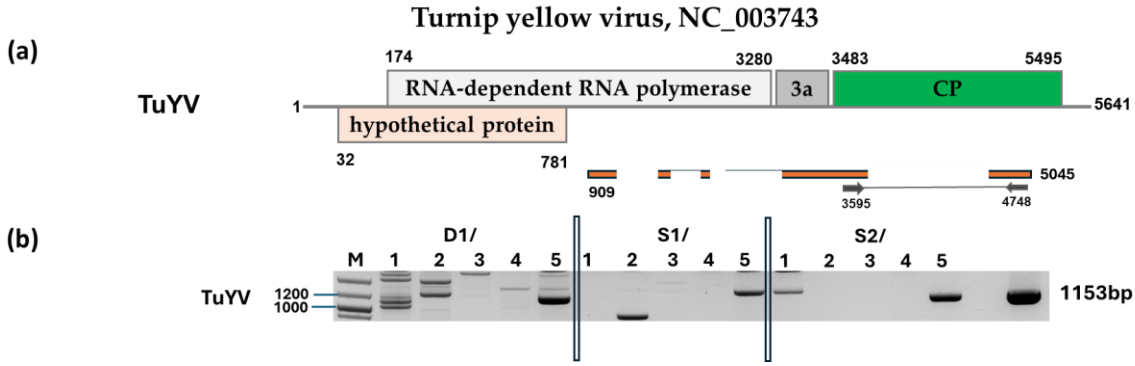

Figure 16. Summarized result of HTS and its validation for the presence of TuYV (a) Illustration representing the TuYV genome and the position of primers used for RT-PCR validation. The orange line indicates the region covered by HTS sequencing results. (b) shows results of validation of the presence of TuYV using RT-PCR. M - represents the GeneRuler 100 bp Plus DNA Ladder, D1/ 1-5 - indicates the *Datura stramonium* individuals of Field I, S1/1-5 – *Solanum nigrum* pool of field I, S2/1-5 – *Solanum nigrum* individuals of field II.

The RT-PCR assays shown in (Figure 16b) confirmed the presence of Turnip yellows virus (TuYV) in samples D1/5 and S2/5, as indicated by the amplification of virus-specific fragments of the expected size.

5.6 RT-PCR Validation of HTS Results for the Keszthely, 2023 Weed Survey

5.6.1 Molecular Detection and Phylogenetic Analysis of PVM

From the sequencing data, six contigs were assembled, and a total of 582,615 reads mapped to the PVM genome, resulting in substantial genome coverage of 82% and providing a detailed view of the viral sequence within these host plants (Figure 17a; Table 14).

Detection of PVM in the species pools revealed that every individual of *Solanum nigrum* (S3) and *Solanum dulcamara* was infected, indicating a widespread presence of this virus in the sampled populations (Figure 17b).

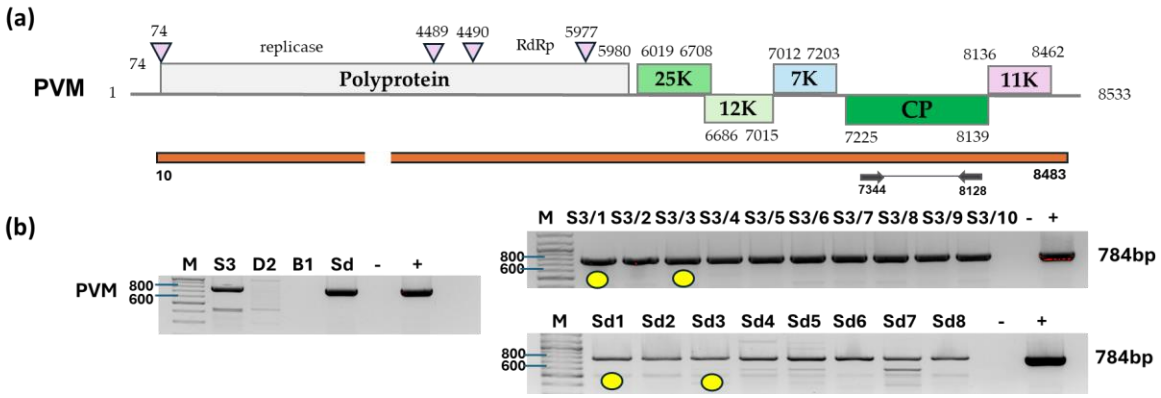

Figure 17. Summarized result of the HTS and its validation for the presence of PVM (a) Illustration representing the PVM genome and the position of primers used for RT-PCR validation. The orange line indicates the region covered by HTS sequencing results. (b) shows results of validation of the presence of PVM using RT-PCR. M - represents the GeneRuler 100 bp Plus DNA Ladder, S3 - indicates the *Solanum nigrum* pool of Field III, D2 – *Datura stramonium* pool of field II, B1 – *Brassica napus* pool of Field II, Sd – *Solanum dulcamara* pool, - / + stands for negative and positive controls, S3: 1-10 denotes individuals of *Solanum nigrum* from Field III while Sd: 1-8 denotes individuals of *Solanum dulcamara*. Yellow dots indicate the products which were cloned and sequenced.

For PVM, samples S3/1, S3/3, Sd1 and Sd3 were cloned. The PCR products obtained from these individuals were cloned and Sanger sequenced. The resulting sequences, derived from cDNA of the respective samples, were investigated for the presence of SNPs. As no SNPs were detected in any of the cloned sequences, they were used for the phylogenetic analysis.

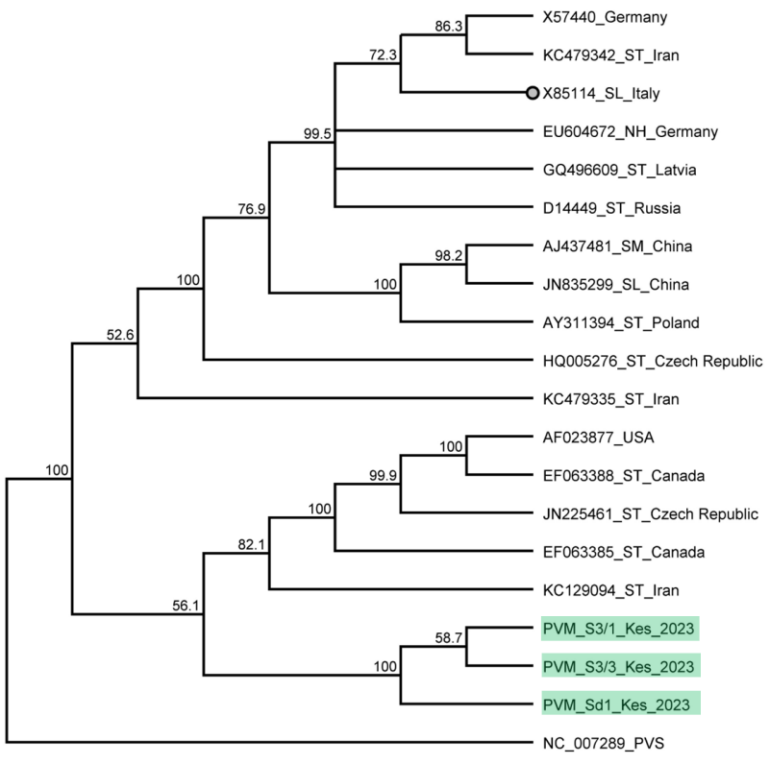

Figure 18. Phylogenetic analysis of PVM variants. The phylogenetic analysis was performed using the Geneious Tree Builder, applying the Tamura–Nei model and the neighbour-joining method with 1000 bootstrap replicates. The PVM variants identified in our investigation are highlighted with green boxes. The sequences are indicated by their GenBank accession numbers. The middle panel of these indicates the host plant species by using the following abbreviations: ST — *Solanum tuberosum*, SL — *Solanum lycopersicum,* NH — *Nicotiana hesperis*, SM — *Solanum muricatum*.

5.6.2 Molecular Detection of PVH

For PVH, a total of 11 contigs were identified across the sampled plants, with 90,905 reads mapping to the viral genome (Figure 19a). This resulted in 90% genome coverage, providing a comprehensive representation of the virus and confirming its active presence within the infected hosts (Table 14). Testing of PVH in the individuals of *S. dulcamara* after this pool appeared positive revealing that Sd1, Sd6 and Sd7 were infected (Figure 19b).

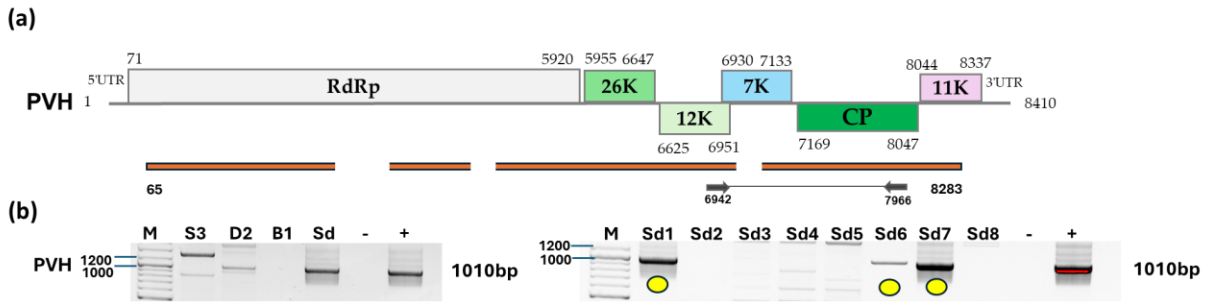

Figure 19. Summarized result of HTS and its validation for the presence of PVH (a) Illustration showing the PVH genome and the positions of primers used for RT-PCR validation. The orange line indicates the region covered by HTS sequencing results. (b) shows the results of validation of the presence of BBWV2 using RT-PCR. M - represents the GeneRuler 100 bp Plus DNA Ladder, S3 - indicates the *Solanum nigrum* pool of Field III, D2 – *Datura stramonium* pool of field II, B1 – *Brassica napus* pool, Sd – *Solanum dulcamara* pool, - / + stand for negative and positive controls, Sd: 1-8 denotes individuals of *Solanum dulcamara*. Yellow dots represent PCR products that were purified and subjected to sequencing.

5.6.3 Molecular Detection and Phylogenetic Analysis of ObPV

For ObPV, a total of 2 contigs were assembled (Figure 20a), with only 47 reads mapping to the viral genome, resulting in relatively low coverage of 33% (Table 14). Although the number of reads was very small and the genome coverage limited, the virus could still be successfully detected and amplified in three positive individuals (Figure 20b), demonstrating that even with minimal sequencing data, ObPV was present and active in the sampled plants.

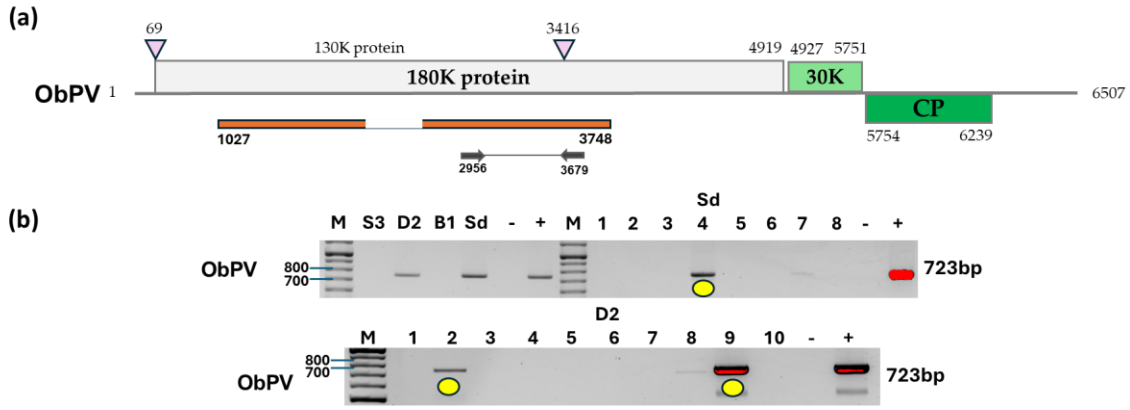

Figure 20. Summarized result of HTS and its validation for the presence of ObPV (a) Illustration showing the ObPV genome and the positions of primers used for RT-PCR validation. The orange line indicates the region covered by HTS sequencing results. (b) shows the results of validation of the presence of BBWV2 using RT-PCR. M - represents the GeneRuler 100 bp Plus DNA Ladder, S3 - indicates the *Solanum nigrum* pool of Field III, D2 – *Datura stramonium* pool of field II, B1 – *Brassica napus* pool, Sd – *Solanum dulcamara* pool, - / + stand for negative and positive controls, Sd: 1-8 denotes individuals of *Solanum dulcamara* while D2: 1-10 denotes individuals of *Datura stramonium* from field III. Yellow dots indicate the products which were cloned and sequenced.

To confirm the presence of ObPV across different species and individuals, primers were designed based on contig sequences (Table 6). RT-PCR detected ObPV in samples Sd/4, D2/2, and D2/9 (Figure 20b). The PCR products from these cDNA samples were then purified, cloned, and Sanger sequenced. Each sequence was checked for nucleotide variations, and since no SNPs were identified, the sequences were included in the phylogenetic analysis (Figure 21).

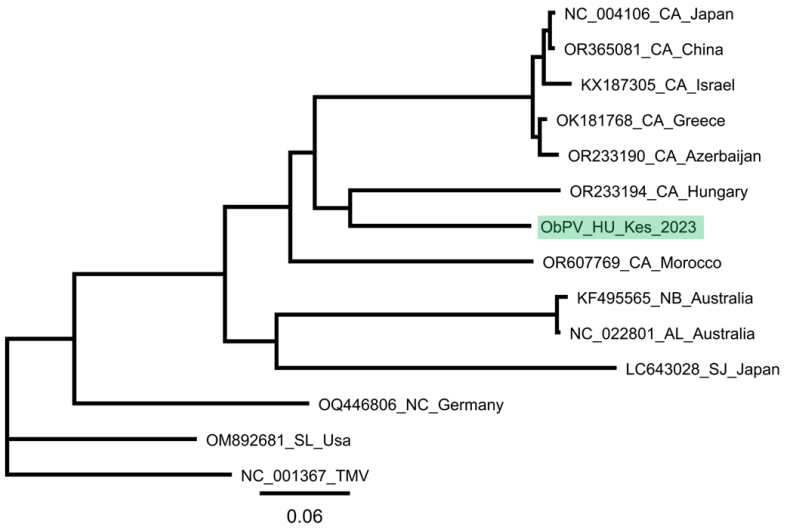

Figure 21. Phylogenetic analysis of ObPV. The phylogenetic analysis was performed using the Geneious Tree Builder, applying the Tamura–Nei model and the neighbor-joining method with 1000 bootstrap replicates. The ObPV variant identified in our investigation is highlighted with green box. The sequences are indicated by their GenBank accession numbers. The middle panel of these indicates the host plant species by using the following abbreviations: CA — *Capsicum annuum*, NB — *Nicotiana benthamiana,* AL— *Anthocercis littorea*, SJ — *Scopolia japonica,* NC — *Nic. Clevelandii*. SL— *Solanum lycopersicum*.

5.6.4 Molecular Detection and Phylogenetic Analysis of LBVaV

For LBVaV, both RNA1 and RNA2 segments were represented by a single contig each (Figure 22a). A total of 56,368 reads mapped to RNA1 and 16,005 reads mapped to RNA2, resulting in high genome coverage of 99% for both segments (Table 14). These results provide strong evidence of the virus's presence and indicate that both genomic segments were well represented in the sequencing data, allowing for a nearly complete characterization of LBVaV in the sampled plants.

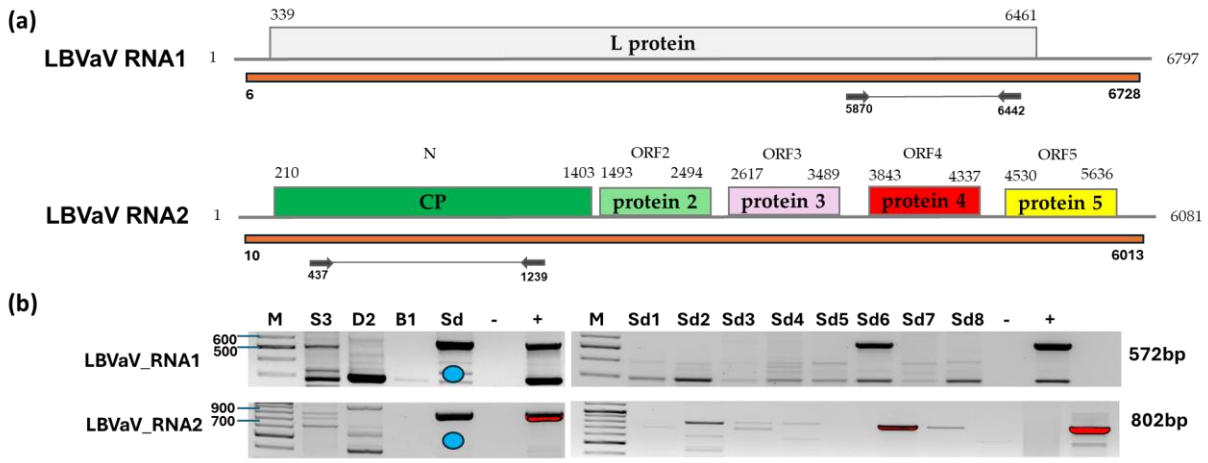

Figure 22. Summarized result of HTS and its validation for the presence of LBVaV (a) Illustration showing the LBVaV genome and the positions of primers used for RT-PCR validation. The orange line indicates the region covered by HTS sequencing results. (b) shows the results of validation of the presence of BBWV2 using RT-PCR. M - represents the GeneRuler 100 bp Plus DNA Ladder, S3 - indicates the *Solanum nigrum* pool of Field III, D2 – *Datura stramonium* pool of field II, B1 – *Brassica napus* pool of field II, Sd – *Solanum dulcamara* pool, - / + stand for negative and positive controls, Sd: 1-8 denotes individuals of *Solanum dulcamara*. Blue dots represent PCR products that were purified and subjected to sequencing.

To confirm the presence of LBVaV and evaluate its distribution across different species and individuals, primers were designed based on the contig sequences obtained from the sequencing data. RT-PCR detected LBVaV in both RNAs, RNA1 and RNA2, but only in the individual Sd/6 (Figure 22b). The PCR products from the pools were purified and then carefully checked for the presence of any single nucleotide polymorphisms (SNPs). As no SNPs were observed, the sequences were included in the phylogenetic analysis to assess their relationship with other LBVaV isolates.

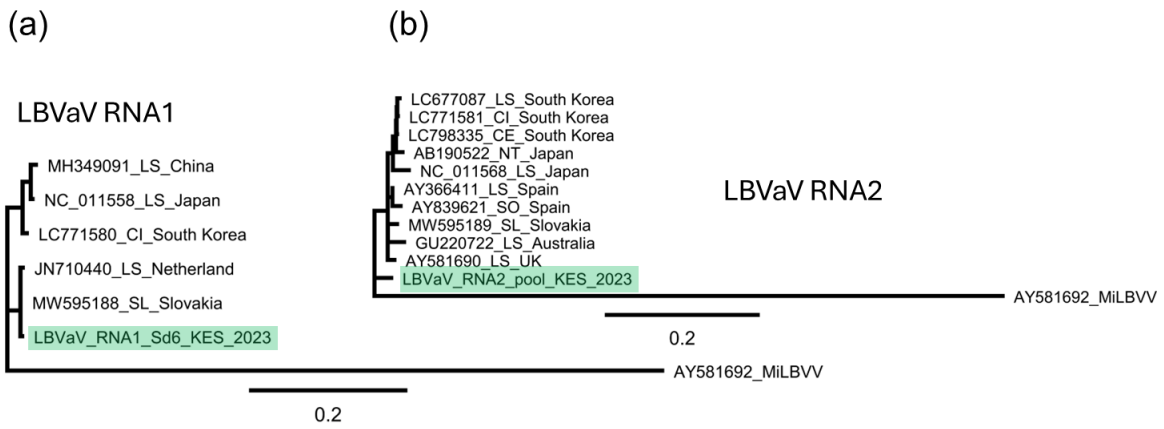

Figure 23. Phylogenetic analysis of LBVaV variants (a) LBVaV RNA1 and (b) LBVaV RNA2. The phylogenetic analysis was performed using the Geneious Tree Builder, applying the Tamura–Nei model and the neighbor-joining method with 1000 bootstrap replicates. The LBVaV variants identified in our investigation are highlighted with green boxes. The sequences are indicated by their GenBank accession numbers. The middle panel of these indicates the host plant species by using the following abbreviations: LS—*Lactuca sativa*, CI—*Cichorium intybus*, SL—*Solanum lycopersicum*, CE—*Cichorium endivia*, NT—*Nicotiana tabacum*, SO—*Sonchus oleraceus*.

The LBVaV RNA1 sequence obtained from *S. dulcamara* in experiment K2023 clusters within the main LBVaV lineage (Figure 23a). According to the pairwise identity matrix, its closest relative is JN710440_LS_Netherland, a *Lactuca sativa*–derived isolate, showing 98.295% nucleotide identity, indicating a highly similar but not identical variant. The LBVaV RNA2 sequence from experiment K2023 clusters in a different sub-branch than the RNA1 isolate (Figure 23b). According to the identity matrix, its closest relative is the *Solanum lycopersicum* isolate MW595189_SL_Slovakia, with 96.381% nucleotide identity.

5.6.5 Molecular Detection and Phylogenetic Analysis of OxruMV1

OxruMV1 was detected with a total of six contigs, and a relatively high number of 411,315 reads, mapped to the viral genome, resulting in coverage of 72% (Figure 24a; Table 14). These results indicate a substantial presence of OxruMV1 in the sampled plants, with the sequencing data capturing a significant portion of the viral genome and allowing for a reliable characterization of the infection.

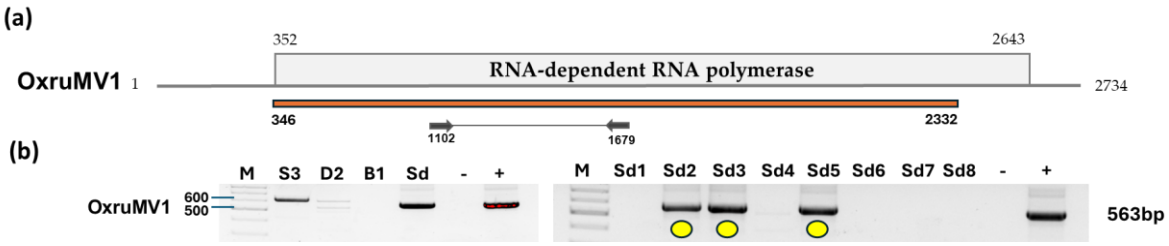

Figure 24. Summarized result of HTS and its validation for the presence of OxruMV1 (a) Illustration showing the ObPV genome and the positions of primers used for RT-PCR validation. The orange line indicates the region covered by HTS sequencing result. (b) shows the results of validation of the presence of BBWV2 using RT-PCR. M - represents the GeneRuler 100 bp Plus DNA Ladder, S3 - indicates the *Solanum nigrum* pool of Field III, D2 – *Datura stramonium* pool of field II, B1 – *Brassica napus* pool of field II, Sd – *Solanum dulcamara* pool, - / + stand for negative and positive controls, Sd: 1-8 denotes individuals of *Solanum dulcamara*. Yellow dots represent PCR products that were purified and subjected to sequencing.

To confirm the presence of OxruMV1 and to check its distribution across different species and individuals, primers were designed based on contig sequences (Table 6). RT-PCR identified OxruMV1 in the *Solanum dulcamara* pool within samples Sd/2, Sd/3, and Sd/5 (Figure 24b). The corresponding PCR products were purified, cloned, and Sanger sequenced. These sequences were then incorporated into phylogenetic analyses.

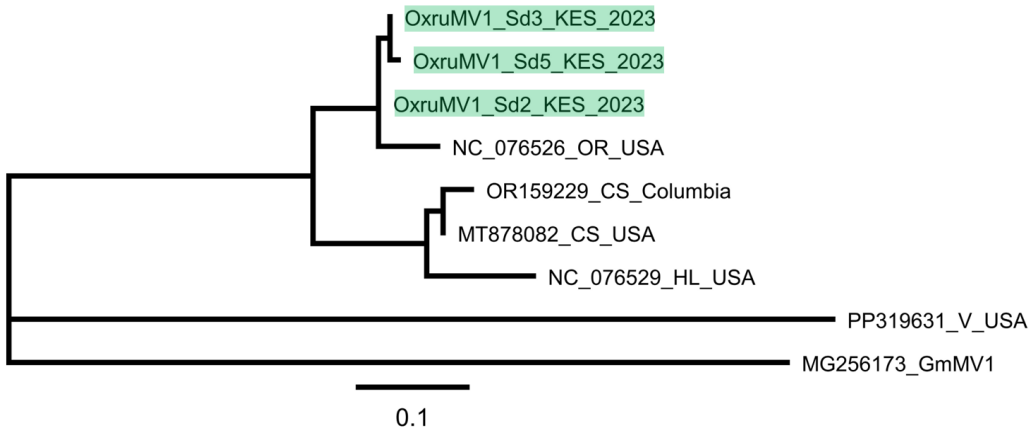

Figure 25. Phylogenetic analysis of OxruMV1 variants. The phylogenetic analysis was performed using the Geneious Tree Builder, applying the Tamura–Nei model and the neighbor-joining method with 1000 bootstrap replicates. The OxruMV1 variants identified in our investigation are highlighted with green boxes. The sequences are indicated by their GenBank accession numbers. The middle panel of these indicates the host plant species using the following abbreviations: OR — *Oxybasis rubra,* CS — *Cannabis sativa,* HL — *Humulus lupulus.*

5.6.6 Molecular Detection and Phylogenetic Analysis of TVCV

TVCV was detected with a total of 11 contigs corresponding, covering 45% of the viral genome, and a total of 2,452 reads mapped to the virus (Figure 26a; Table 14).

Detection of TVCV showed that almost all individuals of *Solanum nigrum* S3 tested positive, with the exception of plant S3/5, for which no RT-PCR amplification was obtained (Figure 26b). This indicates a high infection rate within the S3 population. TVCV was also detected in *Datura stramonium*, D2, where two individuals, D2/1 and D2/7, were confirmed as infected (Figure 26b).

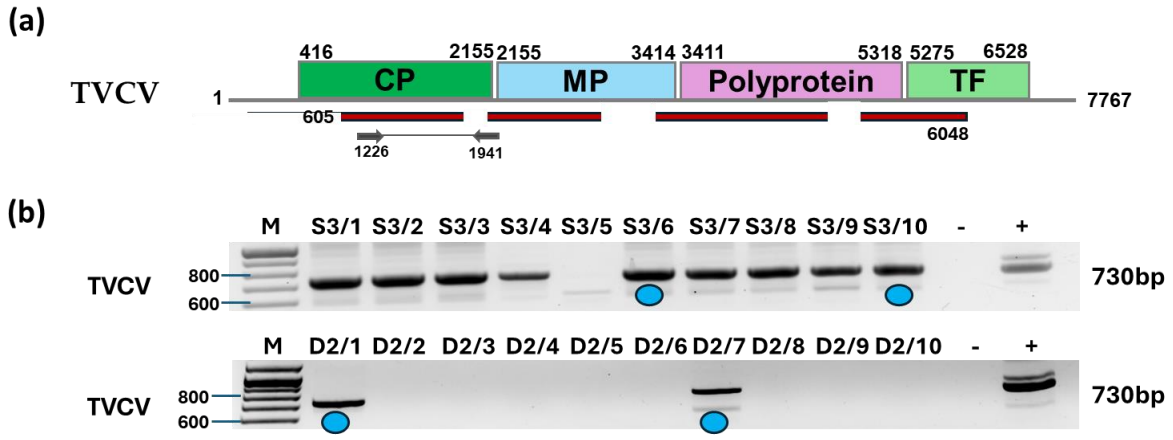

Figure 26: Summarized result of HTS and its validation for the presence of TVCV in experiment K2023. (a) Illustration representing the TVCV genome and the position of primers used for RT-PCR validation. The orange line indicates the region covered by HTS sequencing result. (b) shows the results of validation of the presence of TVCV using RT-PCR. M - represents the GeneRuler 100 bp Plus DNA Ladder, S3/1-10 – *Solanum nigrum* individuals of field III, D2/1-10 - indicates the *Datura stramonium* individuals of Field II,. Blue dots indicate the products which were purified and sequenced.

5.7 RT-PCR Validation of HTS Results for the Kosovo, 2023 Crop Survey

5.7.1 Molecular Detection and Phylogenetic Analysis of CMV

In the case of CMV, we had three, four and nine contigs mapped to the three segments of the CMV genome, respectively (Figure 27a). 387,085 reads mapped to RNA1, 319,933 reads mapped to RNA2 and 1,248,670 reads mapped to RNA3 covering 100% of the CMV genome (Table 16).

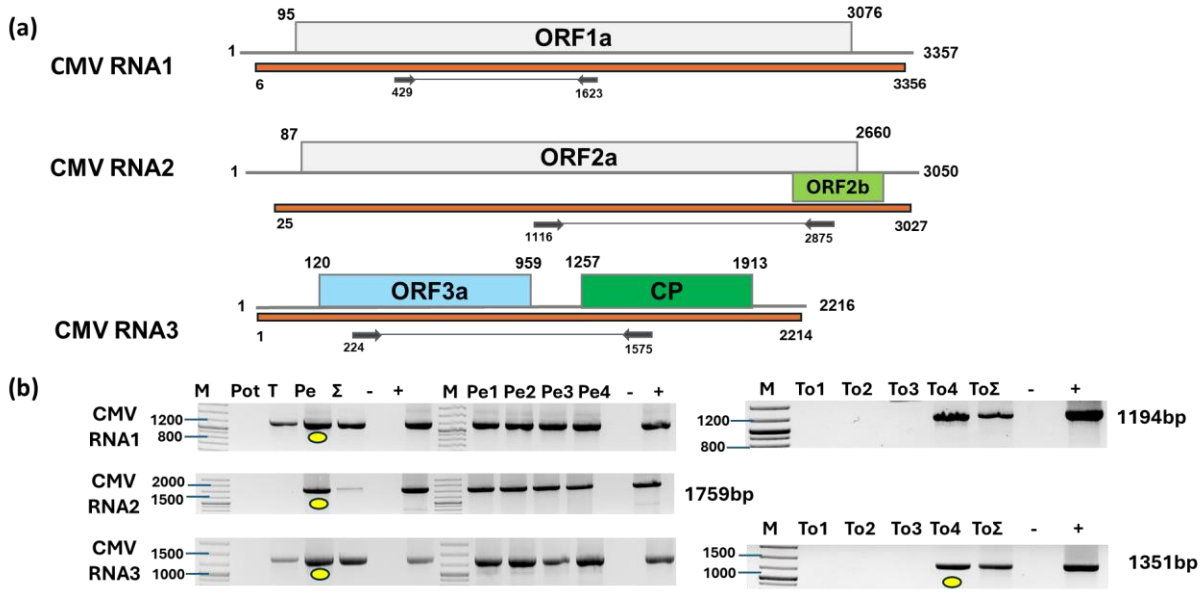

Figure 27. Results indicating the presence of CMV (a) Schematic representation of the CMV genome showing the positions of primers designed for RT-PCR validation. The orange represents the genomic region covered by HTS sequencing data. (b) RT-PCR validation results for CMV detection. M indicates the GeneRuler 100 bp Plus DNA Ladder; Pot refers to potato samples; T to tomato; and Pe to the pepper pool. The symbol Σ represents the combined pool of Pot, T, and Pe samples that were subjected to sequencing. The symbols − and + denote the negative and positive controls, respectively. Pe1, Pe2, Pe3, and Pe4 correspond to individual pepper plants, while To1, To2, To3, and To4 correspond to individual tomato plants. Yellow dots indicate the amplicons that were cloned and subsequently sequenced.

To validate the presence of both three segments of the CMV and inspect its presence in the different species and individuals we designed primers based on the contig sequences and sequences of diverse CMV variants (Table 6). RT-PCR revealed the presence of CMV in tomato and pepper. Only one tomato, but all four pepper individuals were infected with the virus (Figure 27b). In the case of tomato, we cloned and sequenced the PCR product of RNA 3 originating from the PCR using the cDNA prepared from the individuals as a template (GenBank accession number PV102684). In case of pepper the PCR product originating from the PCR, when the cDNA prepared from the pepper pool was the template, which was sequenced and checked for the possible presence of SNPs. As the sequences of these PCR products showed no SNP, we cloned and sequenced these products amplified from the RNA1, RNA2 and RNA3 (GenBank accession number PV020939-41) and used them for phylogenetic analysis. Sequencing of the presenting CMV variants revealed that the tomato plant was infected with a variant belonging to the less virulent subgroup II of CMV (Figure 28).

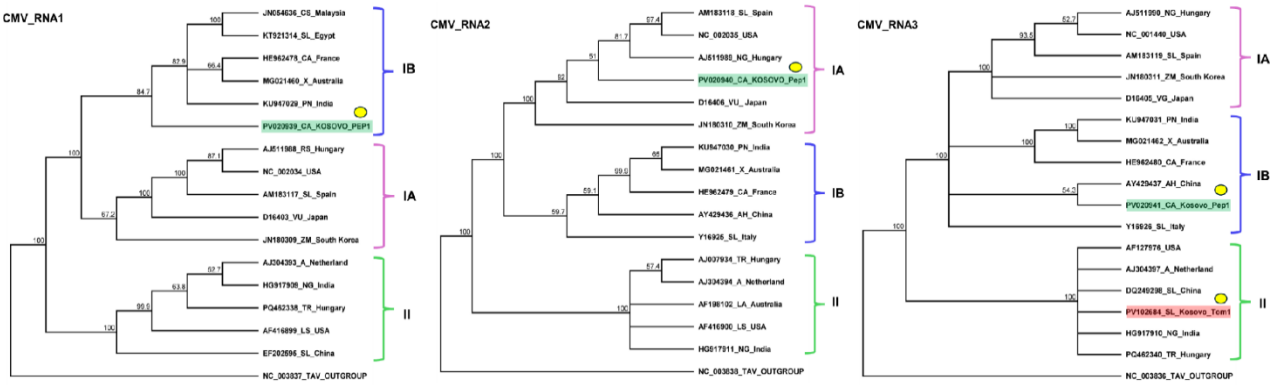

Figure 28. Phylogenetic analysis of CMV variants found in Kosovo. The phylogenetic analysis was performed using the Geneious Tree Builder, applying the Tamura–Nei model and the neighbor-joining method with 1000 bootstrap replicates. Distinct colors represent the clustering of CMV subgroups. The CMV variants identified in pepper and tomato are highlighted with green and red boxes, respectively. Yellow dots indicate the variants sequenced in this study. The sequences are indicated by their GenBank accession numbers. The middle panel of these indicates the host plant species by using the following abbreviations: CA—*Capsicum annuum*, CS—*Cucumis sativus*, SL—*Solanum lycopersicum*, X—*Xanthosoma*, PN—*Piper nigrum*, RS—*Raphanus sativus*, VU—*Vigna unguiculata*, ZM—*Zea mays*, A—*Alstroemeria*, NG—*Nicotiana glutinosa*, TR—*Trifolium repens*, LS—*Lactuca saligna*, AH—*Arachis hypogaea*, and LA—*Lupinus angustifolius*.

The CMV variant identified in pepper appeared to represent a reassortant within subgroup I variants. Specifically, RNA1 and RNA3 were grouped within subgroup IB, while RNA2 clustered within subgroup IA. The RNA1 segment of the KOSPep variant showed a notable divergence from other CMV variants available in GenBank, sharing the highest nucleotide identity (92.552%) with an isolate obtained from *Capsicum* sp. in France (accession number HE962478). In contrast, the closest homolog of KOSPep CMV RNA2 was identified as a tomato-derived variant from Spain (AM183118), showing 60.356% identity, although the two variants did not appear to be directly related phylogenetically. Furthermore, KOSPep RNA3 displayed the highest similarity (91.985%) to an Italian tomato isolate (Y16926), while the KOSTom RNA3 sequence exhibited the greatest similarity (97.498%) to a Hungarian *Trifolium repens* variant (PQ462340).

5.7.2 Molecular Detection and Phylogenetic Analysis of BBWV2

Seven and five contigs showed high identity to BBWV2 RNA1 and RNA2, respectively While 124,493 reads could be mapped to RNA1, 211,548 reads could be mapped to RNA2 resulting 96% and 99% coverage of the BBWV2 segments (Figure 29a; Table 16).

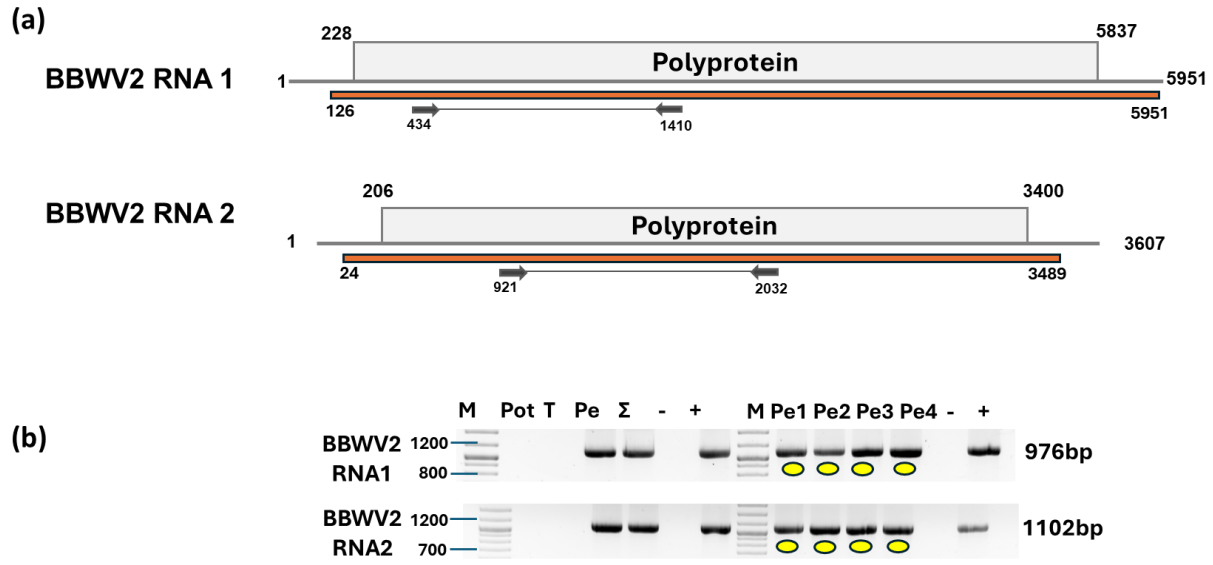

Figure 29. Results indicating the presence of BBWV2 (a) Schematic representation of the BBWV2 genome showing the positions of primers designed for RT-PCR validation. The orange line represents the genomic region covered by HTS sequencing data. (b) Validation of the presence of BBWV2 using RT-PCR. M represents the GeneRuler 100 bp Plus DNA Ladder; Pot indicates potato; T denotes tomato; Pe indicates the pepper pool; Σ denotes the combined pool of Pot, T, and Pe that was sequenced; −/+ indicate negative and positive controls, respectively; and Pe1, Pe2, Pe3, and Pe4 denote individual pepper plants. Yellow dots indicate the products that were cloned and sequenced.

The validation of BBWV2 revealed that only pepper plants, including all four individual samples, were infected with this virus (Figure 29b). The PCR products obtained from these individuals were cloned and subsequently Sanger-sequenced (GenBank accession numbers PV020942-PV020948). Sequencing of the amplified regions of RNA1 and RNA2 of BBWV2 identified three and four closely related variants, respectively, which clustered within subgroup II and between the two BBWV2 subgroups (Figure 30). These variants showed considerable divergence from previously reported BBWV2 isolates in GenBank, exhibiting 78–92% nucleotide identity for RNA1 and 80–86% for RNA2. The RNA1 sequence of the BBWV2 KOSPep variant showed the highest similarity (92%) to a tomato-derived isolate from China (FN985164, subgroup II), whereas RNA2 displayed the greatest similarity (87%) to a *Vicia faba* isolate from Japan (AB013616, subgroup I).

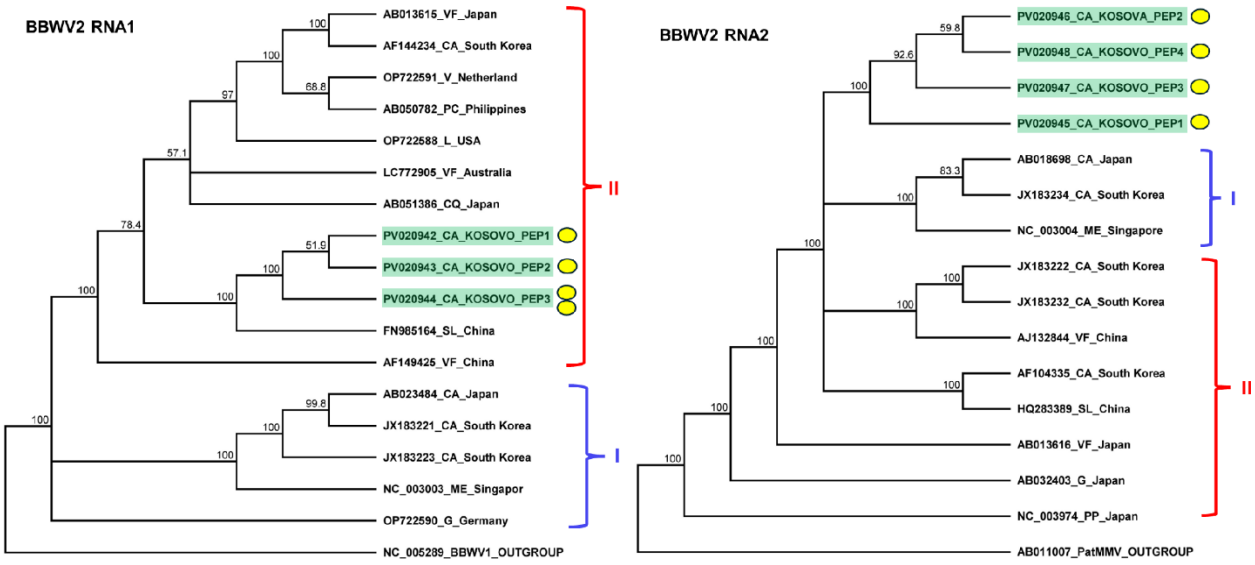

Figure 30. Phylogenetic analysis of the BBWV2 variants found in Kosovo. The phylogenetic analysis was performed using the Geneious Tree Builder, applying the Tamura–Nei model and the neighbor-joining method with 1000 bootstrap replicates. Red and blue lines represent the clustering of BBWV2 subgroup variants. Yellow dots indicate the variants sequenced in the present study. All sequences are labeled with their corresponding GenBank accession numbers. The middle panel of these indicates the host plant species by using the following ab-breviations: VF—*Vicia faba*, CA—*Capsicum annuum*, V—*Verbena*, PC—*Pogostemon cablin*, L—*Lactuca spp.,* CQ—*Chenopodium quinoa*, LE—*Lycopersicon esculentum*, ME—*Megaskepasma erythrochlamys*, G—*Gentiana*, and PP—*Pogostemon patchouli*.

5.7.3 Molecular Detection and Phylogenetic Analysis of PVY

A total of six contigs and 610,666 reads were successfully mapped to Potato virus Y (PVY), providing a nearly complete genome coverage of approximately 99% (Figure 31a; Table 16). This high mapping rate indicates a strong presence of PVY sequences within the sample, confirming its reliable detection and comprehensive representation in the dataset.

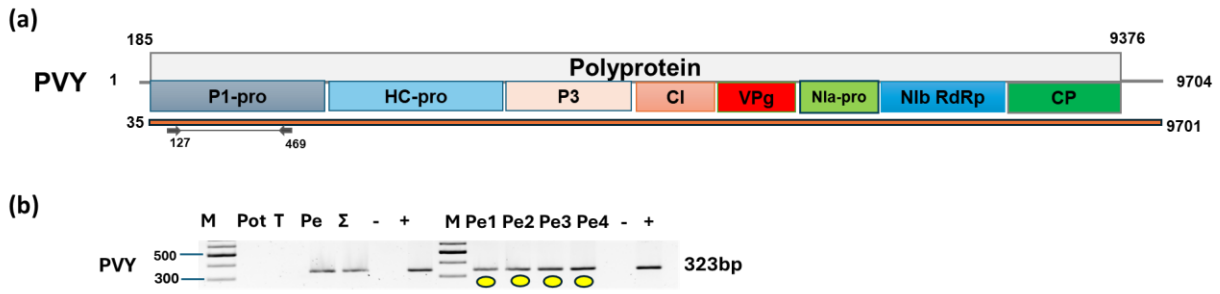

Figure 31. Results indicating the presence of PVY (a) Cartoon representation of the PVY genome and the positions of primers used for RT-PCR validation. The orange line indicates the region covered by the HTS sequencing results. (b) Results validating the presence of PVY RT-PCR. M represents the GeneRuler 100 bp Plus DNA Ladder; Pot indicates potato; T indicates tomato; Pe denotes the pepper pool; Σ denotes the combined pool of Pot, T, and Pe that were sequenced; −/+ denote negative and positive controls, respectively; and Pe1, Pe2, Pe3, and Pe4 denote individual pepper plants. Yellow dots indicate the products that were cloned and sequenced.

The validation of virus presence confirmed that all analyzed pepper samples were infected, whereas both potato and tomato plants tested negative for the virus (Figure 31b). Sanger sequencing of the cloned viral fragments revealed a high sequence identity (greater than 96%) with corresponding variants deposited in GenBank. Phylogenetic analysis further showed that the KOSPep variants formed a distinct cluster within the O clade (Figure 32).

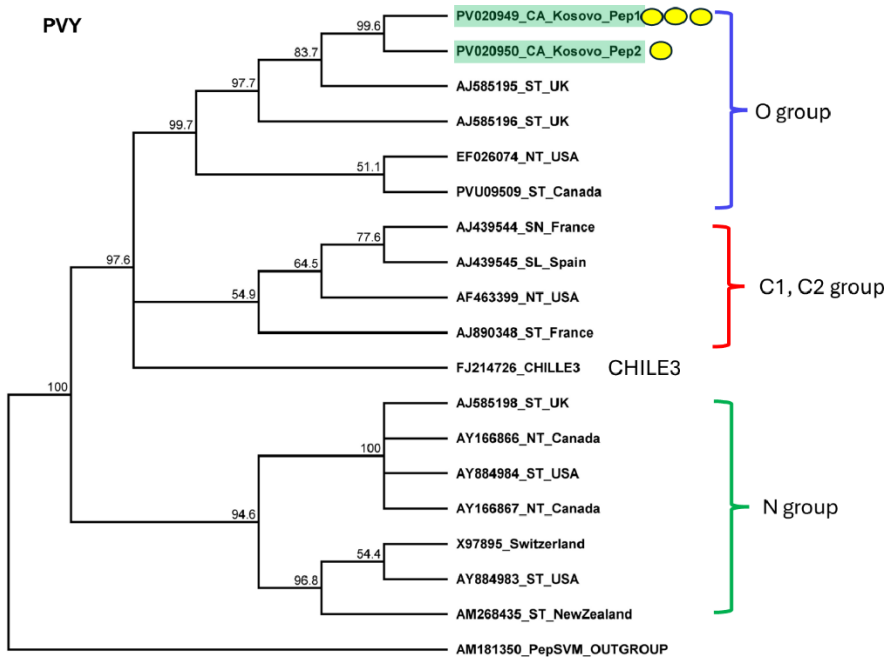

Figure 32. Phylogenetic analysis of Potato virus Y (PVY) variants detected in Kosovo was performed using the Geneious Tree Builder with the Tamura–Nei model, the neighbor-joining method, and 1000 bootstrap replicates. Green boxes indicate the pepper-derived PVY variants sequenced in this study, while the colored lines represent the different PVY subgroups, illustrating the genetic relationships and clustering patterns among the analyzed isolates. Yellow dots indicate the variants sequenced in this study. The sequences are indicated by their GenBank accession numbers. The middle panel of these indicates the host plant by using the following abbreviations: ST—*Solanum tuberosum*, NT—*Nicotiana tabacum*, SN—*Solanum nigrum*, and SL—*Solanum lycopersicum*.

5.7.4 Molecular Detection and Phylogenetic Analysis of PCV2 and BPEV

Two contigs showed sequence identity to the RNA1 segment of Pepper cryptic virus 2 (PCV2), while one contig was mapped to its RNA2 segment. In total, 27,242 and 6,786 reads were aligned to RNA1 and RNA2, respectively, providing 99% coverage of the complete viral genome (Figure 33a; Table 16). Additionally, a single contig corresponding to Bell pepper endornavirus (BPEV) was assembled from 54,178 mapped reads, covering approximately 99% of its genome (Figure 33c; Table 16).

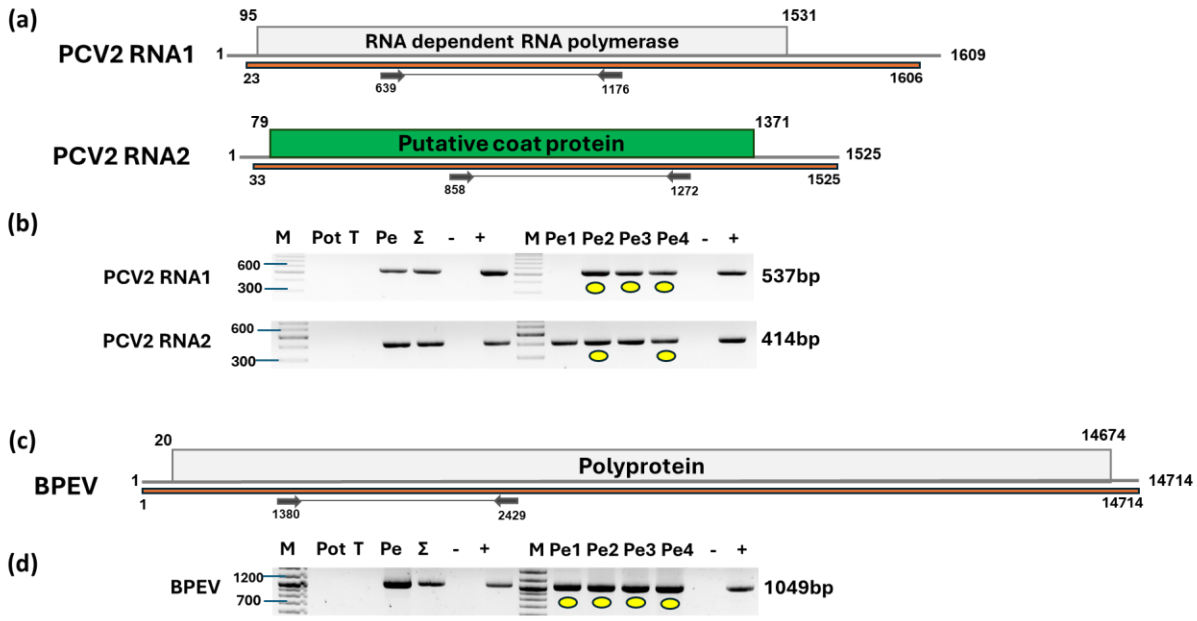

Figure 33. Detection and validation of PCV2 and BPEV in pepper samples (a) and (c) illustrate cartoon representations of the PCV2 and BPEV genomes, respectively, along with the positions of primers designed for RT-PCR validation. The orange line marks the regions covered by HTS sequencing. Panels (b) and (d) display the RT-PCR validation results confirming the presence of PCV2 and BPEV, respectively. M denotes the GeneRuler 100 bp Plus DNA Ladder; Pot represents potato pool; T indicates tomato pool; Pe corresponds to the pepper pool; and Σ represents the combined pool of Pot, T, and Pe that was sequenced. The symbols −/+ refer to negative and positive controls, respectively, while Pe1, Pe2, Pe3, and Pe4 indicate individual pepper plants. Yellow dots highlight the PCR products that were cloned and sequenced for further confirmation.

The validation of PCV2 and BPEV presence confirmed that all analyzed pepper plants were infected with these latent viruses (Figure 33b and d). However, amplification of the RNA1 segment of PCV2 in one pepper plant individual (Pe1) did not yield any product, likely due to a minor nucleotide variation at the primer annealing site of the PCV2 variant present in that individual. Sequencing of the amplified PCV2 RNA2 fragments revealed that the obtained sequences were identical or highly similar (over 99% identity) to corresponding PCV2 RNA2 sequences available in GenBank. The RNA1 sequences of the Kosovo variants were identical among themselves but showed slightly higher variability compared to RNA2, sharing over 97% identity with other PCV2 isolates. The closest homolog of the KOSPep variant was a strain previously reported in Slovakia (Figure 34/a).

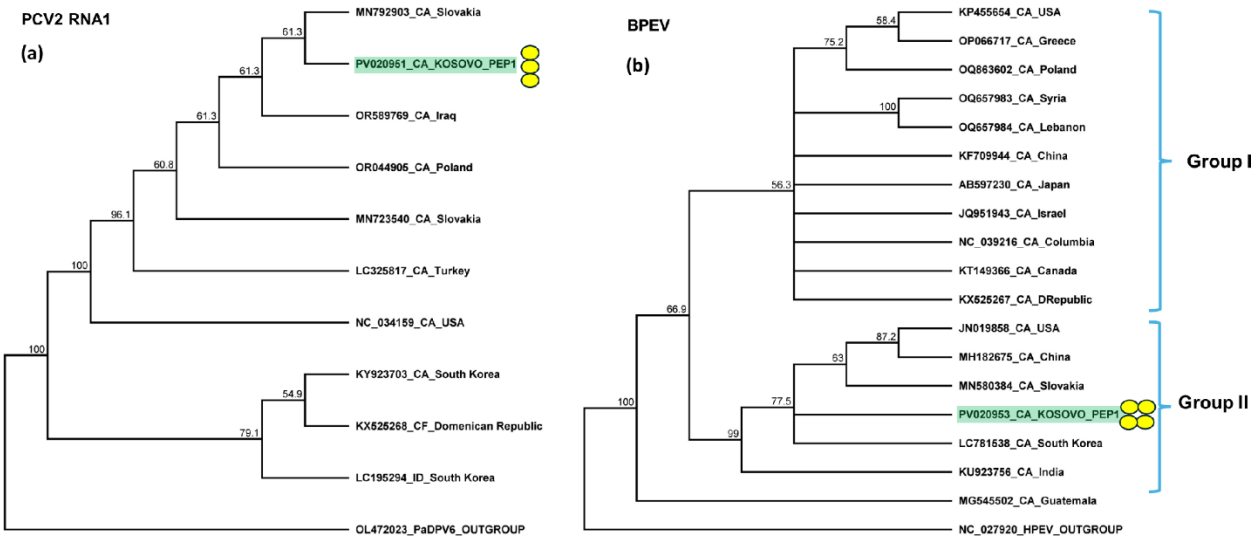

Figure 34. Phylogenetic analysis of the (a) PCV2 and (b) BPEV variants found in Kosovo. The analysis was conducted using Geneious Tree Builder with the Tamura–Nei model, the neighbor-joining method, and 1000 bootstrap replicates. Green boxes highlight the pepper variants sequenced in this study. Subgroups of BPEV are indicated. Yellow dots indicate the variants sequenced in this study. The sequences are indicated by their GenBank accession numbers. The middle panel of these indicates the host plant species by using the following abbreviations: CA—*Capsicum annuum*, CF—*Capsicum frutescens*, and ID—*Ixeridium dentatum*.

Sequencing of the amplified fragments of BPEV KOSPep revealed that all obtained variants were identical and grouped within clade II of this virus (Figure 34/b). The sequence showed 88–99% identity with corresponding BPEV variants deposited in GenBank, indicating a close genetic relationship with previously reported isolates.

5.7.5 Molecular Detection and Phylogenetic Analysis of RWMV

We found two contigs highly similar to RWMV RNA1. Mapping of the reads revealed 227 mapped reads, covering 99% of this reference genome. Direct BLAST search of these contigs revealed hits to an RWMV RNA1 (OR879093) sequence, which was indeed 3621nt longer than the NC_043389 reference genome. OR879093 was sequenced at DSMZ, together with three other RNAs originating from different segments of RWMV. BLAST of the contigs to these four RWMV genome segments revealed additional hits (three contigs could be mapped to RNA1, while an additional three were highly similar to RNA2, RNA3 and RNA4 of the virus) (Figure 35a). Remapping of the reads to each four segments resulted in 494, 1037, 2460 and 8800 mapped reads

to RNA1, RNA2, RNA3 and RNA4, respectively, and covering 98% of the viral genome in case of RNA1, 98% in case of RNA2, 97% in case of RNA3 and 97% in case of RNA4 (Table 16).

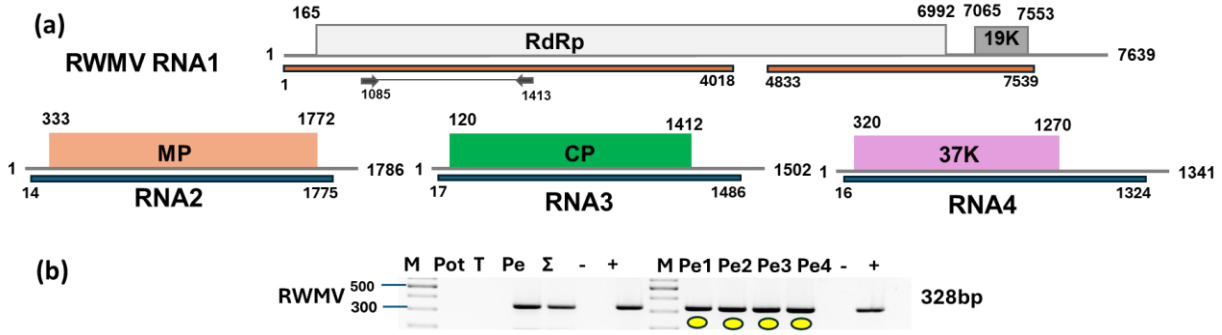

Figure 35. Results confirming the presence of Ranunculus white mottle virus (RWMV). (a) Schematic representation of the RWMV genome, showing RNA1, RNA2, RNA3, and RNA4, along with the positions of primers designed for RT-PCR validation. The orange line indicates the genomic regions covered by the HTS sequencing results. (b) RT-PCR validation confirming the presence of RWMV in the analyzed samples. M represents the GeneRuler 100 bp Plus DNA Ladder; Pot indicates potato; T indicates tomato; Pe indicates the pepper pool; Σ denotes the combined pool of Pot, T, and Pe that was se-quenced; −/+ denote negative and positive controls, respectively; Pe1, Pe2, Pe3, and Pe4 denote in-dividual pepper plants. Yellow dots indicate the products that were cloned and sequenced.

For validation of presence of the virus we tested the presence of RNA1. Our results showed that all pepper individuals were infected by RWMV (Figure 35b). Sequences of the cloned parts of the RMWV variants present in the individuals were identical and 92-95% identical to the other variants of the virus whose sequences are available in GenBank. The variant present in Kosovo clusters with the variants sequenced in Slovenia (Figure 36)

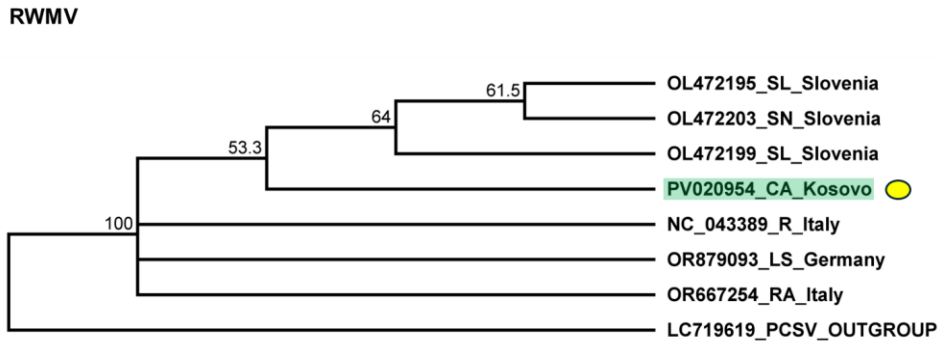

Figure 36. Phylogenetic analysis of the Ranunculus white mottle virus (RWMV) variant identified in Kosovo. The analysis was performed using Geneious Tree Builder, applying the Tamura–Nei model, the neighbor-joining method, and 1000 bootstrap replicates. Green boxe highlight the pepper-derived RWMV variants sequenced in this study, while yellow dots indicate the variant sequenced in this study. All sequences are labeled with their corresponding GenBank accession numbers. The middle panel of these indicates the host plant by using the following abbreviations: SL—*Solanum lycopersicum*, SN—*Solanum nigrum*, CA—*Capsicum annuum*, R—*Ranunculus spp*., LS—*Lactuca sativa*, and RA—*Ranunculus asiaticus*.

5.8 Discussion of the results

Over the past decade, high-throughput sequencing (HTS) has greatly advanced crop-virome studies by enabling sensitive, broad-range detection of known and novel plant viruses, including mixed and low-titer infections that are often missed by conventional diagnostic approaches (Maclot et al., 2020, Bester et al., 2023). Increasingly, HTS-based investigations have highlighted the importance of sampling not only cultivated crops but also surrounding weed communities, which are now widely recognized as important virus reservoirs that maintain viral populations and facilitate spillover into crops (Kyrychenko et al., 2021). Detecting viruses in both crops and nearby weed reservoirs is crucial for effective plant protection and disease management . In this study, weeds and cultivated crops were surveyed to assess their roles as virus reservoirs. Symptomatic and asymptomatic plants were sampled and analyzed using sRNA-HTS, RNA-Seq, and RT-PCR. Combined bioinformatics analyses revealed a diverse virome across the three sampling sites (K2022, K2023, and Ko2023), identifying CMV, BBWV1/2, TVCV, TuYV, PVM, PVH, ObPV, LBVaV, OxruMV1, PotLV, PVY, PCV2, BPEV, RWMV, TAV, and a CMV satellite RNA, several of which appeared in multiple datasets (Table 17). The virus diversity detected in this study is comparable to previous HTS-based surveys of crops and associated weeds, which consistently report complex viromes and frequent mixed infections across host species. Similar to our findings, (Ma et al., 2020) demonstrated extensive virome overlap between cultivated tomato and the neighboring weed *Solanum nigrum*, supporting the role of solanaceous weeds as active reservoirs facilitating virus exchange within agroecosystems. Likewise, metagenomic analyses of weeds and wild plants have repeatedly revealed the presence of economically important crop viruses, often in asymptomatic hosts, highlighting their epidemiological relevance for virus persistence and spread (Hasiów-Jaroszewska et al., 2021). Comparable levels of virome complexity and mixed infections were also reported in tomato–weed agroecosystems by (Rivarez et al., 2023), who showed that HTS uncovers diverse and overlapping virus communities across cultivated and non-cultivated hosts. More broadly, plant virus ecology studies show that wild plants and weeds serve as long-term reservoirs influencing virus diversity and emergence in crops, consistent with the patterns observed (Roossinck, 2014).

Clear differences in virus prevalence and diversity were observed across study years and locations.

In the Keszthely, 2022 sampling experiment, four viruses, CMV, BBWV1, TVCV, and TuYV, were detected. This site, previously used for horticultural crops such as pepper, tomato, and eggplant, and recently for wheat, with a history of potato cultivation, was surrounded by diverse dicot weed species. These surrounding weeds likely contributed to virus circulation and maintenance within the field. CMV was detected in one *Solanum nigrum* individual from Field I (S1/5), which carried all three viral RNAs. BBWV1 was found in one *Solanum nigrum* plant from Field II (S2/1), and was validated with both RNAs of the virus. TVCV was detected in all *Solanum nigrum* individuals from both fields, whereas none of the *Datura stramonium* plants were infected. TuYV was detected in one *Solanum nigrum* plant from Field I (S1/5), in two individuals of *Solanum nigrum* from Field II (S2/1 and S2/5), and in one *Datura stramonium* (D/5). Although all sampled plants appeared asymptomatic at the time of sampling, all viruses were successfully amplified, indicating that *S. nigrum* and *Datura stramonium* can act as an efficient reservoir host capable of sustaining latent infections

In the Keszthely, 2023 sampling experiment, seven viruses, PVM, PVH, ObPV, TVCV, LBVaV, OxruMV1, and PotLV, were detected, demonstrating broader viral diversity and greater reservoir potential in the field. This increase reflects the capacity of weed and wild plant species to harbor multiple viruses simultaneously, acting as persistent sources of infection that facilitate virus spread to adjacent crops. *Solanum nigrum*, which had tested positive for CMV, BBWV1, TVCV and TuYV in 2022, was positive for PVM in 2023, with all individuals from Field III infected (S3/1–S3/10), illustrating temporal shifts in virus prevalence that may result from vector dynamics, crop rotations, or competitive interactions among viruses. TVCV was detected in all *S. nigrum* individuals from Field III except S3/5, highlighting widespread infection within the population. *Datura stramonium*, was positive for Obuda pepper virus in 2023, with two individuals from Field III infected (D2/2 and D2/9), and two individuals also positive for TVCV (D2/1 and D2/7), indicating yearly changes in virus circulation influencing infection patterns. *Brassica napus*, grown alongside infected weeds, tested negative for all viruses, suggesting that viruses present in surrounding wild hosts either do not efficiently infect *Brassica* or were below detectable levels. *Solanum dulcamara* showed the highest virus diversity, with all individuals from Field IV infected with PVM (SD1–SD8). PVH was detected in three *S. dulcamara* individuals (Sd1, Sd6, Sd7), ObPV in one individual (Sd4), LBVaV in Sd6 with both RNAs confirmed, and OxruMV1 in three individuals (Sd2, Sd3, Sd6). For PotLV, no further analyses were performed, BLAST of its contigs

showed higher similarity to PVM and PVH, likely due to conserved genomic regions among these related viruses. Mixed infections were common, for example, Sd7 harboring three viruses simultaneously (PVM, PVH and both RNAs of LBVaV), emphasizing the role of *S. dulcamara* as a key reservoir species capable of maintaining viruses across seasons. Sampling in 2023 was more extensive, including leaves, flowery shoots, seeds, and fruits, likely contributing to higher detection rates and observed diversity.

The sampling experiment in Kososvo, 2023 showed the highest virus diversity, with the presence of CMV, BBWV2, PVY, PCV2, BPEV, RWMV, TVCV, TAV, and the CMV satellite RNA. This site was used for potato cultivation and bordered by uncultivated or mixed-use areas such as bean, pepper, and tomato fields, creating conditions favorable for virus spillover between crops and weeds. All sampled pepper plants were positive for several viruses, including CMV, BBWV2, PVY, PCV2, BPEV, and RWMV reflecting strong inoculum pressure, high host susceptibility, and efficient vector-mediated transmission. In contrast, only one individual of tomatoes was infected with CMV, likely due to differences in host susceptibility or vector exposure. For TVCV, TAV, and CMV satellite, assembled contigs were shorter than full genomes or partially aligned with known viruses. BLAST comparisons indicated high similarity to Solanaceae host sequences, suggesting many hits originated from the plant genome rather than active infections. TAV and CMV satellite regions were particularly short, likely representing artifacts or remnants, while TVCV contigs showed longer identity regions, possibly reflecting host-integrated viral sequences from past infections

Table 17. Summary of the sRNA-HTS, RNAseq and RT-PCR results.

K2022										
Library	Diagnostic method	CMV			BBWV1		TVCV	TuYV		
		RNA1	RNA2	RNA3	RNA1	RNA2				
255_KSOL	sRNA								Low incidence	
SOL_KES_10	RNAseq								Moderate incidence	
	RT-PCR	1 of 15	1 of 15	1 of 15	1 of 15	1 of 15	10 of 15	2 of 15	High incidence	
K2023										
Library	Diagnostic method	PVM	PVH	ObPV	LBVaV		OxruMV1	TVCV		
					RNA1	RNA2				
SOL_KES_17	RNAseq									
	RT-PCR	18 of 31	3 of 31	3 of 31	1 of 31		3 of 31	11 of 31		
Ko2023												
Library	Diagnostic method	CMV			BBWV2		PVY	PCV2		BPEV	RWMV
		RNA1	RNA2	RNA3	RNA1	RNA2		RNA1	RNA2		RNA1
SOL_KOS_18	RNAseq										
	RT-PCR	5 of 12	4 of 12	5 of 12	4 of 12	4 of 12	4 of 12	3 of 13	4 of 12	4 of 12	4 of 12

6. CONCLUSIONS

Detection of plant viruses in both crops and surrounding weeds is essential for sustainable agricultural production. The viromes of solanaceous weeds and cultivated solanaceous crops were investigated, with the focus on the role of weeds as virus reservoirs. Field surveys, visual inspections, and multi-tissue sampling enabled the collection of plants ranging from asymptomatic to highly symptomatic, which were analyzed using sRNA-HTS, RNA-Seq, and RT-PCR to characterize the viromes and validate virus detection results.

The results revealed that solanaceous weeds, including *Solanum nigrum, Datura stramonium*, and *Solanum dulcamara*, consistently harbored multiple viruses across years, often maintaining mixed infections. Cultivated crops were also affected by infections, with pepper plants showing multiple virus infections and a tomato individual infected with a virus, highlighting differences in host susceptibility and virus exposure. Temporal and spatial variations in virus prevalence reflect the influence of vector dynamics, crop rotations, and virus–virus interactions. Some viral-like contigs represented host-integrated sequences rather than active infections.

Overall, these findings demonstrate that solanaceous weeds serve as persistent and dynamic virus reservoirs, sustaining a broad diversity of plant viruses across seasons and locations. By harboring single and mixed infections, these weeds contribute to the continuous circulation of viruses, enabling spillover to cultivated crops and potentially influencing disease outbreaks in agricultural systems. Furthermore understanding the viromes of weed species is essential for predicting virus emergence and managing infection risks in crops. These observations underscore the importance of multi-year, multi-tissue surveillance to accurately capture virus prevalence, diversity, and tissue-specific distribution.

6.1 Recommendations

Based on the findings of this study, several recommendations can be made to improve plant virus monitoring, management, and research in both cultivated crops and surrounding wild plant populations. First, continuous multi-year and multi-tissue surveillance is essential, as virus prevalence and diversity vary temporally and spatially. Sampling multiple plant organs including leaves, flowers, seeds, and fruits ensures more accurate detection of both symptomatic and asymptomatic infections. Second, the integration of high-throughput sequencing approaches, such as small RNA-HTS and RNA-Seq, with targeted molecular validation methods like RT-PCR, is recommended for comprehensive virome analysis. This combined approach allows the detection of both known and emerging viruses, including those involved in mixed infections, which are common in wild and weed hosts. Third, monitoring surrounding weed species, particularly wild Solanaceae such as *Solanum nigrum*, *Datura stramonium* and *Solanum dulcamara*, is critical because these plants serve as important virus reservoirs capable of sustaining and amplifying multiple viruses over time, increasing the risk of spillover into crop fields. Fourth, agronomic practices such as crop rotation, field hygiene, and vector management should be optimized to reduce virus transmission between crops and wild hosts. Fifth, given the ongoing global movement of plant materials and the potential effects of climate change on vector populations, routine diagnostic protocols must be flexible and adaptable to emerging viral threats. Finally, capacity building for plant health monitoring, including the development of standardized and accredited diagnostic pipelines, is essential to support early detection, rapid response, and sustainable plant virus management strategies. Implementing these recommendations will enhance the ability to manage virus outbreaks, protect economically important crops, and maintain resilient agricultural systems.

7. NEW SCIENTIFIC RESULTS

1. The virome of solanaceous weeds in Keszthely was evaluated using high-throughput sequencing (HTS), providing the first sequences of CMV, BBWV1, TVCV, and TuYV obtained from *Solanum nigrum* in Hungary.
2. The sequence of the ObPV variant detected from *Datura stramonium* represents the first sequence of this virus from this host.
3. We described *Solanum dulcamara* as a host of PVH, LBVaV, and OxruMV1 for the first time.
4. Mixed infections occurred in pepper plants in Kosovo, where CMV, BBWV2, PVY, PCV2, BPEV, and RWMV were confirmed by HTS and RT-PCR, providing the first partial molecular sequences of these viruses in the country.
5. BBWV2 was reported for the first time in the Balkan region.
6. The partial sequence of CMV infecting tomato in Kosovo was described for the first time.

8. SUMMARY

In this research, we investigated the virus infections of endemic plants and invasive weeds and evaluated their role as virus reservoirs. solanaceous weeds represent an important challenge for agriculture, as they grow rapidly, adapt easily to field conditions, and compete with cultivated crops for nutrients. Major solanaceous crops such as tomato, pepper, potato, and eggplant are cultivated worldwide, and the presence of solanaceous weeds in production fields poses a significant risk to these crops. Their ability to survive under various environmental conditions enables them to harbor plant viruses and contribute to their persistence, survival, and spread.

Investigation of the virome of solanaceous weeds in Keszthely, Hungary using both small RNA sequencing and RNA-seq was pursued. The results clearly demonstrated that solanaceous weeds serve as important virus reservoirs. *Solanum nigrum*, previously described as a host, was confirmed by HTS as a natural host of CMV, BBWV1, TVCV, and TuYV in Keszthely, Hungary, with variants partially sequenced for the first time in this host, *Datura stramonium* was confirmed as a natural host of ObPV, providing the first ObPV sequence from this host in GenBank and *Solanum dulcamara* was newly recognized as a host for PVH, LBVaV, and OxruMV1.

In Kosovo, CMV, BBWV2, PVY, PCV2, BPEV, and RWMV were detected using HTS, providing the first official HTS-based documentation and the first partial molecular sequences of these viruses in the country. BBWV2 was also reported for the first time in the Balkan region, expanding the known geographical distribution of this virus. In addition, mixed infections involving up to six viruses were detected in pepper plants in Kosovo, showing the complexity of co-infection patterns and highlighting the epidemiological importance of local weed reservoirs. CMV was also detected in a tomato field with one individual infected.

To obtain these results, a total of 15 weed samples were collected in Keszthely, Hungary, during the summer of 2022, including *Solanum nigrum* and *Datura stramonium*. In 2023, an additional 31 samples were collected, including *Solanum nigrum*, *Datura stramonium*, *Brassica napus*, and *Solanum dulcamara*. Nucleic acids were extracted, and both small RNA and RNA-seq libraries were prepared and sequenced on the Illumina platform. Sequencing data were analyzed using bioinformatics pipelines in CLC Genomics Workbench, and all virus hits were validated using RT-PCR.

Bioinformatics analysis revealed virus hits corresponding to CMV, BBWV1, TVCV, TuYV, PVM, PVH, ObPV, LBVaV, OxruMV1, PotLV, BBWV2, PVY, PCV2, BPEV, RWMV, TAV, and CMVs variant, with several viruses detected repeatedly across sampling years. RT-PCR confirmed the presence of CMV in *Solanum nigrum*, *Capsicum annuum*, and *Solanum lycopersicum*; BBWV1 in *Solanum nigrum*; PVM in *Solanum nigrum* and *Solanum dulcamara*; PVH in *Solanum dulcamara*; ObPV in *Datura stramonium* and *Solanum dulcamara*; LBVaV and OxruMV1 in *Solanum dulcamara*; BBWV2, PVY, PCV2, BPEV, and RWMV in *Capsicum annuum*.

Overall, the results clearly demonstrate that solanaceous weeds play an important role in the maintenance, persistence, and spread of plant viruses in agricultural ecosystems. Their ability to host numerous viruses, including several newly reported at national, regional, or global levels, confirms their significance as persistent virus reservoirs and highlights the need to consider weeds as key components in plant virus epidemiology and disease management strategies. The detection of mixed infections and repeated virus occurrences across sampling years further indicates that these weeds can support complex viral communities capable of influencing disease dynamics in nearby crops. For Kosovo, the detection of mixed infections in pepper and one CMV infection in tomato indicates that Kosovo's crop fields already harbor diverse and active viral populations. These findings highlight the need and importance for continued virus monitoring and suggest that local crop production may be influenced or affected by a wider range of previously unreported viruses circulating in the region.

9. REFERENCES

NCBI BLAST, National Center for Biotechnology Information.

ABASS, M. O. & LAHUF, A. A. 2023. High-Throughput Sequencing and Bioinformatic Analysis Reveal Presence of the Endogenous Pararetrovirus Tobacco vein clearing virus Genome in the Tomato (Solanum lycopersicum) Host Genome. *Arab journal of plant protection,* 41.

ABOU KUBAA, R., SAPONARI, M., HEINOUN, K., JREIJIRI, F. & CHOUEIRI, E. 2024. First report of bell pepper endornavirus in pepper in Syria and Lebanon. *Journal of Plant Pathology,* 106**,** 781-781.

ABOUELNASR, H., LI, Y.-Y., ZHANG, Z.-Y., LIU, J.-Y., LI, S.-F., LI, D.-W., YU, J.-L., MCBEATH, J. & HAN, C.-G. 2014. First report of Potato virus H on Solanum muricatum in China. *Plant Disease,* 98**,** 1016-1016.

ALBERT, R., ALMÁSI, K., KÜNSTLER, A., SALAMON, P. & KIRÁLY, L. 2019. First Report of Lettuce Big-Vein Disease Associated with Mirafiori Lettuce Big-Vein Virus and Lettuce Big-Vein Associated Virus on Lettuce in Hungary. *Plant Disease,* 103**,** 1801-1801.

ALFARO-FERNÁNDEZ, A., CEBRIÁN, M., HERRERA-VÁSQUEZ, J., CÓRDOBA-SELLÉS, M., SÁNCHEZ-NAVARRO, J. A. & JORDÁ, C. 2010. Molecular variability of Spanish and Hungarian isolates of Tomato torrado virus. *Plant pathology,* 59**,** 785-793.

ALVAREZ-QUINTO, R., GRINSTEAD, S., JONES, R. & MOLLOV, D. 2023. Complete genome sequence of a new mitovirus associated with walking iris (Trimezia northiana). *Archives of Virology,* 168**,** 273.

AMER, M., SHAKEEL, M., KHALID, Z., AL-SHAHWAN, I. & AL-SALEH, M. 2025. SEROLOGICAL AND MOLECULAR CHARACTERIZATION OF CUCURBIT APHID BORNE YELLOWS VIRUS AFFECTING SQUASH, CUCUMBER AND ARABLE WEEDS IN SAUDI ARABIA. *Journal of Animal & Plant Sciences,* 35**,** 780-790.

AMRUTA, B., LAXMIDEVI, V., RAMEGOWDA, G., SEETHARAMU, G., USHARANI, T. & KRISHNAREDDY, M. 2020. First report of Groundnut bud necrosis virus infecting anthurium (Anthurium andreanum) in India. *New Disease Reporter,* 41**,** 2044-0588.2020.

ANSAR, M., AGNIHOTRI, A. K., RANJAN, T., KARN, M., A, S., KUMAR, R. R. & BHAGAT, A. P. 2021. Nightshade (Solanum nigrum), an intermediate host between tomato and cucurbits of Tomato leaf curl New Delhi virus. *Phytopathologia Mediterranea,* 60**,** 409-420.

ASAD, Z., ASHFAQ, M. & AHSAN, M. 2019. Serological and Molecular Identification Based on Coat Protein (CP) Gene of Cucumber mosaic virus (CMV) Infecting Cucumber (Cucumis sativus L) in Pothwar Region of Pakistan. *J Plant Biochem Physiol,* 7**,** 2.

BAULCOMBE, D. 2004. RNA silencing in plants. *Nature,* 431**,** 356-363.

BELABESS, Z., DALLOT, S., EL-MONTASER, S., GRANIER, M., MAJDE, M., TAHIRI, A., BLENZAR, A., URBINO, C. & PETERSCHMITT, M. 2015. Monitoring the dynamics of emergence of a non-canonical recombinant of Tomato yellow leaf curl virus and displacement of its parental viruses in tomato. *Virology,* 486**,** 291-306.

BERGUA, M., LUIS-ARTEAGA, M. & ESCRIU, F. 2014. Genetic diversity, reassortment, and recombination in Alfalfa mosaic virus population in Spain. *Phytopathology,* 104**,** 1241-1250.

BERNAL-VICENTE, A., DONAIRE, L., TORRE, C., GÓMEZ-AIX, C., SÁNCHEZ-PINA, M. A., JUAREZ, M., HERNANDO, Y. & ARANDA, M. A. 2018. Small RNA-seq to characterize viruses responsible of Lettuce big vein disease in Spain. *Frontiers in Microbiology,* 9**,** 3188.

BERTRAN, A. G., OLIVEIRA, A. S., NAGATA, T. & RESENDE, R. O. 2011. Molecular characterization of the RNA-dependent RNA polymerase from groundnut ringspot virus (genus Tospovirus, family Bunyaviridae). *Arch Virol,* 156**,** 1425-9.

BESTER, R., MASSART, S., FONTDEVILA PARETA, N., KHALILI, M., MAACHI, A., RIVAREZ, M., ROLLIN, J., SALAVERT, F., TEMPLE, C. & ARANDA, M. 2023. Managing the deluge of newly discovered plant viruses and viroids: an optimized scientific and regulatory framework for their characterization and risk analysis.

BI, J., ZHENG, H., LU, Y., PENG, J., LIN, L., CHEN, Z., SONG, B., CHEN, J. & YAN, F. 2020. First Report of Tobacco Vein Banding Mosaic Virus Naturally Infecting Black Nightshade (Solanum nigrum) in China. *Plant Disease,* 104**,** 1265-1265.

BISWAS, K. K., BALRAM, N., ELANGOVAN, M., PALCHOUDHURY, S., BHATTACHARYYA, U. K., KHATOON, H., AGGARWAL, S., GODARA, S.,

KUMAR, P. & SAIN, S. K. 2025. Divergent Cotton leaf curl Multan betasatellite and three different alphasatellite species associated with cotton leaf curl disease outbreak in Northwest India. *PLoS One,* 20**,** e0313844.

BRAGARD, C., CACIAGLI, P., LEMAIRE, O., LOPEZ-MOYA, J., MACFARLANE, S., PETERS, D., SUSI, P. & TORRANCE, L. 2013. Status and prospects of plant virus control through interference with vector transmission. *Annual review of phytopathology,* 51**,** 177-201.

BRIDDON, R. W., BEDFORD, I. D., TSAI, J. H. & MARKHAM, P. G. 1996. Analysis of the nucleotide sequence of the treehopper-transmitted geminivirus, tomato pseudo-curly top virus, suggests a recombinant origin. *Virology,* 219**,** 387-94.

BUXTON-KIRK, A., ADAMS, I., FREW, L., WARD, R., KELLY, M., FORDE, S., SKELTON, A., HARJU, V., BAUCAS, N. & BAS-ILAN, M. 2021. First report of Turnip yellows virus in cabbage in the Philippines. *New Disease Reports,* 44.

CAVILEER, T., CLARKE, R., CORSINI, D. & BERGER, P. 1998. A new strain of potato carlavirus M. *Plant disease,* 82**,** 98-102.

CHAUDHARY, P., KAUR, A., SINGH, B., KUMAR, S., HALLAN, V. & NAGPAL, A. K. 2023. First report of tomato chlorosis virus (ToCV) and detection of other viruses in field-grown tomatoes in North-Western region of India. *VirusDisease,* 34**,** 56-75.

CHAUDHARY, P., KUMARI, R., SINGH, B., HALLAN, V. & NAGPAL, A. K. 2019. First report of potato virus M, potato virus Y and cucumber mosaic virus infection in Solanum nigrum in India. *Journal of Plant Pathology,* 101**,** 419-419.

CHENG, Y., DENG, T., CHEN, C., LIAO, J., CHANG, C. & CHIANG, C. 2011. First report of pepper mottle virus in bell pepper in Taiwan. *Plant disease,* 95**,** 617-617.

CHIKH ALI, M., MAOKA, T., NATSUAKI, T. & NATSUAKI, K. 2010. PVYNTN-NW, a novel recombinant strain of Potato virus Y predominating in potato fields in Syria. *Plant Pathology,* 59**,** 31-41.

CLARK, M. F. & ADAMS, A. 1977. Characteristics of the microplate method of enzyme-linked immunosorbent assay for the detection of plant viruses. *Journal of general virology,* 34**,** 475-483.

CSILLERY, G., TOBIAS, I. & RUSKO, J. 1983. A new pepper strain of tomato mosaic virus. *Acta Phytopathol Acad Sci Hung. 1983,* 18:195–200.

D'AGOSTINO, N., GOLAS, T., VAN DE GEEST, H., BOMBARELY, A., DAWOOD, T., ZETHOF, J., DRIEDONKS, N., WIJNKER, E., BARGSTEN, J. & NAP, J.-P. 2013. Genomic analysis of the native European Solanum species, S. dulcamara. *BMC genomics,* 14**,** 356.

DE OLIVEIRA, F. F., FAVARA, G. M., FERRO, C. G., KRAIDE, H. D., CARMO, E. Y. N., KITAJIMA, E. W. & REZENDE, J. A. M. 2022. First report of groundnut ringspot virus infecting Zinnia sp. in Brazil. *Plant Disease,* 106.

DEBRECZENI, D. E., RUIZ-RUIZ, S., ARAMBURU, J., LOPEZ, C., BELLIURE, B., GALIPIENSO, L., SOLER, S. & RUBIO, L. 2011. Detection, discrimination and absolute quantitation of Tomato spotted wilt virus isolates using real time RT-PCR with TaqMan® MGB probes. *Journal of virological methods,* 176**,** 32-37.

DELFINO, J., SILVA, H., DE LEÓN, I. P., HOFFMAN, E. & AGORIO, A. 2025. First report of turnip yellow virus infecting rapeseed (Brassica napus) in Uruguay. *New Disease Reports,* 51**,** e70031.

DENG, Z., MA, L., ZHANG, P. & ZHU, H. 2022. Small RNAs participate in plant–virus interaction and their application in plant viral defense. *International journal of molecular sciences,* 23**,** 696.

DIAS, N. P., HU, R., HALE, F. A., HANSEN, Z. R., WSZELAKI, A., DOMIER, L. L. & HAJIMORAD, M. R. 2023. Viromes of Field-Grown Tomatoes and Peppers in Tennessee Revealed by RNA Sequencing Followed by Bioinformatic Analysis. *Plant Health Progress,* 24**,** 207-213.

DOLJA, V. V., KRUPOVIC, M. & KOONIN, E. V. 2020. Deep roots and splendid boughs of the global plant virome. *Annual review of phytopathology,* 58**,** 23-53.

DONG, J., LUO, Y., DING, M., ZHANG, Z. & YANG, C. 2007. First report of Tomato yellow leaf curl China virus infecting kidney bean in China. *Plant pathology,* 56.

DOOLITTLE, S. P. 1916. A new infectious mosaic disease of cucumber. *Phytopathology,* 6**,** 145-147.

DUFFUS, J. E. 1971. Role of weeds in the incidence of virus diseases. *Annual Review of Phytopathology,* 9**,** 319-340.

EFSA. 2020. Pest categorisation of non-EU viruses and viroids of potato. Available: https://www.efsa.europa.eu/en/efsajournal/pub/6157 [Accessed 30 November 2025].

FAN, H., KAI, G., ZHOU, Y., ZHU, M. & ZHAO, Y. 2021. First report of natural infection of potato virus Y on Solanum nigrum L. in China. *Journal of Plant Pathology,* 103**,** 691-691.

FANIGLIULO, A., COMES, S., PACELLA, R., HARRACH, B., MARTIN, D. & CRESCENZI, A. 2005. Characterisation of Potato virus Y nnp strain inducing veinal necrosis in pepper: a naturally occurring recombinant strain of PVY. *Archives of virology,* 150**,** 709-720.

FERRER, R. M., FERRIOL, I., MORENO, P., GUERRI, J. & RUBIO, L. 2011. Genetic variation and evolutionary analysis of broad bean wilt virus 2. *Archives of virology,* 156**,** 1445-1450.

FERRER, R. M., GUERRI, J., LUIS-ARTEAGA, M., MORENO, P. & RUBIO, L. 2005. The complete sequence of a Spanish isolate of Broad bean wilt virus 1 (BBWV-1) reveals a high variability and conserved motifs in the genus Fabavirus. *Archives of virology,* 150**,** 2109-2116.

FERRIOL, I., AMBROS, S., DA SILVA JR, D. M., FALK, B. W. & RUBIO, L. 2016. Molecular and biological characterization of highly infectious transcripts from full-length cDNA clones of broad bean wilt virus 1. *Virus research,* 217**,** 71-75.

FERRIOL, I., FERRER, R. M., LUIS-ARTEAGA, M., GUERRI, J., MORENO, P. & RUBIO, L. 2014. Genetic variability and evolution of broad bean wilt virus 1: role of recombination, selection and gene flow. *Archives of Virology,* 159**,** 779-784.

FIALLO-OLIVÉ, E., CHIRINOS, D. T., GERAUD-POUEY, F., MORIONES, E. & NAVAS-CASTILLO, J. 2013. Complete genome sequences of two begomoviruses infecting weeds in Venezuela. *Archives of Virology,* 158**,** 277-280.

FIALLO-OLIVÉ, E., TRENADO, H. P., LOURO, D. & NAVAS-CASTILLO, J. 2019. Recurrent speciation of a tomato yellow leaf curl geminivirus in Portugal by recombination. *Scientific Reports,* 9**,** 1332.

FILARDO, F., NANCARROW, N., KEHOE, M., MCTAGGART, A. R., CONGDON, B., KUMARI, S., AFTAB, M., TRĘBICKI, P., RODONI, B. & THOMAS, J. 2021. Genetic diversity and recombination between turnip yellows virus strains in Australia. *Archives of Virology,* 166**,** 813-829.

FLATKEN, S., UNGEWICKELL, V., MENZEL, W. & MAISS, E. 2008. Construction of an infectious full-length cDNA clone of potato virus M. *Archives of virology,* 153**,** 1385-1389.

FORDE, S., HARJU, V., SKELTON, A., ADAMS, I., FOWKES, A., PUFAL, H., MCGREIG, S., CONYERS, C., WARD, R. & FREW, L. 2023. First report of Snowdrop virus Y and Turnip yellows virus in Narcissus sp. in the United Kingdom. *New Disease Reports,* 48.

FOWKES, A. R., MCGREIG, S., PUFAL, H., DUFFY, S., HOWARD, B., ADAMS, I. P., MACARTHUR, R., WEEKES, R. & FOX, A. 2021. Integrating high throughput sequencing into survey design reveals turnip yellows virus and soybean dwarf virus in pea (Pisum sativum) in the United Kingdom. *Viruses,* 13**,** 2530.

FOX, A., FOWKES, A., SKELTON, A., HARJU, V., BUXTON-KIRK, A., KELLY, M., FORDE, S., PUFAL, H., CONYERS, C. & WARD, R. 2019. Using high-throughput sequencing in support of a plant health outbreak reveals novel viruses in Ullucus tuberosus (Basellaceae). *Plant Pathology,* 68**,** 576-587.

GAIRE, B. P. & SUBEDI, L. 2013. A review on the pharmacological and toxicological aspects of Datura stramonium L. *Journal of integrative medicine,* 11**,** 73-79.

GALIPIENSO, L., ELVIRA-GONZÁLEZ, L., VELASCO, L., HERRERA-VÁSQUEZ, J. & RUBIO, L. 2021. Detection of Persistent Viruses by High-Throughput Sequencing in Tomato and Pepper from Panama: Phylogenetic and Evolutionary Studies. *Plants (Basel),* 10.

GARCIA-RUIZ, H., GARCIA RUIZ, M. T., GABRIEL PERALTA, S. M., MIRAVEL GABRIEL, C. B. & EL-MOUNADI, K. 2016. Mechanisms, applications, and perspectives of antiviral RNA silencing in plants. *Revista mexicana de fitopatología,* 34**,** 286-307.

GARCÍA, M. L., BÓ, E. D., DA GRAÇA, J. V., GAGO-ZACHERT, S., HAMMOND, J., MORENO, P., NATSUAKI, T., PALLÁS, V., NAVARRO, J. A., REYES, C. A., LUNA, G. R., SASAYA, T., TZANETAKIS, I. E., VAIRA, A. M., VERBEEK, M. & ICTV REPORT, C. 2017. ICTV Virus Taxonomy Profile: Ophioviridae. *J Gen Virol,* 98**,** 1161-1162.

GAVRILI, V., LOTOS, L., VASILEIOU, N., KATIS, N. & MALIOGKA, V. 2024. First report of ranunculus white mottle virus and lettuce ring necrosis virus in pepper in Greece. *Journal of Plant Pathology,* 106.

GE, B., HE, Z., ZHANG, Z., WANG, H. & LI, S. 2014. Genetic variation in potato virus M isolates infecting pepino (Solanum muricatum) in China. *Archives of virology,* 159**,** 3197-3210.

GEBHARDT, C. 2016. The historical role of species from the Solanaceae plant family in genetic research. *Theoretical and Applied Genetics,* 129**,** 2281-2294.

GENBANK, N. 2023. Genome record for accession NC_076526. Available: https://www.ncbi.nlm.nih.gov/nuccore/NC_076526 [Accessed 30 November 2025].

GERGERICH, R. C. & DOLJA, V. V. 2006. Introduction to plant viruses, the invisible foe. *The plant health instructor,* 478.

GLASA, M., SOLTYS, K., PREDAJNA, L., SIHELSKÁ, N., BUDIS, J., MRKVOVÁ, M., KRAIC, J., MIHÁLIK, D. & RUIZ-GARCÍA, A. B. 2019. High-throughput sequencing of Potato virus M from tomato in Slovakia reveals a divergent variant of the virus. *Plant Protection Science,* 55**,** 159-166.

GOLDBACH, R., BUCHER, E. & PRINS, M. 2003. Resistance mechanisms to plant viruses: an overview. *Virus research,* 92**,** 207-212.

GOLUBEVA, T. S., CHERENKO, V. A. & ORISHCHENKO, K. E. 2021. Recent advances in the development of exogenous dsRNA for the induction of RNA interference in cancer therapy. *Molecules,* 26**,** 701.

GREER, S., NEWBERT, M., RODRIGUES, L., OLIVEIRA, A., CHAVES, A., CALEGARIO, R., BARKER, G., EIRAS, M. & WALSH, J. A. 2021. First report of turnip yellows virus in Brazil. *New Disease Reports,* 44.

GRIECO, F., DI FRANCO, A. & GALLITELLI, D. 1997. Potato virus M in tomato crops in Southern Italy. *Journal of Plant Pathology***,** 45-49.

HALABI, M. H., OLADOKUN, J. O., BALDODIYA, G. M., BORAH, B. K. & NATH, P. D. 2021. Identification, prevalence and genetic diversity study of potato viruses in Northeastern states of India. *Annals of Applied Biology,* 179**,** 185-194.

HAMIDSON, H., DAMIRI, N. & ANGRAINI, E. Effect of medicinal plants extracts on the incidence of mosaic disease caused by cucumber mosaic virus and growth of chili. IOP Conference Series: Earth and Environmental Science, 2018. IOP Publishing, 012062.

HANČINSKÝ, R., MIHÁLIK, D., MRKVOVÁ, M., CANDRESSE, T. & GLASA, M. 2020. Plant viruses infecting Solanaceae family members in the cultivated and wild environments: A review. *Plants,* 9**,** 667.

HASIÓW-JAROSZEWSKA, B., BOEZEN, D. & ZWART, M. P. 2021. Metagenomic studies of viruses in weeds and wild plants: a powerful approach to characterise variable virus communities. *Viruses,* 13**,** 1939.

HAYES, R. J., WINTERMANTEL, W. M., NICELY, P. A. & RYDER, E. J. 2006. Host resistance to Mirafiori lettuce big-vein virus and Lettuce big-vein associated virus and virus sequence diversity and frequency in California. *Plant Disease,* 90**,** 233-239.

HENSON, J. M. & FRENCH, R. C. 1993. The polymerase chain reaction and plant disease diagnosis. *Papers in Plant Pathology***,** 2.

HERNANDEZ, A., TORRES, D., BELTRÁN-ACOSTA, C. & KOBAYASHI, S. 2020. First Report of Lettuce Big-Vein Disease Associated with Mirafiori Lettuce Big-Vein Virus and Lettuce Big-Vein Associated Virus in Colombia. *Plant Disease,* 104**,** 1000.

HOBBS, H., EASTBURN, D., D'ARCY, C., KINDHART, J., MASIUNAS, J., VOEGTLIN, D., WEINZIERL, R. & MCCOPPIN, N. 2000. Solanaceous weeds as possible sources of Cucumber mosaic virus in southern Illinois for aphid transmission to pepper. *Plant disease,* 84**,** 1221-1224.

HOSSEINI, S. A. & SALARI, K. 2017. Detection and molecular characterisation of potato virus S of weed reservoirs in Iran. *Archives of Phytopathology and Plant Protection,* 50**,** 828-838.

HOSSEINZADEH, M. R., SHAMS-BAKHSH, M., OSALOO, S. K. & BROWN, J. K. 2014. Phylogenetic relationships, recombination analysis, and genetic variability among diverse variants of tomato yellow leaf curl virus in Iran and the Arabian Peninsula: further support for a TYLCV center of diversity. *Archives of virology,* 159**,** 485-497.

HULL, R. 1984. Caulimovirus group. *CAB/AAB Descriptions of Plant Viruses.*

HYODO, K. & OKUNO, T. 2020. Hijacking of host cellular components as proviral factors by plant-infecting viruses. *Advances in virus research.* Elsevier.

IBABA, J. D. & GUBBA, A. 2020. High-throughput sequencing application in the diagnosis and discovery of plant-infecting viruses in Africa, a decade later. *Plants,* 9**,** 1376.

IGWEGBE, E. 1983. Some properties of a tobacco mosaic virus strain isolated from pepper (Capsicum annuum) in Nigeria.

IKEDA, R., WATANABE, E., WATANABE, Y. & OKADA, Y. 1993. Nucleotide sequence of tobamovirus Ob which can spread systemically in N gene tobacco. *Journal of general virology,* 74**,** 1939-1944.

IQBAL, M. J., ZIA-UR-REHMAN, M., ILYAS, M., HAMEED, U., HERRMANN, H. W., CHINGANDU, N., MANZOOR, M. T., HAIDER, M. S. & BROWN, J. K. 2023. Sentinel plot surveillance of cotton leaf curl disease in Pakistan-a case study at the cultivated cotton-wild host plant interface. *Virus Research,* 333**,** 199144.

JACQUAT, A. G., THEUMER, M. G. & DAMBOLENA, J. S. 2023. Putative mitoviruses without in-frame UGA (W) codons: evolutionary implications. *Viruses,* 15**,** 340.

JAIN, R., SHARMA, A., GUPTA, S., SARETHY, I. P. & GABRANI, R. 2011. Solanum nigrum: current perspectives on therapeutic properties. *Altern Med Rev,* 16**,** 78-85.

JEONG, J.-J., JU, H.-J. & NOH, J. 2014. A review of detection methods for the plant viruses. *Research in Plant Disease,* 20**,** 173-181.

JO, Y., CHOI, H., LEE, J. H., MOH, S. H. & CHO, W. K. 2022. Viromes of 15 Pepper (Capsicum annuum L.) Cultivars. *Int J Mol Sci,* 23.

JONES, R. A. 2006. Control of plant virus diseases. *Advances in Virus Research,* 67**,** 205-244.

KARANFIL, A. 2022. Phylogenetic relationship and genetic diversity of Turkish peanut viruses. *Molecular Biology Reports,* 49**,** 2293-2301.

KARAPETSI, L., CHATZIVASSILIOU, E. K., KATIS, N. I. & MALIOGKA, V. I. 2021. Artichoke yellow ringspot virus as the causal agent of a new viral disease of lettuce: Epidemiology and molecular variability. *Plant Pathology,* 70**,** 594-603.

KAZINCZI, G., LUKACS, D., TAKACS, A., HORVATH, J., GABORJANYI, R., NADASY, M. & NADASY, E. 2006. Biological decline of Solanum nigrum due to virus infections. *ZEITSCHRIFT FUR PFLANZENKRANKHEITEN UND PFLANZENSCHUTZ-SONDERHEFT-,* 20**,** 325.

KHALED-GASMI, W., SOUISSI, R. & BOUKHRIS-BOUHACHEM, S. 2020. Temporal distribution of three pepper viruses and molecular characterization of two Cucumber mosaic virus isolates in Tunisia.

KIM, M.-K., KWAK, H.-R., LEE, S.-H., KIM, J.-S., KIM, K.-H., CHA, B.-J. & CHOI, H.-S. 2011. Characteristics of Cucumber mosaic virus isolated from Zea mays in Korea. *The Plant Pathology Journal,* 27**,** 372-377.

KIMARU, S., KILALO, D., MUIRU, W., KIMENJU, J. & THUKU, C. 2020. Molecular detection of cucumber mosaic virus and tobacco mosaic virus infecting African Nightshades (Solanum scabrum Miller). *International Journal of Agronomy,* 2020**,** 8864499.

KIRANMAI, G., SREENIVASULU, P. & NAYUDU, M. 1998. Epidemiology of cucumber mosaic cucumovirus isolates naturally infecting three solanaceous vegetable crops around Tirupati. *Indian Phytopathology,* 51**,** 315-318.

KNIERIM, D., TSAI, W.-S. & KENYON, L. 2013. Analysis of sequences from field samples reveals the presence of the recently described pepper vein yellows virus (genus Polerovirus) in six additional countries. *Archives of virology,* 158**,** 1337-1341.

KOBAYASHI, Y., NAKANO, M., KASHIWAZAKI, S., NAITO, T., MIKOSHIBA, Y., SHIOTA, A., KAMEYA-IWAKI, M. & HONDA, Y. 1999. Sequence analysis of RNA-2 of different isolates of broad bean wilt virus confirms the existence of two distinct species. *Archives of virology,* 144**,** 1429-1438.

KOBAYASHI, Y. O., KOBAYASHI, A., NAKANO, M., HAGIWARA, K., HONDA, Y. & OMURA, T. 2003. Analysis of genetic relations between Broad bean wilt virus 1 and Broad bean wilt virus 2. *Journal of general plant pathology,* 69**,** 320-326.

KOENIG, R. & PAUL, H. 1982. Variants of ELISA in plant virus diagnosis. *Journal of Virological Methods,* 5**,** 113-125.

KOH, L., COOPER, J. & WONG, S. 2001. Complete sequences and phylogenetic analyses of a Singapore isolate of broad bean wilt fabavirus. *Archives of virology,* 146**,** 135-147.

KUMAR, A., KATIYAR, A., JAILANI, A. A. K., CHACKRABORTY, A. & MANDAL, B. 2023. Genetic diversity of Potato virus M (PVM) in the major potato growing region in the Indo-Gangetic plain and characterization of a distinct strain of PVM occurring in India. *Frontiers in Microbiology,* 14**,** 1265653.

KUMAR, M., GUPTA, P. K. & KUMAR, Y. 2024. Chapter-15 Papaya Mosaic Virus. *Viral Diseases of Vegetable & Fruit Crops,* 33**,** 207.

KUMARI, N., SHARMA, V., PATEL, P. & SHARMA, P. 2023. Pepper mild mottle virus: A formidable foe of capsicum production—A review. *Frontiers in Virology,* 3**,** 1208853.

KUTNJAK, D., ELENA, S. F. & RAVNIKAR, M. 2017. Time-sampled population sequencing reveals the interplay of selection and genetic drift in experimental evolution of potato virus Y. *Journal of Virology,* 91**,** 10.1128/jvi. 00690-17.

KUTNJAK, D., RUPAR, M., GUTIERREZ-AGUIRRE, I., CURK, T., KREUZE, J. F. & RAVNIKAR, M. 2015. Deep sequencing of virus-derived small interfering RNAs and RNA from viral particles shows highly similar mutational landscapes of a plant virus population. *Journal of virology,* 89**,** 4760-4769.

KWAK, H.-R., KIM, M.-K., LEE, Y.-J., SEO, J.-K., KIM, J.-S., KIM, K.-H., CHA, B. & CHOI, H.-S. 2013a. Molecular characterization and variation of the broad bean wilt virus 2 isolates based on analyses of complete genome sequences. *The plant pathology journal,* 29**,** 397.

KWAK, H.-R., KIM, M.-K., NAM, M., KIM, J.-S., KIM, K.-H., CHA, B. & CHOI, H.-S. 2013b. Genetic compositions of Broad bean wilt virus 2 infecting red pepper in Korea. *The plant pathology journal,* 29**,** 274.

KWAK, M., TROIANO, E., KIL, E.-J. & PARRELLA, G. 2024. High-throughput sequencing detected a virus–viroid complex in a single pokeweed plant. *Frontiers in Plant Science,* 15**,** 1435611.

KYRYCHENKO, A., SHCHERBATENKO, I. & KOVALENKO, A. 2021. Viruses of wild plants and current metagenomic methods for their investigation. *Cytology and Genetics,* 55**,** 248-255.

LEE, U., HONG, J., CHOI, J., KIM, K., KIM, Y., CURTIS, I., NAM, H. & LIM, P. 2000. Broad bean wilt virus causes necrotic symptoms and generates defective RNAs in Capsicum annuum. *Phytopathology,* 90**,** 1390-1395.

LI, N., YU, C., YIN, Y., GAO, S., WANG, F., JIAO, C. & YAO, M. 2020. Pepper crop improvement against cucumber mosaic virus (CMV): A review. *Frontiers in plant science,* 11**,** 598798.

LI, Y.-Y., ZHANG, R.-N., XIANG, H.-Y., ABOUELNASR, H., LI, D.-W., YU, J.-L., MCBEATH, J. H. & HAN, C.-G. 2013. Discovery and characterization of a novel carlavirus infecting potatoes in China. *PLoS One,* 8**,** e69255.

LI, Z., TANG, Y., SHE, X., LAN, G., YU, L. & HE, Z. 2023. First report of tomato yellow mottle-associated virus infecting Solanum nigrum in China. *Plant Disease,* 107**,** 592.

LIM, S., KIM, K. H., ZHAO, F., YOO, R. H., IGORI, D., LEE, S. H. & MOON, J. S. 2015. Complete genome sequence of a novel endornavirus isolated from hot pepper. *Arch Virol,* 160**,** 3153-6.

LIU, J., ZHANG, L., XU, F., CHAI, M., WU, X., KIM, U., LV, D., WU, X., WU, X. & CHENG, X. 2020. Molecular analysis of a divergent isolate of Potato virus H from potato reveals novel evolutionary feature of Carlaviruses. *Canadian Journal of Plant Pathology,* 42**,** 116-124.

LOBIN, K. K., BOOLUCK, K., RAMESSUR, I. & TALEB-HOSSENKHAN, N. 2023. First report of tomato yellow leaf curl virus (TYLCV) infecting Solanum nigrum plants in Mauritius. *Journal of Plant Pathology,* 105**,** 591-592.

LOCKHART, B. E., MENKE, J., DAHAL, G. & OLSZEWSKI, N. E. 2000. Characterization and genomic analysis of tobacco vein clearing virus, a plant pararetrovirus that is transmitted vertically and related to sequences integrated in the host genome. *Journal of General Virology,* 81**,** 1579-1585.

LÓPEZ, M. M., LLOP, P., OLMOS, A., MARCO-NOALES, E., CAMBRA, M. & BERTOLINI, E. 2009. Are molecular tools solving the challenges posed by detection of plant pathogenic bacteria and viruses? *Current issues in molecular biology,* 11**,** 13-45.

MA, Y., MARAIS, A., LEFEBVRE, M., FAURE, C. & CANDRESSE, T. 2020. Metagenomic analysis of virome cross-talk between cultivated Solanum lycopersicum and wild Solanum nigrum. *Virology,* 540**,** 38-44.

MACCARONE, L. D., BARBETTI, M. J., SIVASITHAMPARAM, K. & JONES, R. A. 2010. Comparison of the coat protein genes of Lettuce big-vein associated virus isolates from Australia with those of isolates from other continents. *Archives of virology,* 155**,** 765-770.

MACKIE, A. E., RODONI, B., BARBETTI, M. J., MCKIRDY, S. & JONES, R. A. 2016. Potato spindle tuber viroid: alternative host reservoirs and strain found in a remote subtropical irrigation area. *European Journal of Plant Pathology,* 145**,** 433-446.

MACKIE, J., CAMPBELL, P. R., KEHOE, M. A., TRAN-NGUYEN, L. T., RODONI, B. C. & CONSTABLE, F. E. 2023. Genome characterisation of the CGMMV virus population in Australia—informing plant biosecurity policy. *Viruses,* 15**,** 743.

MACLOT, F., CANDRESSE, T., FILLOUX, D., MALMSTROM, C. M., ROUMAGNAC, P., VAN DER VLUGT, R. & MASSART, S. 2020. Illuminating an ecological blackbox: using high throughput sequencing to characterize the plant virome across scales. *Frontiers in Microbiology,* 11**,** 578064.

MAINA, S., DONOVAN, N. J., PLETT, K., BOGEMA, D. & RODONI, B. C. 2024. High-throughput sequencing for plant virology diagnostics and its potential in plant health certification. *Frontiers in Horticulture,* 3**,** 1388028.

MAREE, H. J., FOX, A., AL RWAHNIH, M., BOONHAM, N. & CANDRESSE, T. 2018. Application of HTS for routine plant virus diagnostics: State of the art and challenges. *Frontiers in plant science,* 9**,** 1082.

MARIA LAURA, G. 2012. Ophioviruses: State of the Art. *In:* MARIA LAURA, G. & VICTOR, R. (eds.) *Viral Genomes.* Rijeka: IntechOpen.

MARSHALL, S. H. 2016. *Genetic diversity of Tomato spotted wilt virus.* Washington State University.

MASSART, S., ADAMS, I., AL RWAHNIH, M., BAEYEN, S., BILODEAU, G. J., BLOUIN, A. G., BOONHAM, N., CANDRESSE, T., CHANDELLIER, A. & DE JONGHE, K. 2022. Guidelines for the reliable use of high throughput sequencing technologies to detect plant pathogens and pests. *Peer Community Journal,* 2.

MATSUSHITA, Y., YANAGISAWA, H., KHIUTTI, A., MIRONENKO, N., OHTO, Y. & AFANASENKO, O. 2021. Genetic diversity and pathogenicity of potato spindle tuber viroid and chrysanthemum stunt viroid isolates in Russia. *European Journal of Plant Pathology,* 161**,** 529-542.

MEHLE, N., TUŠEK ŽNIDARI, M., TORNOS, T. & RAVNIKAR, M. 2008. First report of Broad bean wilt virus 1 in Slovenia. *Plant Pathology,* 57.

MEHRVAR, M., ALINIZI, H. R., KERAMATI, M. R. & MORADI, Z. 2024. First report of broad bean wilt virus 1 infecting Plantago lanceolata in Iran. *Journal of Plant Pathology,* 106**,** 1863-1863.

MIHARA, T., NISHIMURA, Y., SHIMIZU, Y., NISHIYAMA, H., YOSHIKAWA, G., UEHARA, H., HINGAMP, P., GOTO, S. & OGATA, H. 2016. Linking virus genomes with host taxonomy. *Viruses,* 8**,** 66.

MINICKA, J., TABERSKA, A., BORODYNKO-FILAS, N., KAŹMIŃSKA, K., BARTOSZEWSKI, G. & HASIÓW-JAROSZEWSKA, B. 2024. Viruses infecting Capsicum crops in Poland and molecular characterization of newly detected bell pepper alphaendornavirus (BPEV). *Crop Protection,* 176**,** 106478.

MISHCHENKO, L., DUNICH, A., TARAN, O., DASHCHENKO, A., POLISCHUK, V. & KONDRATYUK, O. 2018. Phylogenetic relationships of two Ukrainian tomato isolates of potato virus M and genetic variability analysis of its population. *Acta virologica,* 62**,** 214-219.

MNARI-HATTAB, M., ZAMMOURI, S., PELLEGRIN, F. & GAUTHIER, N. 2014. Natural occurrence of begomovirus recombinants associated with tomato yellow leaf curl disease co-existing with parental viruses in tomato crops and weeds in Tunisia. *Journal of Plant Pathology,* 96**,** 195-200.

MOCHIZUKI, T. & OHKI, S. T. 2012. Cucumber mosaic virus: viral genes as virulence determinants. *Molecular plant pathology,* 13**,** 217-225.

MOHAMMED, H., EL SIDDIG, M., EL HUSSEIN, A., NAVAS-CASTILLO, J. & FIALLO-OLIVÉ, E. 2018. A novel strain of the begomovirus tomato leaf curl Sudan virus infecting Datura stramonium in Sudan. *Plant Disease,* 102**,** 1863.

MOODLEY, V., IBABA, J. D., NAIDOO, R. & GUBBA, A. 2014. Full-genome analyses of a Potato Virus Y (PVY) isolate infecting pepper (Capsicum annuum L.) in the Republic of South Africa. *Virus Genes,* 49**,** 466-476.

MOURA, M. F., SOMAN, M., MITUTI, T., PAVAN, M. A. & KRAUSE-SAKATE, R. 2014. Solanum americanum: reservoir for Potato virus Y and Cucumber mosaic virus in sweet pepper crops. *Summa Phytopathologica,* 40**,** 78-80.

MOURY, B., CHARRON, C., JANZAC, B., SIMON, V., GALLOIS, J.-L., PALLOIX, A. & CARANTA, C. 2014. Evolution of plant eukaryotic initiation factor 4E (eIF4E) and potyvirus genome-linked protein (VPg): A game of mirrors impacting resistance spectrum and durability. *Infection, genetics and evolution,* 27**,** 472-480.

MOURY, B., MOREL, C., JOHANSEN, E. & JACQUEMOND, M. 2002. Evidence for diversifying selection in Potato virus Y and in the coat protein of other potyviruses. *Journal of General Virology,* 83**,** 2563-2573.

MUKHTAR, Y., TUKUR, S. & BASHIR, R. 2019. An overview on Datura stramonium L.(Jimson weed): A notable psychoactive drug plant. *Am. J. Nat. Sci,* 2**,** 1-9.

MUÑOZ-BAENA, L., MARÍN-MONTOYA, M. & GUTIÉRREZ, P. A. 2017. Genome sequencing of two Bell pepper endornavirus (BPEV) variants infecting Capsicum annuum in Colombia. *Agronomía Colombiana,* 35**,** 44-52.

MURPHY, F. A., FAUQUET, C. M., BISHOP, D. H., GHABRIAL, S. A., JARVIS, A. W., MARTELLI, G. P., MAYO, M. A. & SUMMERS, M. D. 2012. *Virus taxonomy: classification and nomenclature of viruses*, Springer Science & Business Media.

NADU, K., KARTHIKEYAN, G., DAMAYANTI, T. A., OLUFEMI, A. & RAYAPADI, N. 2009. First report of the natural occurrence of Chilli veinal mottle virus in Solanum nigrum and Physalis floridana in India.

NAGENDRAN, K., PRIYANKA, R., ARAVINTHARAJ, R., BALAJI, C., PRASHANT, S., BASAVARAJ, B., MOHANKUMAR, S. & KARTHIKEYAN, G. 2018. Characterization of cucumber mosaic virus infecting snake gourd and bottle gourd in India. *Physiological and Molecular Plant Pathology,* 103**,** 102-106.

NAKAMURA, S., IWAI, T. & HONKURA, R. 1998. Complete nucleotide sequence and genome organization of Broad bean wilt virus 2. *Japanese Journal of Phytopathology,* 64**,** 565-568.

NAVARRO, J., TOROK, V., VETTEN, H. & PALLAS, V. 2005a. Genetic variability in the coat protein genes of Lettuce big-vein associated virus and Mirafiori lettuce big-vein virus. *Archives of virology,* 150**,** 681-694.

NAVARRO, J. A., BOTELLA, F., MARHUENDA, A., SASTRE, P., SANCHEZ-PINA, M. A. & PALLAS, V. 2005b. Identification and partial characterisation of Lettuce big-vein associated virus and Mirafiori lettuce big-vein virus in common weeds found amongst Spanish lettuce crops and their role in lettuce big-vein disease transmission. *European journal of plant pathology,* 113**,** 25-34.

NAVARRO, J. A., BOTELLA, F., MARUHENDA, A., SASTRE, P., SÁNCHEZ-PINA, M. A. & PALLAS, V. 2004. Comparative infection progress analysis of Lettuce big-vein virus and

Mirafiori lettuce virus in lettuce crops by developed molecular diagnosis techniques. *Phytopathology,* 94**,** 470-477.

NIBERT, M. L., VONG, M., FUGATE, K. K. & DEBAT, H. J. 2018. Evidence for contemporary plant mitoviruses. *Virology,* 518**,** 14-24.

NICAISE, V. 2014. Crop immunity against viruses: outcomes and future challenges. *Frontiers in plant science,* 5**,** 660.

NURULITA, S., GEERING, A. D., CREW, K. S., HARPER, S. M. & THOMAS, J. E. 2022. Detection of two poleroviruses infecting garlic (Allium sativum) in Australia. *Australasian Plant Pathology,* 51**,** 461-465.

OCHOA-CORONA, F., TANG, J., LEBAS, B., RUBIO, L., GERA, A. & ALEXANDER, B. 2010. Diagnosis of Broad bean wilt virus 1 and Verbena latent virus in Tropaeolum majus in New Zealand. *Australasian Plant Pathology,* 39**,** 120-124.

OCHOA-MARTÍNEZ, D., ALFONSINA-HERNÁNDEZ, J., SÁNCHEZ-ESCUDERO, J., RODRÍGUEZ-MARTÍNEZ, D. & VERA-GRAZIANO, J. 2014. First report of Lettuce big-vein associated virus (Varicosavirus) infecting lettuce in Mexico. *Plant Disease,* 98**,** 573-573.

OKADA, R., KIYOTA, E., SABANADZOVIC, S., MORIYAMA, H., FUKUHARA, T., SAHA, P., ROOSSINCK, M. J., SEVERIN, A. & VALVERDE, R. A. 2011. Bell pepper endornavirus: molecular and biological properties, and occurrence in the genus Capsicum. *J Gen Virol,* 92**,** 2664-2673.

OLMSTEAD, R. G., BOHS, L., MIGID, H. A., SANTIAGO-VALENTIN, E., GARCIA, V. F. & COLLIER, S. M. 2008. A molecular phylogeny of the Solanaceae. *Taxon,* 57**,** 1159-1181.

ORFANIDOU, C., LOTOS, L., TSIOLAKIS, G., STEFANIDIS, S., TSIALTAS, J., KATIS, N. & MALIOGKA, V. 2021. Molecular characterization of poleroviruses isolated from oilseed rape in Greece. *Virus Genes,* 57**,** 289-292.

ORMEÑO, J., SEPÚLVEDA, P., ROJAS, R. & ARAYA, J. E. 2006. Datura Genus Weeds as an Epidemiological Factor of Alfalfa mosaic virus (AMV), Cucumber mosaic virus (CMV), and Potato virus Y (PVY) on Solanaceus Crops. *Agricultura Técnica,* 66**,** 333.

PADGETT, H. S. & BEACHY, R. N. 1993. Analysis of a tobacco mosaic virus strain capable of overcoming N gene-mediated resistance. *The Plant Cell,* 5**,** 577-586.

PAPAYIANNIS, L., KATIS, N., IDRIS, A. & BROWN, J. 2011. Identification of weed hosts of Tomato yellow leaf curl virus in Cyprus. *Plant Disease,* 95**,** 120-125.

PAPPI, P. G., MALIOGKA, V. I., AMOUTZIAS, G. D. & KATIS, N. I. 2016. Genetic variation of eggplant mottled dwarf virus from annual and perennial plant hosts. *Archives of virology,* 161**,** 631-639.

PAVAN, M. A., KRAUSE-SAKATE, R., SILVA, N. D., ZERBINI, F. M. & LE GALL, O. 2008. Virus diseases of lettuce in Brazil. *Plant viruses,* 2**,** 35-41.

PECMAN, A., KUTNJAK, D., MEHLE, N., ŽNIDARIČ, M. T., GUTIÉRREZ-AGUIRRE, I., PIRNAT, P., ADAMS, I., BOONHAM, N. & RAVNIKAR, M. 2018. High-throughput sequencing facilitates characterization of a "forgotten" plant virus: The case of a Henbane mosaic virus infecting tomato. *Frontiers in microbiology,* 9**,** 2739.

PELÁEZ, A., MCLEISH, M. J., PASWAN, R. R., DUBAY, B., FRAILE, A. & GARCÍA-ARENAL, F. 2021. Ecological fitting is the forerunner to diversification in a plant virus with broad host range. *Journal of evolutionary biology,* 34**,** 1917-1931.

PERRY, K. & MCLANE, H. 2011. Potato virus m in bittersweet nightshade (Solanum dulcamara) in New York State. *Plant Disease,* 95**,** 619-619.

PIMENTA, R. J., MACLEOD, K., BABB, R., COLEMAN, K., MACDONALD, J., ASARE-BEDIAKO, E., NEWBERT, M. J., JENNER, C. E. & WALSH, J. A. 2024. Genetic variation of turnip yellows virus in arable and vegetable brassica crops, perennial wild brassicas, and aphid vectors collected from the plants. *Plant Disease,* 108**,** 616-623.

PLCHOVA, H., VACULIK, P., CEROVSKA, N., MORAVEC, T. & DEDIC, P. 2015. Molecular and biological analysis of Potato virus M (PVM) isolates from the Czech Republic. *Journal of Phytopathology,* 163**,** 1031-1035.

PRINS, M. 2003. Broad virus resistance in transgenic plants. *Trends in Biotechnology,* 21**,** 373-375.

RANI, Y. S., REDDY, V. J., BASHA, S. J., KOSHMA, M., HANUMANTHU, G. & SWAROOPA, P. 2017. A review on Solanum nigrum. *World J. Pharm. Pharm. Sci,* 6**,** 293-303.

RASHID, M.-O., LI, J.-H., LIU, Q., WANG, Y. & HAN, C.-G. 2021. Molecular detection and identification of eight potato viruses in Gansu province of China. *Current Plant Biology,* 25**,** 100184.

RASHID, M.-O., WANG, Y. & HAN, C.-G. 2020. Molecular detection of potato viruses in Bangladesh and their phylogenetic analysis. *Plants,* 9**,** 1413.

RASOULPOUR, R. & IZADPANAH, K. 2008. Properties and taxonomic position of hoary cress strain of Cucumber mosaic virus. *Journal of Plant Pathology***,** 97-102.

RIVAREZ, M. P. S., PECMAN, A., BAČNIK, K., MAKSIMOVIĆ, O., VUČUROVIĆ, A., SELJAK, G., MEHLE, N., GUTIÉRREZ-AGUIRRE, I., RAVNIKAR, M. & KUTNJAK, D. 2023. In-depth study of tomato and weed viromes reveals undiscovered plant virus diversity in an agroecosystem. *Microbiome,* 11**,** 60.

ROOSSINCK, M. J. 2014. Plant Virus Metagenomics: What We Know and Why We Need to Know More. *Frontiers in Plant Science,* 5.

RUPASOV, V., MOROZOV, S. Y., KANYUKA, K. & ZAVRIEV*, S. 1989. Partial nucleotide sequence of potato virus M RNA shows similarities to potexviruses in gene arrangement and the encoded amino acid sequences. *Journal of General Virology,* 70**,** 1861-1869.

SABANADZOVIC, S. & VALVERDE, R. A. 2011. Properties and detection of two cryptoviruses from pepper (Capsicum annuum). *Virus Genes,* 43**,** 307-12.

SAHA, A., SAHA, B. & SAHA, D. 2014. Molecular detection and partial characterization of a begomovirus causing leaf curl disease of potato in sub-Himalayan West Bengal, India. *Journal of Environmental Biology,* 35**,** 601.

SALAMON, P. 2006. Viral diseases and viruses of cultivated and wild Solanaceae plants in Hungary. 6. Woody nightshade (Solanum dulcamara L.) as a natural host of a new strain of Potato virus M (PVM).

SALEM, N., ODEH, S., MUSLEM, M. A. & TAHZIMA, R. 2020. Occurrence and partial genetic characterisation of Lettuce big-vein associated virus and Mirafiori lettuce big-vein virus infecting lettuce in Jordan. *Annals of Applied Biology,* 177**,** 90-100.

SALEM, N. M., ABUMUSLEM, M., TURINA, M., SAMARAH, N., SULAIMAN, A., ABU-IRMAILEH, B. & ATA, Y. 2022. New weed hosts for tomato brown rugose fruit virus in wild Mediterranean vegetation. *Plants,* 11**,** 2287.

SANCHES, M. M., KRAUSE-SAKATE, R. & PAVAN, M. A. 2008. Sequence diversity in the coat protein gene of lettuce big-vein associated virus and Mirafiori lettuce big-vein virus infecting lettuce in Brazil. *Summa Phytopathologica,* 34**,** 175-177.

SANTALA, J. & VALKONEN, J. P. 2018. Sensitivity of small RNA-based detection of plant viruses. *Frontiers in microbiology,* 9**,** 939.

SARITHA, R. K., JAIN, P., BARANWAL, V. K., JAIN, R. K., SRIVASTAVA, A. & KALIA, P. 2016. First record of Pepper cryptic virus 2 in chilli (Capsicum annuum) in India. *Virusdisease,* 27**,** 327-328.

SASAYA, T., ISHIKAWA, K. & KOGANEZAWA, H. 2002. The nucleotide sequence of RNA1 of Lettuce big-vein virus, genus Varicosavirus, reveals its relation to nonsegmented negative-strand RNA viruses. *Virology,* 297**,** 289-297.

SASAYA, T., KUSABA, S., ISHIKAWA, K. & KOGANEZAWA, H. 2004. Nucleotide sequence of RNA2 of Lettuce big-vein virus and evidence for a possible transcription termination/initiation strategy similar to that of rhabdoviruses. *Journal of general virology,* 85**,** 2709-2717.

SCHOLTHOF, K. B. G., ADKINS, S., CZOSNEK, H., PALUKAITIS, P., JACQUOT, E., HOHN, T., HOHN, B., SAUNDERS, K., CANDRESSE, T. & AHLQUIST, P. 2011. Top 10 plant viruses in molecular plant pathology. *Molecular plant pathology,* 12**,** 938-954.

SELA, N., LURIA, N. & DOMBROVSKY, A. 2012. Genome assembly of bell pepper endornavirus from small RNA. *J Virol,* 86**,** 7721.

SENSHU, H., YAMAJI, Y., MINATO, N., SHIRAISHI, T., MAEJIMA, K., HASHIMOTO, M., MIURA, C., NERIYA, Y. & NAMBA, S. 2011. A dual strategy for the suppression of host antiviral silencing: two distinct suppressors for viral replication and viral movement encoded by potato virus M. *Journal of Virology,* 85**,** 10269-10278.

SEO, J.-K., KWAK, H.-R., CHOI, B., HAN, S.-J., KIM, M.-K. & CHOI, H.-S. 2017. Movement protein of broad bean wilt virus 2 serves as a determinant of symptom severity in pepper. *Virus research,* 242**,** 141-145.

SHAKEEL, M., AL-SALEH, M., AMER, M. A., AL-SHAHWAN, I., UMAR, M., DIMOU, N., ORFANIDOU, C., ZAKRI, A. & KATIS, N. 2017. Molecular characterization and natural host range of Tomato chlorosis virus in Saudi Arabia. *Journal of Plant Pathology***,** 415-421.

SHUKLA, D., WARD, C. & BRUNT, A. 1994. The Potyviridae. CAB International, Wallingford. *VIRAL DISEASES,* 33.

SINGH, R. P. 1998. Reverse-transcription polymerase chain reaction for the detection of viruses from plants and aphids. *Journal of Virological methods,* 74**,** 125-138.

SLAVÍKOVÁ, L., IBRAHIM, E., ALQUICER, G., TOMAŠECHOVÁ, J., ŠOLTYS, K., GLASA, M. & KUNDU, J. K. 2022. Weed hosts represent an important reservoir of turnip yellows virus and a possible source of virus introduction into oilseed rape crop. *Viruses,* 14**,** 2511.

STANKOVIĆ, I., BULAJIĆ, A., VUČUROVIĆ, A., RISTIĆ, D., MILOJEVIĆ, K., BERENJI, J. & KRSTIĆ, B. 2011. Status of tobacco viruses in Serbia and molecular characterization of Tomato spotted wilt virus isolates. *Acta virologica,* 55**,** 337-347.

STOIMENOVA, E. 1984. New strain of tobacco mosaic virus (TMV) in red pepper. *Plovdiv/Bulgaria: Eucarpia 83,* 1983. pp. 161–164.

SU, X., WU, K., ZHANG, L. Z., RAHMAN, M. S., ZHENG, K., LI, T., ZHANG, Z. & DONG, J. 2017. Complete genome sequence of a new isolate of potato virus M in Yunnan, China. *Archives of Virology,* 162**,** 2485-2488.

SUN, M., JING, C., WU, G., SUN, X., LIU, Y. & QING, L. 2017. First report of pepper cryptic virus 2 infecting pepper in China.

TABASINEJAD, F., JAFARPOUR, B., ZAKIAGHL, M., SIAMPOUR, M., ROUHANI, H. & MEHRVAR, M. 2014. Genetic structure and molecular variability of potato virus M populations. *Archives of virology,* 159**,** 2081-2090.

TABASINEJAD, F., JAFARPOUR, B., ZAKIAGHL, M., SIAMPOUR, M., ROWHANI, H. & MEHRVAR, M. 2015. Molecular variability in the cysteine rich protein of Potato virus M. *VirusDisease,* 26**,** 117-122.

TEMPLE, C., BLOUIN, A. G., BOEZEN, D., BOTERMANS, M., DURANT, L., DE JONGHE, K., DE KONING, P., GOEDEFROIT, T., MINET, L. & STEYER, S. 2024. Biological characterization of Physostegia chlorotic mottle virus, an emergent virus infecting vegetables in diversified production systems. *Phytopathology®,* 114**,** 1680-1688.

THOMSON, D. & DIETZGEN, R. G. 1995. Detection of DNA and RNA plant viruses by PCR and RT-PCR using a rapid virus release protocol without tissue homogenization. *Journal of Virological Methods,* 54**,** 85-95.

TOMAŠECHOVÁ, J., HANČINSKÝ, R., PREDAJŇA, L., KRAIC, J., MIHÁLIK, D., ŠOLTYS, K., VÁVROVÁ, S., BÖHMER, M., SABANADZOVIC, S. & GLASA, M.

2019. High-Throughput Sequencing Reveals Bell Pepper Endornavirus Infection in Pepper (Capsicum annum) in Slovakia and Enables Its Further Molecular Characterization. *Plants (Basel),* 9.

TOMAŠECHOVÁ, J., PREDAJŇA, L., MIHÁLIK, D., MRKVOVÁ, M., CEJNAR, P., ŠOLTYS, K., SABANADZOVIC, S. & GLASA, M. 2021. Characterization of an isolate of Lettuce big-vein associated virus (LBVaV) detected in naturally infected tomato (Solanum lycopersicum L.) in Slovakia. *Plant Protection Science,* 57**,** 344-348.

TOMAŠECHOVÁ, J., PREDAJNA, L., SIHELSKÁ, N., KRAIC, J., MIHÁLIK, D., ŠOLTYS, K. & GLASA, M. 2020. First report of pepper cryptic virus 2 infecting pepper (Capsicum annum) in Slovakia. *Plant Disease,* 104**,** 1565-1565.

VAIRA, A. M., ACCOTTO, G. P., LISA, V., VECCHIATI, M., MASENGA, V. & MILNE, R. G. MOLECULAR DIAGNOSIS OF RANUNCULUS WHITE MOTTLE VIRUS IN TWO ORNAMENTAL SPECIES. 2002. International Society for Horticultural Science (ISHS), Leuven, Belgium, 29-33.

VAIRA, A. M., MILNE, R. G., ACCOTTO, G. P., LUISONI, E., MASENGA, V. & LISA, V. 1997. Partial characterization of a new virus from ranunculus with a divided RNA genome and circular supercoiled thread-like particles. *Archives of Virology,* 142**,** 2131-2146.

VALVERDE, R. A., KHALIFA, M. E., OKADA, R., FUKUHARA, T., SABANADZOVIC, S. & ICTV REPORT, C. 2019. ICTV Virus Taxonomy Profile: Endornaviridae. *J Gen Virol,* 100**,** 1204-1205.

VAN DER WANT, J. & DIJKSTRA, J. 2006. A history of plant virology. *Archives of virology,* 151**,** 1467-1498.

VENKATARAVANAPPA, V., ASHWATHAPPA, K., HIREMATH, S., MANJUNATHA, L., SHANKARAPPA, K., KRISHNA REDDY, M. & LAKSHMINARAYANA REDDY, C. 2023. Begomovirus and DNA-satellites association with mosaic and leaf curl disease of Solanum nigrum and Physalis minima: the new hosts for chilli leaf curl virus. *VirusDisease,* 34**,** 504-513.

VERBEEK, M., DULLEMANS, A., VAN BEKKUM, P. & VAN DER VLUGT, R. 2013. Evidence for Lettuce big-vein associated virus as the causal agent of a syndrome of necrotic rings and spots in lettuce. *Plant Pathology,* 62**,** 444-451.

VILLAMOR, D., HO, T., AL RWAHNIH, M., MARTIN, R. & TZANETAKIS, I. 2019. High throughput sequencing for plant virus detection and discovery. *Phytopathology,* 109**,** 716-725.

WEBSTER, C. G., DE JENSEN, C. E., RIVERA-VARGAS, L. I., RODRIGUES, J. C. V., MERCADO, W., FRANTZ, G., MELLINGER, H. C. & ADKINS, S. 2013. First report of Tomato chlorotic spot virus (TCSV) in tomato, pepper, and jimsonweed in Puerto Rico. *Plant Health Progress,* 14**,** 47.

WREN, J. D., ROOSSINCK, M. J., NELSON, R. S., SCHEETS, K., PALMER, M. W. & MELCHER, U. 2006. Plant virus biodiversity and ecology. *PLoS biology,* 4**,** e80.

WYLIE, S. J., ADAMS, M., CHALAM, C., KREUZE, J., LÓPEZ-MOYA, J. J., OHSHIMA, K., PRAVEEN, S., RABENSTEIN, F., STENGER, D. & WANG, A. 2017. ICTV virus taxonomy profile: Potyviridae. *Journal of General Virology,* 98**,** 352-354.

XIANG, H.-Y., DONG, S.-W., SHANG, Q.-X., ZHOU, C.-J., LI, D.-W., YU, J.-L. & HAN, C.-G. 2011. Molecular characterization of two genotypes of a new polerovirus infecting brassicas in China. *Archives of Virology,* 156**,** 2251-2255.

XU, W., LI, H., SIVASITHAMPARAM, K., TRAN, D. T., JONES, M. G., CHEN, X. & WYLIE, S. J. 2022. Spillover of a Tobamovirus from the Australian indigenous flora to invasive weeds. *Viruses,* 14**,** 1676.

XU, Z., WENG, H., YANG, Z., WANG, L., MAO, Q., CAO, Y., SONG, X., RAO, S., CHEN, J. & LI, Y. 2024. First report of potato virus H infecting tomato (Solanum lycopersicum) in China. *Plant Disease,* 108**,** 3204.

YANAGISAWA, H., MATSUSHITA, Y., KHIUTTI, A., MIRONENKO, N., OHTO, Y. & AFANASENKO, O. 2021. Occurrence and distribution of viruses infecting potato in Russia. *Letters in Applied Microbiology,* 73**,** 64-72.

ZELYÜT, F. R. & ERTUNÇ, F. 2021. Population genetic analysis of lettuce big-vein disease viruses and their vector fungi Olpidium virulentus in Ankara province, Turkey. *Physiological and Molecular Plant Pathology,* 113**,** 101593.

ZHANG, L., SHANG, J., JIA, Q., GONG, G., ZHANG, M. & YANG, W. 2019. The complete genome sequence of wild tomato mosaic virus isolated from Solanum nigrum reveals recombination in the P1 cistron. *Archives of Virology,* 164**,** 903-906.

ZIEBELL, H., MURPHY, A. M., GROEN, S. C., TUNGADI, T., WESTWOOD, J. H., LEWSEY, M. G., MOULIN, M., KLECZKOWSKI, A., SMITH, A. G. & STEVENS, M. 2011. Cucumber mosaic virus and its 2b RNA silencing suppressor modify plant-aphid interactions in tobacco. *Scientific reports,* 1**,** 187.

10. ACKNOWLEDGEMENTS

First and foremost, I would like to thank the Almighty God, the Most Merciful, the Most Compassionate, for His endless guidance, mercy, and blessings, which made it possible for me to complete this PhD journey with health, strength, and perseverance. Without His divine support, none of this would have been achievable.

I am very grateful to all those who supported me throughout this journey. This work was financially supported by NKFIH K146087, and I sincerely thank the Hungarian Government for awarding me the Stipendium Hungaricum scholarship, which made this PhD study possible. I would also like to thank my home country, Kosovo, as a sending partner, for nominating me to obtain this opportunity.

Special thanks are due to my beloved supervisors, Dr. Várallyay Éva, DSc., and my co-supervisor, Dr. habil. András Péter Takács, for their invaluable guidance, expertise, and support. I am sincerely grateful for their exceptional mentorship and insightful advice throughout this work.

I would also like to express my gratitude to all my colleagues at the Plant Protection Institute in Gödöllő for their support, collaboration, and the stimulating research environment that enriched this project. I am equally thankful to all my friends for the good moments we shared and for their companionship throughout this journey.

Finally, yet far from least, I owe heartfelt thanks to my family for their unwavering support and encouragement throughout my PhD. I am particularly grateful to my father, Xhevat Ismajli, my mother, Mirvete Ismajli, my sister, Fitore Ismajli, and my brother, Festim Ismajli, whose love and constant belief in me have strengthened and inspired me throughout this journey.

I would like to dedicate this success to my beloved grandmother, with whom I began this journey. Though she left before seeing its completion, her love and inspiration stayed with me at every step. Each time I left home for Hungary, she used to ask me, *'E kur vjen tash o djali jem?'* (And when are you coming back to visit us next, my son?) but that time she did not wait for my return. I know she would have been deeply proud, and I carry her memory with me as I celebrate this success.

Author's Scientific Publications

Publications in Peer-Reviewed Journals with Impact Factor

- **Ismajli, B**., Galbács, Z. N., Takács, A. P., & Várallyay, É. (2025). The First High-Throughput Sequencing-Based Study of Viruses Infecting Solanaceous Crops in Kosovo Reveals Multiple Infections in Peppers by Six Plant Viruses. Plants, 14(9), 1273, https://doi.org/10.3390/plants14091273. IF: 4.1 (Q1).
- **Ismajli, B**., Pásztor, G., Takács, A., & Várallyay, É. (2024). Investigation of Viromes of Solanaceous Weeds. GEORGIKON FOR AGRICULTURE, 28(Suppl. 1), 13-17, https://journal.uni-mate.hu/index.php/gfa/article/view/6098.
- **Ismajli, Burim**, Zsuzsanna N. Galbács , Lilla Dorottya Péri, György Pasztor, András Takács, Várallyay, Éva. Reinvestigating the viromes of solanaceous weeds in Hungary after several decades confirmed the original results and added new insights. (Under review)

Scientific Talks Presented at Conferences

- **Burim Ismajli**, György Pásztor, András Takács, Éva Várallyay
  Investigation of viromes of Solanaceae weeds
  „MATE Növényvédelmi Intézet Növényvédelmi Tanszék PhD hallgatóinak bemutatkozása" Keszthely, 2023.november 14.
- **Burim Ismajli**, György Pásztor, András Takács, Éva Várallyay
  Investigation of viromes of Solanaceae weeds
  Slovene-Hungarian PhD Student Forum 2023-11-22 Ljubljana, Szlovénia (MTMT 34414572)
- **Burim Ismajli**, György Pásztor, András Takács and Éva Várallyay
  Investigation of viromes of Solanaceae weeds. XXXIII. Keszthelyi Növényvédelmi Fórum, 2024. január 17-19. (MTMT 34414568).
- **Ismajli, Burim**, András Takács, Várallyay, Éva
  Revealing Plant Virus Presence in POTATO, TOMATO and Pepper Cultivars: Kosovo's Debut Virus Report on First-Ever Findings. 2024 LXV. Georgikon Napok Tudományos

Konferencia, Keszthely, május 17-18. https://m2.mtmt.hu/gui2/?mode=browse&params=publication;35059876.

- **Burim Ismajli**; Zsuzsanna, N. Galbács, András Takács, Éva Várallyay
  REVEALING PLANT VIRUS PRESENCE IN PEPPER CULTIVARS: KOSOVO'S DEBUT VIRUS REPORT ON FIRST-EVER FINDINGS. 11th International Plant Protection Symposium at University of Debrecen, 15-17 October 2024. https://m2.mtmt.hu/gui2/?mode=browse&params=publication;35484954
- **Burim Ismajli**; Nagyné Galbács Zsuzsanna, András Takács, Éva Várallyay
  Spicy Trouble in the Fields: Characterization and First-Ever Report of Plant Viruses in Kosovo's Peppers. 34th Plant Protection Forum, Keszthely, 15-17 Jan 2025.
- **Ismajli, Burim**[1]; Pásztor, György[2], András Takács Péter[2],Várallyay, Éva[1]
  30. Tiszántúli Növényvédelmi Fórum: The 12th Plant Protection Symposium
  Conference: Târgu Mureș, Romania 2025.10.14. - 2025.10.16. (Hungarian Chamber of Plant Protection Engineers and Phytopathologists, MTA-DAB Agricultural Committee, Plant Protection Working Committee, Sapientia EMTE Marosvásárhely Faculty, Plant Protection Institute of the University of Debrecen, University of Debrecen MÉK Plant Protection Institute), pp 128-129 (2025) (Transtizan Plant Protection Forum ; 30th TNF) (Book: 36397138). Awarded the 3rd Prize for Best Conference Presentation.
- **Ismajli, Burim**, Zsuzsanna N. Galbács , Lilla Dorottya Péri, György Pasztor, András Takács, Várallyay, Éva
  Exploring Viromes of Solanaceous Weeds at Keszthely using HTS. XXXV. Keszthelyi Növényvédelmi Fórum 2026. január 14-16, MATE Georgikon Campus, Keszthely - A épület 8360 Keszthely, Deák Ferenc utca 16. novenyvedelmi.forum@uni-mate.hu.